

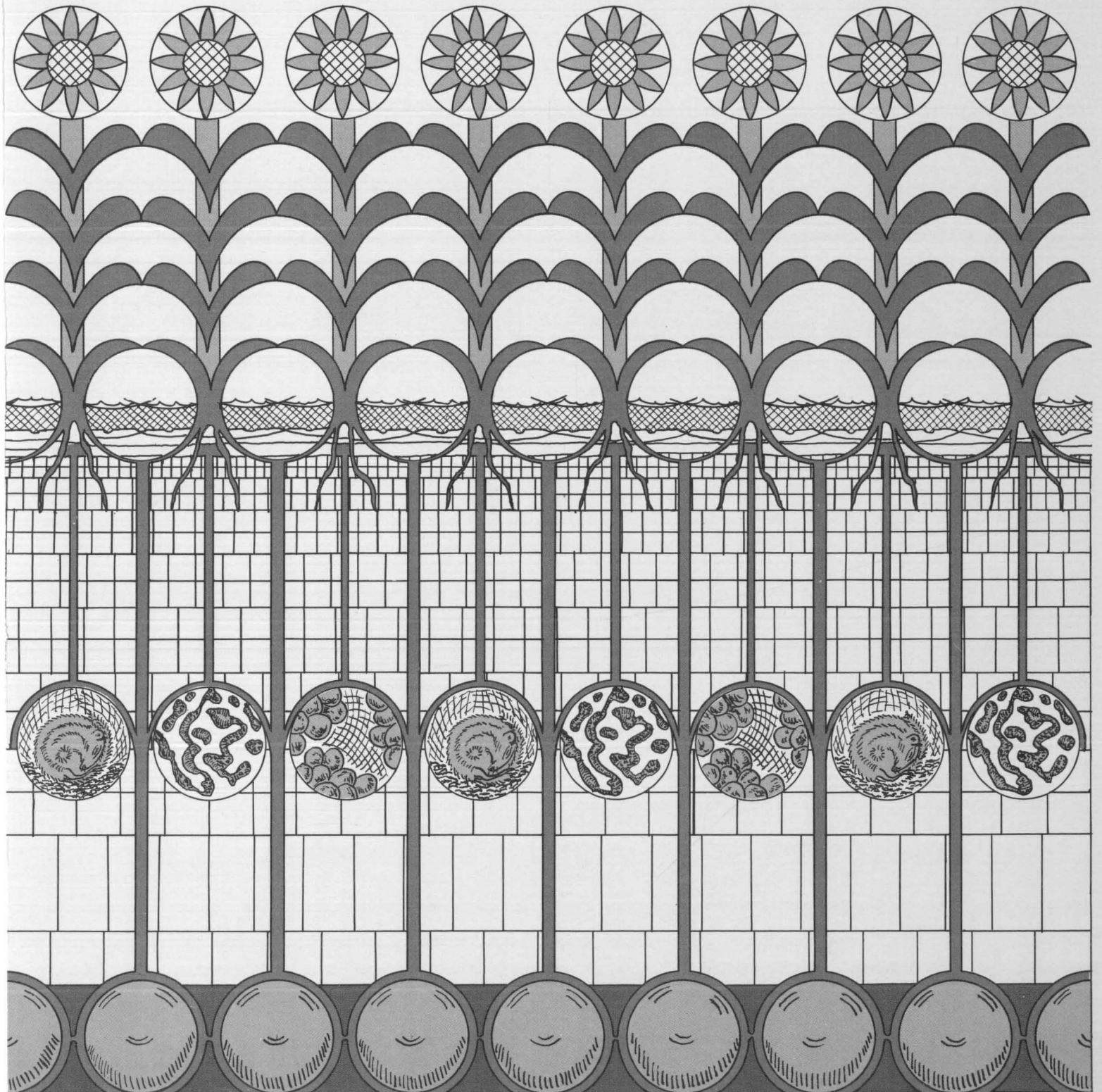
# Measurement of Water Movement in Soil Pedons Above the Water Table

By: J. BOUMA, F. G. BAKER, and P. L. M. VENEMAN

University of Wisconsin-Extension  
GEOLOGICAL AND NATURAL HISTORY SURVEY

University of Wisconsin- Madison  
COLLEGE OF AGRICULTURAL AND LIFE SCIENCES  
Department of Soil Science

INFORMATION CIRCULAR  
NUMBER 27  
1974



University of Wisconsin-Extension  
GEOLOGICAL AND NATURAL HISTORY SURVEY  
Meredith E. Ostrom, Director and State Geologist

INFORMATION CIRCULAR NUMBER 27  
1974

# Measurement of Water Movement in Soil Pedons Above the Water Table

By:

**J. BOUMA, F. G. BAKER, and P. L. M. VENEMAN**

In cooperation with:

University of Wisconsin- Madison  
COLLEGE OF AGRICULTURAL AND LIFE SCIENCES  
Department of Soil Science

Copies available at 1815 University Avenue, Madison, Wisconsin, 53706.  
Price \$3.50

### Affiliations of the Authors and Acknowledgements

J. Bouma is Associate Professor of Soil Science, Department of Soil Science, College of Agricultural and Life Sciences, Madison, Wisconsin 53706 (60%) and Geological and Natural History Survey, University Extension (40%); F. G. Baker is Research Assistant, Geological and Natural History Survey, and P. L. M. Veneman is Research Assistant, Department of Soil Science (Hatch-1973 funds).

Most of these studies were made as part of the Small Scale Waste Management Project, University of Wisconsin, funded by the Upper Great Lakes Regional Commission (1971-74), The State of Wisconsin (1971-current) and the Geological and Natural History Survey (1969-current). Some funds for this study were provided by the U.S. Environmental Protection Agency (Grant R-802874-01) since February 1974.

Cover designed by F. D. Hole.

This manuscript was typed by Mrs. Judy Schroeder.

## TABLE OF CONTENTS

	Page
1. Introduction . . . . .	1
2. Some basic physical characteristics associated with water movement through soils . . . . .	3
Abstract . . . . .	3
2.1. Soil as a three-phase system . . . . .	3
2.2. Physical characterization of liquid in soil materials. .	6
2.2.1. Introduction . . . . .	6
2.2.2. Pressure potential (P) . . . . .	8
2.2.3. Gravitational potential (Z). . . . .	9
2.3. Moisture retention in soil . . . . .	10
2.4. Water movement in soil . . . . .	15
2.5. Literature cited . . . . .	21
3. Measurements and calculations. . . . .	22
3.1. Measurement of soil moisture retention characteristics by P. L. M. Veneman. . . . .	22
3.1.1. Introduction . . . . .	22
3.1.2. Methods. . . . .	27
3.1.2.1. Sampling and pretreatment of samples .	27
3.1.2.2. Measurement in the 0-100 mbar range. .	27
3.1.2.3. Measurement in the 0.1-1 bar range . .	33
3.1.2.4. Measurement at potentials lower than -1 bar. . . . .	36
3.1.2.5. Estimation of the bulk density of undisturbed ring samples. . . . .	37
3.1.3. Calculations . . . . .	37
3.1.3.1. Calculation of moisture contents, 0-100 mbar . . . . .	37
3.1.3.2. Calculation of moisture contents, 0.1-15 bar . . . . .	42
3.1.3.3. The moisture content of saturated soil	44
3.1.4. Literature cited . . . . .	45

	Page
3.2. <i>In situ</i> measurement of saturated hydraulic conductivity: the Bouwer double-tube method . . . . .	46
3.2.1. Introduction. . . . .	46
3.2.2. Procedure . . . . .	46
3.2.3. Literature cited. . . . .	55
3.2.4. Alternative procedures. . . . .	55
3.3. A detailed description of the crust-test procedure for measuring hydraulic conductivities of unsaturated soil <i>in situ</i> . . . . .	56
3.3.1. Introduction. . . . .	56
3.3.2. Installation procedure. . . . .	57
3.3.3. Measurement procedure . . . . .	62
3.3.4. Literature cited. . . . .	66
Appendix - List of materials. . . . .	67
3.4. A detailed description of the instantaneous-profile method for measuring hydraulic conductivities of unsaturated soil <i>in situ</i> , by F. G. Baker. . . . .	68
3.4.1. Introduction. . . . .	68
3.4.2. Theory. . . . .	68
3.4.3. Site selection and preparation. . . . .	69
3.4.4. Instrumentation . . . . .	78
3.4.5. Tensiometry . . . . .	79
3.4.6. Soil moisture content . . . . .	86
3.4.7. Experimental procedure. . . . .	88
3.4.8. Example calculation . . . . .	89
3.4.9. Literature cited. . . . .	95
Appendix A. List of materials. . . . .	95
Appendix B. Profile description of Batavia silt loam .	96
3.5. Calculation of hydraulic conductivities from moisture retention data. . . . .	98
4. Some application of flow theory to specific examples. . . . .	100
4.1. One-dimensional steady saturated flow . . . . .	100
4.1.1. One layer . . . . .	100
4.1.2. Two layers. . . . .	102
4.2. One-dimensional steady unsaturated flow . . . . .	102
4.2.1. One layer . . . . .	102
4.2.2. Two or more layers. . . . .	104

	Page
4.2.3. Flow into crusted soil . . . . .	107
4.3. One-dimensional unsteady unsaturated flow. . . . .	110
4.3.1. Literature cited . . . . .	111
4.4. Some applications of flow theory to soil survey interpretations. . . . .	112

## FIGURES

	Page
Fig. 2.1. Schematic diagram of the soil as a three-phase system	4
Fig. 2.2. Graphical expression of the relationship between tubular pore size and corresponding soil moisture tension	4
Fig. 2.3. Soil moisture retention curves	11
Fig. 2.4. Moisture retention in three schematic soil materials at tensions of 30 and 60 cm	13
Fig. 2.5. Cross section through an idealized void illustrating the hysteresis phenomenon	14
Fig. 2.6. Relationships between sizes of tubular and planar voids and flow rates at defined hydraulic gradients	17
Fig. 2.7. Graphical expression of flow rates through tubular or planar voids as a function of pore size	17
Fig. 2.8. Schematic diagram showing the effect of increasing the degree of crusting or decreasing the rate of application of liquid on flow rates through soil materials	19
Fig. 2.9. Hydraulic conductivity (K) as a function of soil moisture tension	20
Fig. 3.1. Tension-cup assembly for moisture retention measurements in the 0-100 mbar range	23
Fig. 3.2. Schematic laboratory setup of a pressure-plate extractor for retention measurements in the 0.1-15 bar range	25
Fig. 3.3. Modified tension-cup assembly for volumetric moisture retention measurements in the 0-100 mbar range	28
Fig. 3.4. Laboratory setup for low-tension moisture retention measurements	30
Fig. 3.5. Laboratory setup of a series of pressure extractors for moisture retention measurements in the 0.1-15 bar pressure range	34

	Page
Fig. 3.6. Moisture-retention curve for a loam (IIB3 of Batavia silt loam) for the 0-15 bar tension range	43
Fig. 3.7. Moisture-retention curve for a loam (IIB3 of Batavia silt loam) for the 0-15 bar tension range	43
Fig. 3.8. Measurement of the hydraulic conductivity with the Bouwer double-tube method	47+48
Fig. 3.9. Cross section of double-tube method and plotting of experimental data	53
Fig. 3.10. Extrapolation procedure and graphical determination of $K_{sat}$ (after Baumgart)	53
Fig. 3.11. Installation of the crust-test apparatus	58
Fig. 3.12. Two types of tensiometers used to measure soil moisture tensions in the crust-test procedure	59
Fig. 3.13. Hydraulic conductivity (K) as a function of soil moisture tension, measured with the crust test	63
Fig. 3.14. Schematic diagram of the crust-test procedure	64
Fig. 3.15. Picture of crust-test measurement in operation	65
Fig. 3.16. Moisture content as a function of time during drainage of an initially saturated profile, to be used for calculations of the instantaneous-profile method	70
Fig. 3.17. Total potential as a function of depth and time during drainage of an initially saturated profile	70
Fig. 3.18. Diagrams illustrating possible flow patterns occurring when saturating soil for the instantaneous-profile method	71
Fig. 3.19. Soil moisture tensions as a function of time, starting at saturation, in major horizons of a Grays silt loam	75
Fig. 3.20. Picture of prepared plot for the instantaneous-profile method with first plastic sheet installed	75
Fig. 3.21. Pictures of prepared plots with second plastic sheet installed	77
Fig. 3.22. Large excavated column for running the instantaneous-profile method on sites where the regular procedure cannot be applied	77
Fig. 3.23. Schematic diagram showing appropriate locations of tensiometers in a soil profile with three horizons	80

	Page
Fig. 3.24. Installed vertical tensiometer with slurry forced out at the surface to form a cap over the hole	80
Fig. 3.25. Excavated tensiometer cup showing good contact between soil and porous cup and complete filling of the hole above the cup with slurry	82
Fig. 3.26. Tensiometer assemblage, showing the connection of the plastic tube with the manometer board and mercury cup through 1/8" flexible tubing	84
Fig. 3.27. Filling of the 1/8" flexible tubing, using a plastic syringe, which connects the water-filled plastic tube and porous cup and the mercury cup	85
Fig. 3.28. Standard curve for the neutron probe	90
Fig. 3.29. Hydraulic conductivity values determined with the instantaneous-profile method	90
Fig. 4.1. Moisture conditions in cores during steady saturated flow	101
Fig. 4.2. Hydraulic conductivity curves for the Ap and B2 of the Batavia silt loam	103
Fig. 4.3. Calculation tension profiles in the Ap and B2 of the Batavia silt loam at four flow rates	106
Fig. 4.4. Hydraulic conductivity curves for four major types of soil and curves expressing the hydraulic effects of impeding barriers of different resistances	109

## TABLES

	Page
Table 3.1. Laboratory retention data for core samples from a loam (IIB3 of the Batavia silt loam)	39
Table 3.2. Calculations of the double-tube method	54
Table 3.3. Soil moisture probe data for the instantaneous-profile method	92
Table 3.4. Calculation of soil moisture flux	93
Table 3.5. Calculation of hydraulic conductivity	94

## Chapter 1

## INTRODUCTION

This bulletin is the first in a series dealing with water movement and associated soil morphological features in soil pedons above the water table. Part of the material presented has appeared in scientific technical journals and other bulletins, but a need has been felt to rewrite the material so as to make it more accessible for the field soil scientist. Attention will be confined in this bulletin to the occurrence of water in the soil and to water movement in unsaturated soil up to moisture contents corresponding with moisture tensions of approximately 100 cm water. Flow rates become very low at higher tensions and methods of measurement become less reliable. Moreover, data presented herein were generated for a study on soil disposal of liquid waste where flow rates slower than 1 cm/day (0.4 inch/day = 0.24 gals/ft<sup>2</sup>/day) generally corresponding with moisture tensions higher than 100 cm water, are considered marginal. Application of flow theory to plant growth would require more data relating to water movement at much higher tensions, including water vapor dynamics, and to the osmotic potential. Much emphasis will be placed in this bulletin on a thorough description of methods, including details on where to obtain certain components and detailed descriptions and pictures of components and procedures. Chapter 2 was written on the assumption that methods by themselves are useless, and that results obtained should fit somehow into some conceptual scheme. For example, measurement of hydraulic conductivities in unsaturated soil is meaningless if the user does not understand basic principles of unsaturated flow. Unfortunately, this lack of understanding does occur, perhaps because the term "unsaturated" has a strong mathematical smell to it. Much emphasis is therefore also placed on an attempt to explain phenomena of unsaturated flow in a nonmathematical way. Parts of the material presented here have

already been used for other bulletins, for example, the limited edition (June 1973) of the Guide to the study of water movement in soil pedons above the water table, by J. Bouma (Geol. Nat. Hist. Surv.).

Chapter 2  
SOME BASIC PHYSICAL CHARACTERISTICS ASSOCIATED WITH  
WATER MOVEMENT THROUGH SOILS

Abstract

Soil pores in soil materials can be schematically represented by a series of capillary tubes with characteristic diameters. Such diagrams can be used to explain moisture retention and hydraulic conductivity phenomena of specific soils and differences among soils. Capillary forces increase as pore diameters decrease and water in unsaturated soil therefore occurs in the finer pores. Pore size distributions are typical in different soil materials and corresponding moisture retention and hydraulic conductivity ( $K$ ) curves therefore have characteristic shapes.

Several textbooks on soil physics have appeared in the last few years (Rose, 1966; Childs, 1969; Hillel, 1971; Baver, Gardner, and Gardner, 1973) and a discussion of the basic hydraulic properties of soils is central in each of them. This bulletin will not simply repeat what is already in the literature, but will attempt to present a simplified, preferably nonmathematical approach to the description of soil water flow phenomena. The following sections will discuss three aspects:

1. Soil as a three-phase system
2. Physical characterization of water in soil materials
3. Physical characterization of water movement in soil materials

2.1. Soil as a three-phase system

A soil sample consists of solid particles and voids, a fraction of which may be filled with liquid (Fig. 2.1). Assume that the weight of solid particles is  $M$ , that of the water is  $M_w$ , and the total weight

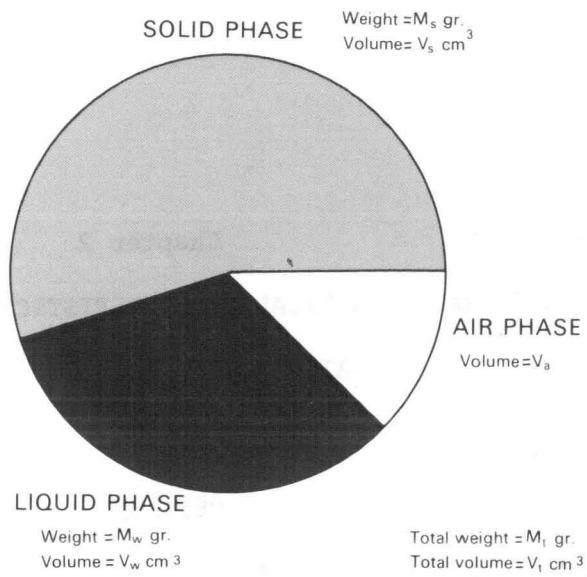


Fig. 2.1. Schematic diagram of the soil as a three-phase system.

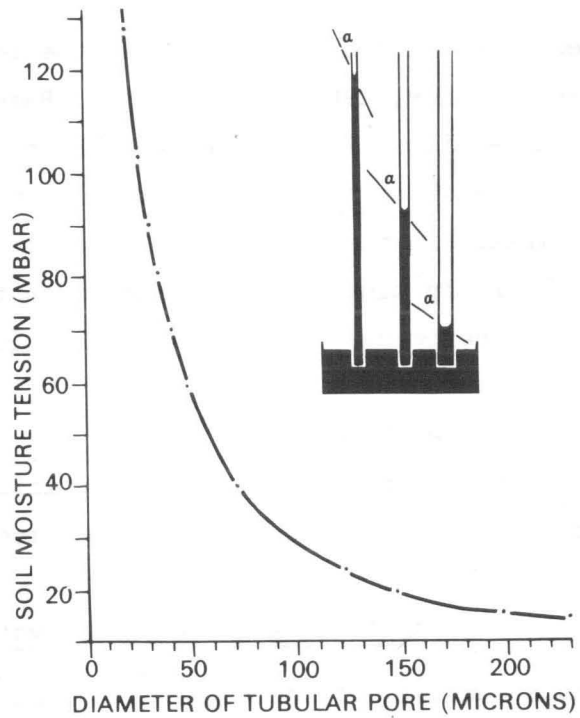


Fig. 2.2. Graphical expression of the relationship between tubular pore size and corresponding soil moisture tension.

is  $M_t$  grams and that the corresponding volumes are:  $V_s$ ,  $V_w$ , and  $V_t$ . Here the volume of pores filled with air ( $V_a$ ) has to be included also, which contributes negligibly to weight but constitutes an important part of the total soil volume. The volume of the pores is  $V_p = V_a + V_w$ . The following characteristics are most commonly distinguished (see also Hillel, 1971).

1. Particle density ( $\rho$ ), which is defined as

$$\rho = \frac{M_s}{V_s} (\text{gr/cm}^3).$$

This value is used to calculate the volume of a certain dry weight of soil. Values are usually about 2.6 - 2.7  $\text{gr/cm}^3$ .

2. Bulk density (B.D.) =  $\frac{M_s}{V_t} = \frac{M_s}{V_a + V_s + V_w}$  (based on dry soil weight).

This value is always smaller than  $\rho$ , because  $V_a$  and  $V_w$  are also included. Sometimes bulk density is determined, including water:

$$\text{B.D. (wet)} = \frac{M_s + M_w}{V_t}.$$

We will use B.D.(dry) exclusively because this is the value used to calculate  $\theta_v$  from  $\theta_w$  (see next section).

3. Porosity ( $p$ ) is defined as

$$p = \frac{V_p}{V_t} = \frac{V_p}{V_p + V_w + V_s}$$

and is normally expressed as a percentage. This value uses the total volume of all pores. Thus, no distinctions can be made between different types of pores with different functions in the soil fabric. Here, morphological analyses may be helpful.

## 2.2. Physical characterization of liquid in soil materials

### 2.2.1. Introduction

Soil wetness can be expressed in two ways:

$$\text{Percentage by weight: } \theta_w = \frac{100 \cdot M_v}{M_s}$$

where  $M_s$  is determined after drying the soil at 105°C, and

$$\text{Percentage by volume: } \theta_v = \frac{100 \cdot V_w}{V_s + V_a + V_w}$$

These two characteristics are interrelated as follows:

$$\theta_v = \frac{\theta_w \cdot \text{B.D. (dry)}}{\rho_w}$$

where  $\rho_w$  = density of water.

Soil volume is a relevant factor in several of the characteristics defined in Section 2.1. This volume may change when dry soil is wetted. Most soil materials containing clay will expand upon wetting, which is mainly due to the mineralogical and chemical nature of the clay minerals and to chemical characteristics of the wetting liquid. Thus, it follows that B.D. and  $\theta_v$  values will be affected. The Saran method has been developed to measure the amount of swelling at different moisture contents (see Sec. 2.3).

Soil wetness refers solely to the total amount of liquid in a soil sample. In addition, it is important to ascertain the distribution of water in the soil at different moisture contents and to understand the natural laws that govern it. As the moisture content of a soil sample decreases, water leaves the larger soil pores but remains in the finer ones. This can be explained by considering the basic phenomena of liquid surface tension and capillarity. Surface tension occurs typically at the interface of a liquid and a gas. Molecules

in the liquid attract each other from all sides. In the surface areas the molecules are attracted into the denser liquid phase by a force greater than the force attracting them into the gaseous phase. The resulting force draws the surface molecules downward, which results in a tendency for liquid to contract. Surface tension has the dimension of dynes/cm. Increased salt concentrations tend to increase the surface tension of water, whereas organic solubles like detergents tend to decrease it. Capillarity refers to the well-known phenomenon of the rise of water into a capillary tube inserted in water, due to its surface tension (Fig. 2.2.). The finer the tube, the higher the capillary rise and the greater the negative pressures below the water meniscus in the tube. This negative pressure ( $p$ ) is a result of the curvature of the meniscus, which increases as tubes become smaller, and can be calculated (in dynes/cm<sup>2</sup>) as follows (assuming that the contact angle between water and tube is zero):

$$p = \frac{2\delta}{r} \quad (1)$$

where  $\delta$  = surface tension of the water (dynes/cm), and  $r$  = radius of the capillary (cm). The height of capillary rise (cm) is

$$h = \frac{2\delta}{\rho g r}$$

where  $\rho$  = density of the water (gr/cm<sup>3</sup>) and  $g$  = gravitational constant (cm/sec<sup>2</sup>). Function (1) can be pictured as a continuous graph, relating capillary radius to corresponding pressure (Fig. 2.2.). The negative pressure below the meniscus in the water can thus be expressed in terms of the height of the column of water (cm) that can be "pulled" from a cup of water by the capillary tube. Fig. 2.2. illustrates that fine pores can exercise a larger "pull" than large pores. For example, a cylindrical pore radius of 100 microns corresponds with a relatively low capillary rise of 28 cm water (pressure below meniscus = -28 cm water), a radius of 30 microns with a relatively high rise of 103 cm (pressure -103 cm water). These figures imply that it takes a larger force (more energy) to remove water from a small pore than from a large one, which, in turn, implies that water in small pores has a higher level of energy than water in large pores.

To represent the porosity of a certain soil material as a bundle of capillaries with a characteristic size range is, of course, an unrealistic model as real pores in the soil have a much more complex configuration, with varying sizes and discontinuities. This representation can nevertheless be helpful to visualize the energy condition of water in soil and flow phenomena, particularly when soil moisture contents are relatively close to saturation.

A more scientific expression of the common observation that water flows downhill is one stating that water moves from points where it has a higher to points where it has a lower energy status. The energy status is referred to as the "water potential," a central concept in soil physics. A thorough and clear discussion of this concept has been given by Rose (1966) and only a brief summary will be presented in this bulletin. The total potential (or energy per-unit-quantity) of water ( $\psi$ ) is defined as the mechanical work required to transfer unit quantity (e.g., unit mass weight or volume) of water from a standard reference state ( $\psi = 0$ ) to the situation where the potential has the defined value. The total potential of water (which in the following will be expressed in terms of energy per unit of weight because this results in the simplest expression) is composed of several components, which will now be discussed separately.

### 2.2.2. Pressure potential (P)

Water in unsaturated soil occurs only in the finer pores and not in the larger ones because the total amount of available water is insufficient to fill all the pores while the smallest pores can "pull" strongest and thus get filled, thereby excluding the larger ones. The pressure in the water is then less than that of the local atmosphere (see Fig. 2.2.). As the available amount of water decreases, the diameter of water-filled pores decreases and the moisture pressure becomes more negative. It is convenient, but not necessary, to refer to a negative (less than atmospheric) pressure as a "tension" or "suction." A tension or suction of, for example, 30 cm water represents a soil water pressure of -30 cm water. The terms: "tension", "suction" and "pressure" are used throughout this bulletin to alert

the reader to errors that may occur if only a single expression is used and references are studied in which a different procedure is followed. For example: low "tensions" or "suctions" are equivalent to relatively high "pressures", whereas high "tensions" or "suctions" are equivalent to relatively low "pressures".

The pressure potential in unsaturated soil is referred to as the matric or capillary potential  $M$ . Expressed per-unit weight, the dimension of the matric potential becomes

$$P/\rho g = \frac{g \cdot \text{cm} \cdot \text{t}^{-2} \cdot \text{cm}^{-2}}{g \cdot \text{cm}^{-3} \cdot \text{cm} \cdot \text{t}^{-2}} = \text{cm}.$$

This notation is more convenient than others expressing the potential per-unit mass or volume (Rose, 1966).

The matric potential, which can be measured by tensiometry (discussed in Sec. 3.3 and 3.4) is the most important component of the pressure potential in most cases because soils above the water table are usually unsaturated. The soil water is at a pressure higher than one atmosphere if submerged beneath a free water surface. The potential associated with this has been called the submergence potential ( $S$ ) by Rose (1966). The submergence and matric potentials are mutually exclusive possibilities; if either of them is nonzero, the other must be zero. Finally, another possible cause of pressure change in soil water is the pneumatic potential ( $G$ ) which follows from a change in the pressure of the air adjacent to it. Gas pressures in natural soil will usually not be different from the atmospheric pressure. In summary:

$$P = M(\text{or } S) + G(\text{cm}).$$

### 2.2.3. Gravitational potential (Z)

The gravitational potential is due to the attraction of every body on the earth's surface toward the center of the earth by a gravitational force equal to the weight of the body. To raise this body against this attraction, work must be done, and this work is stored

by the raised body in the form of gravitational potential energy ( $Z$ ) which is determined at each point by the elevation of the point relative to some arbitrary reference level. Therefore

$$Z = M \cdot g \cdot z$$

where  $Z$  is the gravitational potential energy of a mass  $M$  of water at a height  $z$  above a reference and  $g$  = acceleration of gravity. This potential, expressed per-unit weight, becomes  $Z = z$  (in cm).

The osmotic potential ( $O$ ) describes the effect of solutes on the total potential of soil water and is important for the study of water movement into and through plant roots and for studies of evaporation and vapor movement. This component-potential will not be discussed further here, since it does not significantly affect the mass movement of water through soil between tensions of 0 and 100 cm, which is of most interest in the context of this review.

The total potential ( $\psi$ ) of soil water at any place in the soil is thus equal to the sum of the component-potentials  $P$ ,  $Z$ , and  $O$ . Theory of water flow uses the hydraulic potential (cm), which is the sum of pressure and gravitational potentials previously defined. It is common to refer to the hydraulic potential in terms of the "hydraulic head" ( $H$ ) (cm).

### 2.3. Moisture retention in soil

At zero tension all pores in the soil are filled with water (assuming that isolated air pockets do not exist). With increasing soil moisture tension, progressively smaller pores will empty as the capillary force they can exercise becomes insufficient to retain water against the tension applied. The rate of decrease of water content in a soil sample upon increasing tension is characteristic for each soil material, since it is a function of its pore-size distribution. This simplified discussion assumes that the soil-matrix is rigid and that water extraction does not result in soil shrinkage, thereby releasing water without creating empty voids. This is, however, an important process in clayey soils. Use of the Saran method can yield data on volume changes of soil upon desaturation.

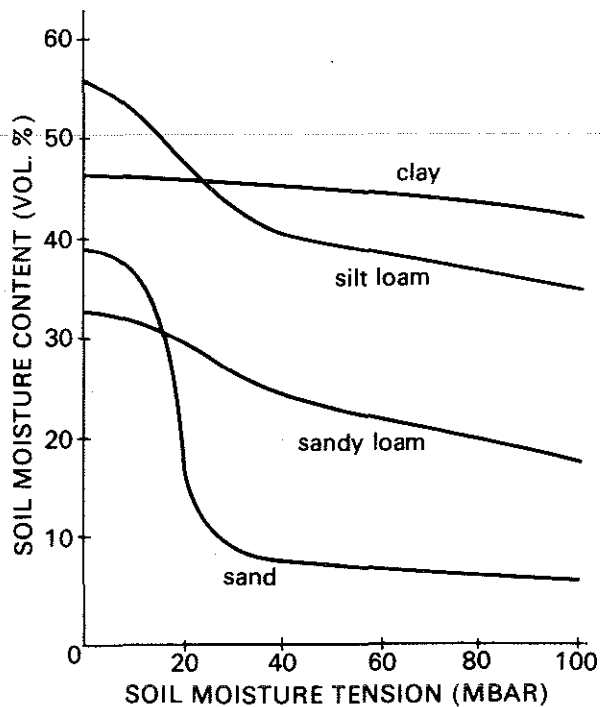


Fig. 2.3. Soil moisture retention curves, relating soil moisture content to moisture tension, for four different soil materials.

This method was introduced by Brasher, et al. (1966) in Soil Science 108 and consists basically of coating a dry soil aggregate with a plastic film. The coated aggregate swells upon wetting and the volume increase can be measured by weighing the aggregate both in air and under water. Calculation details associated with this procedure, including calculation of the coefficient of Linear Extensibility (COLE), were discussed in "Soil Absorption of Septic Tank Effluent" Inf. Circular 20 (1972), Geol. Nat. Hist. Surv., Univ. Ext., Madison, Wis. by J. Bouma, et al. (pages 42-44). This method sometimes offers excessive values for swelling due to use of relatively small samples. Use of larger cores, as discussed in this bulletin, may better resemble natural *in situ* conditions in soils with low or moderate swelling potential.

Techniques are available (Sec. 3.1.) to experimentally determine the so-called soil moisture retention curve, which gives the water content of the soil at any given tension (see Fig. 2.3).

Two techniques can be applied which will be discussed in more detail in Sec. 3.1: 1) air pressure is applied to a saturated soil sample placed on a porous disk with very small pores that remain water filled at all pressures applied. Pores in the soil sample that can exercise capillary forces larger than the applied air pressure remain filled with water, other larger pores with smaller capillary forces will lose their water, which will flow into and through the porous disk; 2) the saturated soil sample is placed on a porous disk as in 1), but this disk is inside a Buchner-type cup to which a tension can be applied by having the point of water outflow at a specific level below the plate (see Fig. 2.4, where application of a tension of 30 cm and 60 cm water is shown schematically).

Figure 2.3. shows moisture retention curves for a sand (C horizon of Plainfield loamy sand), a sandy loam (IIC of Batavia silt loam), a silt loam (B2 of Batavia silt loam), and a clay (B2 of Hibbing loam), demonstrating the effect of their different pore types, three of which schematically represented in Fig. 2.4. The sand has many relatively large pores that drain at relatively low tensions or pressures, whereas the more clayey soils release only a small volume of water because most of it is strongly absorbed in fine pores. The sandy loam has more coarse pores than the clay soil.

Moisture contents in a soil sample are different at corresponding tensions, depending on whether the moisture content was reached by removing water from an initially wetter sample (desorption) or by adding water to an initially drier sample (adsorption). This phenomenon is referred to as hysteresis, and can be illustrated using Fig. 2.5. The water-filled void (top) will drain (desorption) if the applied tension exceeds the relatively large capillary force corresponding with the smallest pore diameter ( $2r$ ) in the system. An air-filled void (bottom) will fill with water (adsorption) as soon as the relatively small capillary force, corresponding with the largest pore diameter ( $2R$ ), is sufficiently strong to pull the

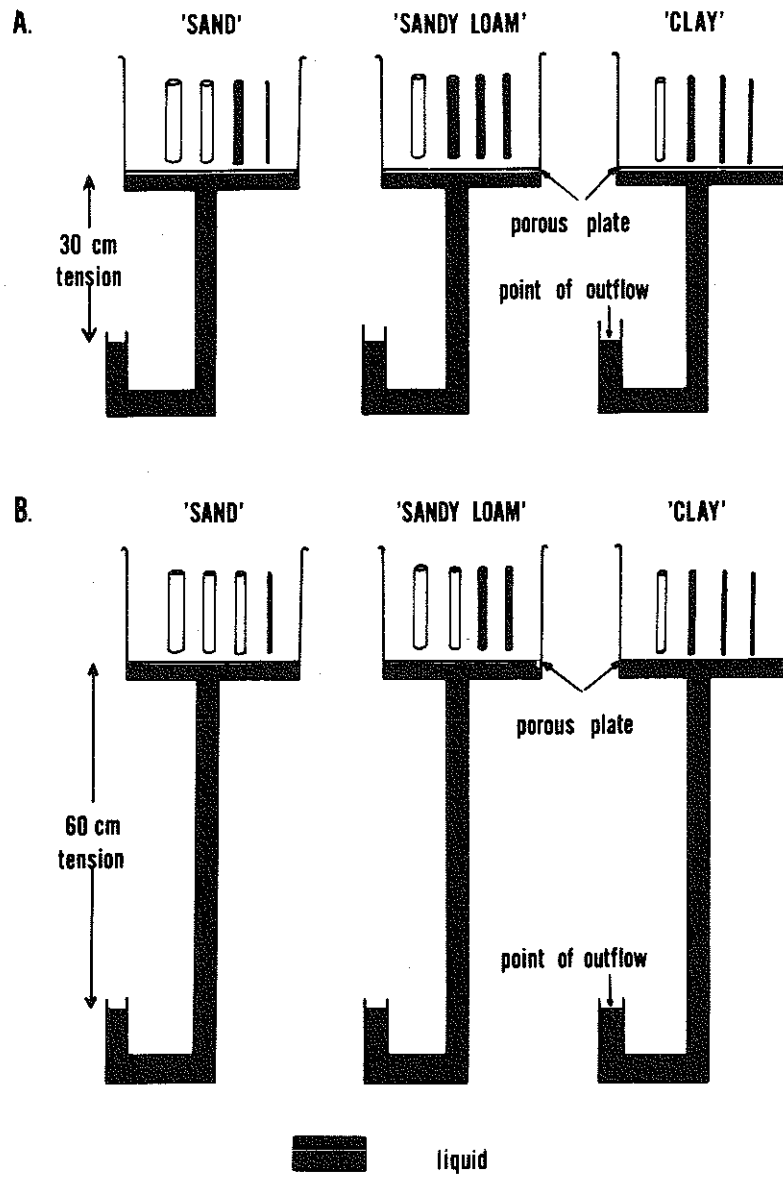
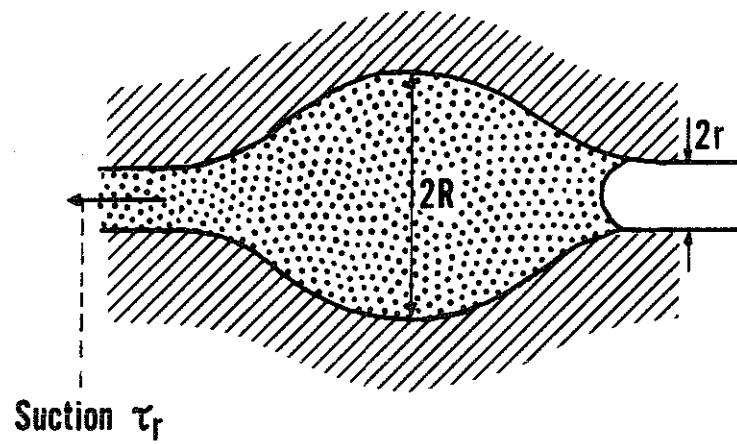
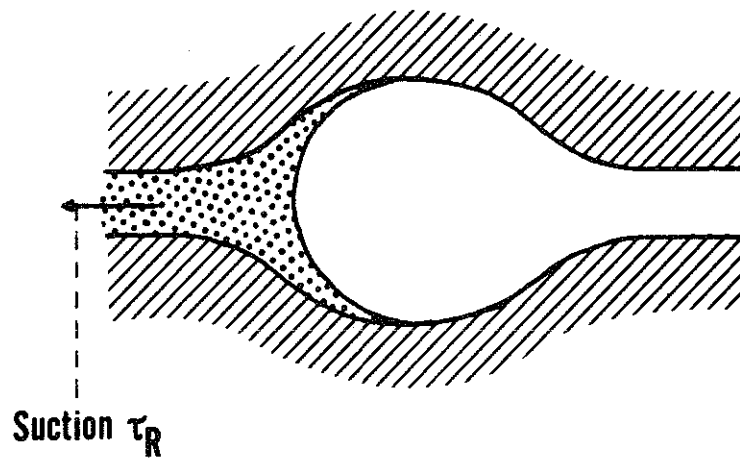


Fig. 2.4. Moisture retention in three schematic soil materials at tensions of 30 and 60 cm.



(a) DESORPTION



(b) ADSORPTION

Fig. 2.5. Cross section through an idealized void illustrating the hysteresis phenomenon.

water in. This comparison shows that the water content of a soil at a given soil moisture tension will be greater following desorption than following adsorption. It takes more energy (it is "more difficult") to get water out of the soil once it is in, than to get it back in, once it is out.

#### 2.4. Water movement in soil

The amount of flow through a soil sample is proportionate to the drop of the hydraulic head, as defined in Sec. 2.2.3, per-unit distance in the direction of flow. This, basically, is Darcy's law as stated for a one-dimensional, steady-state condition of flow:

$$V = K \cdot \frac{\Delta H}{L} \quad (2)$$

where  $V = \text{flux (cm} \cdot \text{t}^{-1}\text{)}$  of water [ $= Q/(A \cdot t)$ ], which is the volume ( $Q$ ) of water flowing through a cross-sectional area  $A$  per time  $t$ .  $K$  is the hydraulic conductivity ( $\text{cm} \cdot \text{t}^{-1}$ ) and  $\Delta H/L$  is the hydraulic gradient (dimensionless). This equation applies to both saturated and unsaturated soils for steady-state conditions of flow.

The flux  $V$  is measured across unit cross-sectional area. Part of that area (at least 40%) is occupied by the solid phase, which implies that the real velocity of flow in the soil pores is larger than  $V$ . If the soil would be composed of simple capillary tubes of specific sizes, calculations of the real flow velocity in those pores would be easy. However, pores vary in shape, width, and direction, and the actual flow velocity in the soil pores is variable. At best, therefore, one can refer to some "average" velocity ( $v'$ ) that can be calculated on the basis of the water-filled porosity at each tension.

$$v' = \frac{V}{\epsilon_w}$$

where  $\epsilon_w$  is the water-filled porosity, as derived from the moisture retention curve. At unit hydraulic gradient, we find

$$v' = \frac{K}{\epsilon_w}$$

Using these relationships, travel times at different moisture contents during steady-state flow can be estimated for different soil horizons if a K curve is available. According to equation (2), flow rates in a given soil material at a certain moisture content can vary considerably with varying hydraulic gradient. The hydraulic conductivity (K), however, is defined as the flux at unit gradient, and can, therefore, be considered a characteristic value for the soil. Methods for measuring hydraulic conductivity (K) in the field will be discussed in Chapter 3. These include: 1) the Bouwer double-tube method for measurement of K of saturated soil (Sec. 3.2); 2) the crust-test and the instantaneous-profile method for measuring K of unsaturated soil (Sec. 3.3 and 3.4).

K curves of different soil materials vary widely due to different pore size distributions in the soils.

Physical equations have been developed for certain types of pores to relate pore sizes to flow rates at a given hydraulic-head gradient (Childs, 1969). For a cylindrical pore of radius r, we find

$$Q/t = \frac{\pi g \rho r^4}{8\eta} \cdot \text{grad } \phi \quad (\text{Fig. 2.6}). \quad (3)$$

For a plane slit of width D, and unit length,

$$Q/t = \frac{g \rho D^3}{12\eta} \cdot \text{grad } \phi \quad (\text{Fig. 2.6}) \quad (4)$$

where  $Q/t$  = flow rate ( $\text{cm}^3/\text{cm}^2/\text{sec}$ ),  $\rho$  = density of water ( $\text{gr}/\text{cm}^3$ ),  $g$  = gravitational constant ( $\text{cm}^2/\text{sec}$ ),  $\eta$  = viscosity ( $\text{dyne}/\text{cm}$ ),  $\text{grad } \phi$  = hydraulic gradient ( $\text{cm}/\text{cm}$ ). These equations are graphically expressed in Fig. 2.7, demonstrating the significant effect of pore size on flow rates. For example, these graphs show that a tubular (cylindrical) pore with a diameter of 100 microns will conduct about  $2 \text{ cm}^3/\text{day}$  at a gradient of  $1 \text{ cm}/\text{cm}$  ( $8 \text{ cm}^3/\text{day}$  at a gradient of  $4 \text{ cm}/\text{cm}$ ). A plane slit with a width of 100 microns (and unit length) will conduct  $700 \text{ cm}^3/\text{day}$ . A plane slit with a length of 4 cm will conduct  $8400 \text{ cm}^3/\text{day}$  if the gradient is  $3 \text{ cm}/\text{cm}$  ( $12 \times 700 \text{ cm}^3/\text{day}$ ).

PLANAR VOID MODEL

TUBULAR VOID MODEL

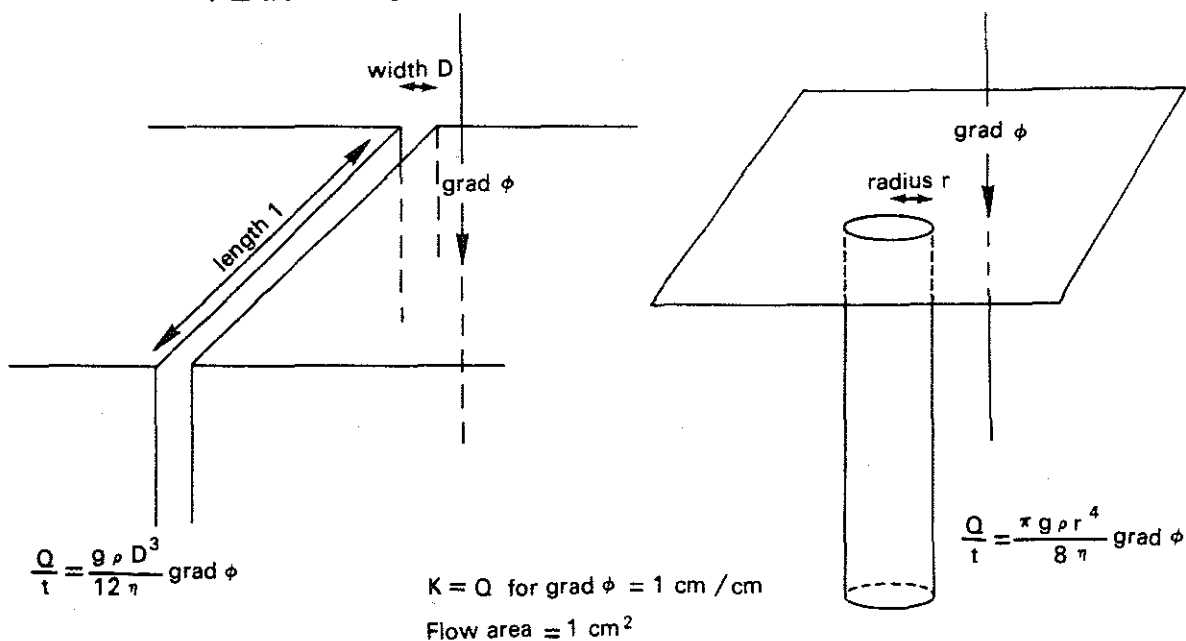


Fig. 2.6. Relationships between sizes of tubular and planar voids and flow rates at defined hydraulic gradients.

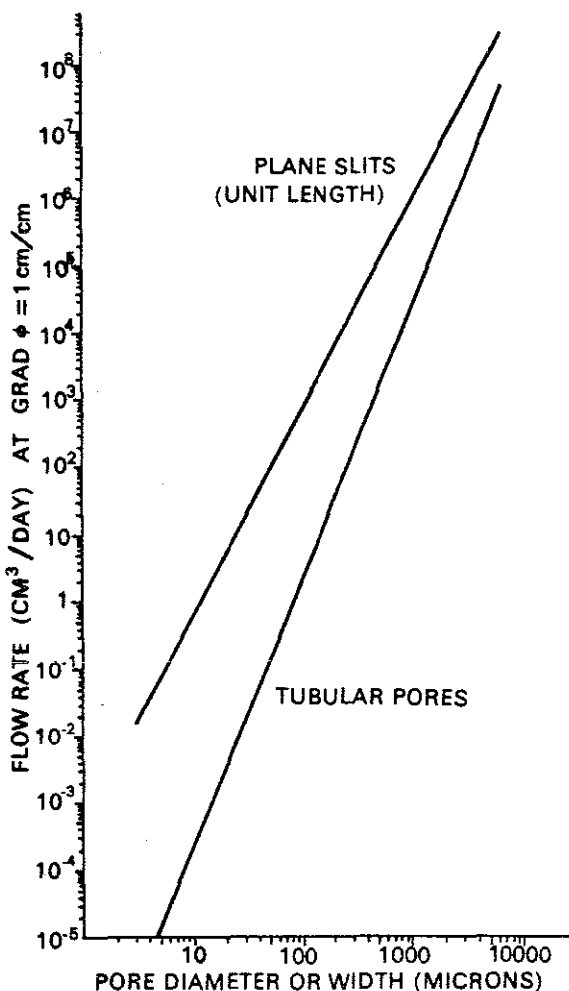


Fig. 2.7. Graphical expression of flow rates through tubular or planar voids as a function of pore size at a hydraulic gradient of 1 cm/cm.

The dominant effect of pore sizes on permeability is evident when comparing K values of a soil material that are measured at different degrees of saturation. Unsaturated soil below an infiltrating surface may have different causes, such as the occurrence of a physical barrier to flow at the surface of infiltration or an application rate which is lower than the saturated hydraulic conductivity. We may assume three different soil materials, with pore size distributions schematically represented in Fig. 2.8. The uppermost "soil" is coarse porous (like a sand) and the lowest one is fine porous (like a clay). Without any physical barrier (a "crust") on the soil surface and with a sufficient supply of water, all pores are filled and each will conduct water downward as a result of the potential gradient of 1 cm/cm, due to gravity. The larger pores will conduct much more water than the smaller ones. (See equation (3) and Figs. 2.6 and 2.7). Suppose a weak crust forms over the tops of the tubes. Pores will fill with water only if the capillary force they can exercise is strong enough to "pull" the water through the crust. The larger the pore, the smaller the capillary force that can be exercised (equation 1). Therefore, larger pores will empty first at increasing crust resistance, creating unsaturated soil and soil moisture tensions (Sec. 2.2) which, in turn, leads to a strong reduction in the hydraulic conductivity of the soil.

With no crusts present, similar processes can occur when the rate of application of water to the capillary system is reduced. With abundant supply, all pores are filled. As this supply (which is supposed to be divided evenly over the infiltrating pore system) is decreased, there is not enough water to keep all pores filled during the downward movement of the water. (It is assumed here that pores are horizontally interconnected.) Larger pores will empty first, as they conduct most liquid, while at the same time they exercise only relatively small capillary forces. *In this system a certain size of pore can be filled with water only if smaller pores have an insufficient capacity to conduct away the applied water.*

The degree of reduction in K upon desaturation and increasing soil moisture tension is thus characteristic for the pore size distribution. Coarse porous soils have a relatively high saturated hydraulic conductivity ( $K_{sat}$ ), but K drops strongly with increasing

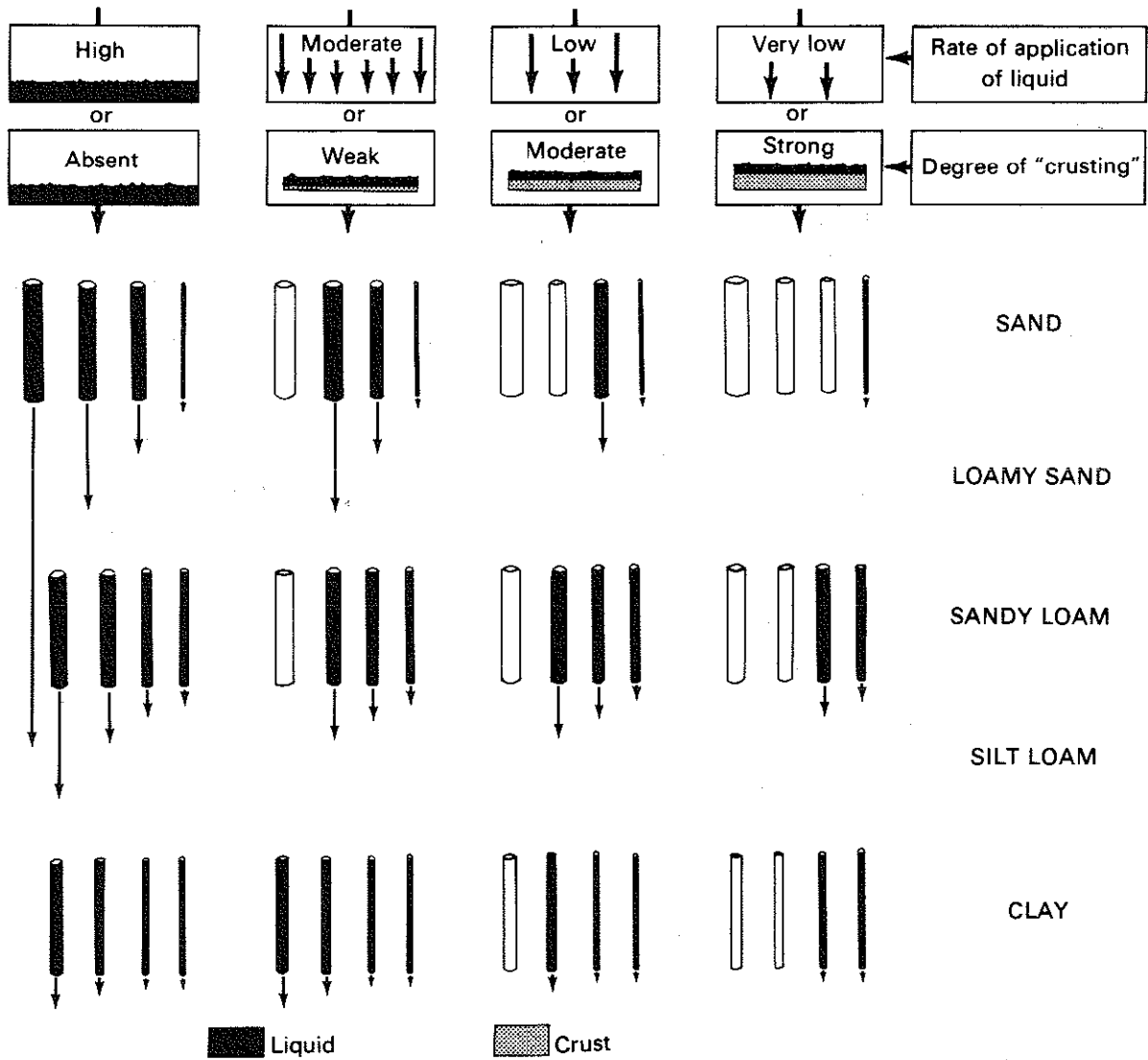


Fig. 2.8. Schematic diagram showing the effect of increasing the degree of crusting or decreasing the rate of application of liquid on the rate of percolation through three "soil materials."

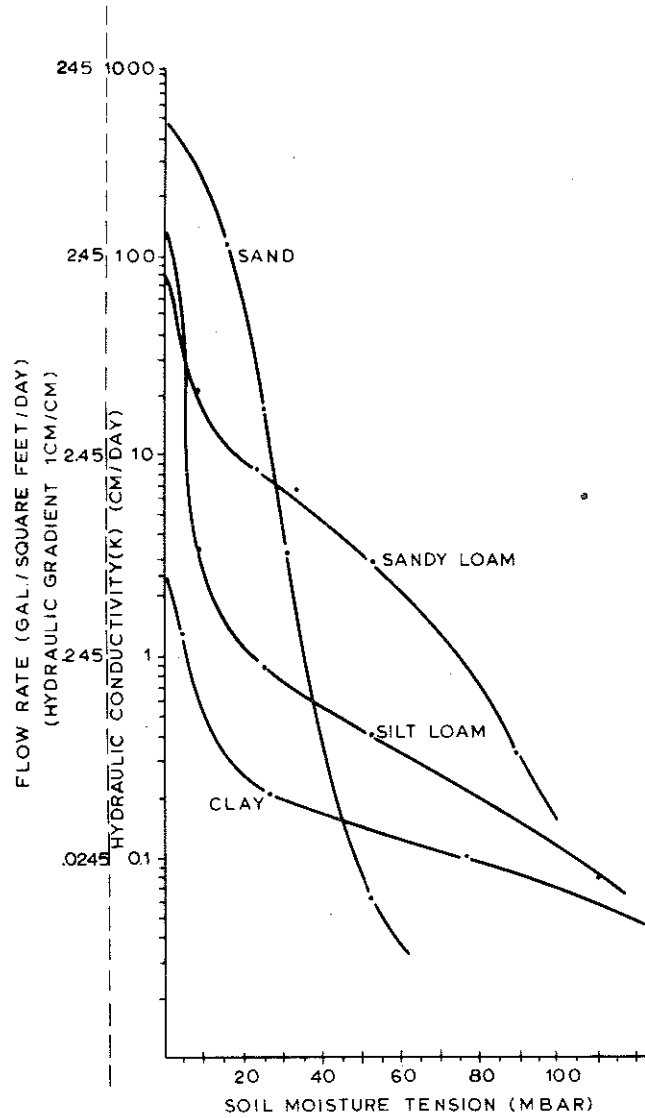


Fig. 2.9. Hydraulic conductivity (K) as a function of soil moisture tension measured *in situ* with the crust-test procedure.

tension. Fine porous soils have a relatively low  $K_{sat}$ , but  $K$  decreases more slowly upon increasing tension. Experimental curves, determined in the field with the crust test (in detail Sec. 3.3) show such patterns for natural soil. Fig. 2.9 shows curves for the sand C horizon of the Plainfield loamy sand, the sandy loam IIC horizon and the silt loam B2 horizon of the Batavia silt loam, and the clay B2 horizon of the Hibbing loam. Moisture retention curves for the same soil horizons were presented in Fig. 2.3. The curves for the pedal silt loam and clay horizons demonstrate the physical effect of the occurrence of relatively large cracks and root and worm channels. Soil structure inside the peds is very fine porous and these fine pores hardly contribute to flow. The large pores between peds and root and worm channels give relatively high  $K_{sat}$  values (140 cm/day for the silt loam), but these pores are not filled with water at low tensions and  $K$  values for these pedal soils drop therefore very strongly between saturation and 20 cm tension (1.5 cm/day for the silt loam). These phenomena, showing relationships between pore size distributions and  $K$ , are schematically represented in Fig. 2.8.

In summary, the higher the "crust" resistance or the lower the steady rate of application of water, the higher the soil moisture tension in the underlying soil and the lower the water content and the relevant hydraulic conductivity ( $K$ ). These characteristics apply to steady-state conditions in a one-dimensional system, where, at a hydraulic gradient of 1 cm/cm, flow rates are equal to the hydraulic conductivity. More complex flow systems, for example, those where the moisture content is changing with time, need more complex mathematical expressions which are beyond the scope of this bulletin.

#### 2.5. Literature cited

- Baver, L. D., W. H. Gardner, and W. R. Gardner. 1972. Soil physics. New York: John Wiley, 498 p.
- Childs, E. C. 1969. The physical basis of soil water phenomena. New York: John Wiley, 493 p.
- Hillel, D. I. 1971. Soil and water: physical principles and processes. New York: Academic Press, 288 p.
- Rose, C. W. 1966. Agricultural physics. Oxford: Pergamon Press.

## Chapter 3

## MEASUREMENTS AND CALCULATIONS

3.1. Measurement of soil moisture retention characteristics

by P. L. M. Veneman.

3.1.1. Introduction

Moisture retention characteristics of a soil can be described as the relationship between soil moisture content and the matric potential. Moisture content of a soil can be expressed by  $\theta_w$  or  $\theta_v$ , as discussed in Chapter 2.

Total soil potential is described by the equation:

$$\psi_T = \psi_m + \psi_g + \psi_p + \psi_o + \psi_b$$

in which  $\psi_T$  is the total soil potential and  $\psi_m$ ,  $\psi_g$ ,  $\psi_p$ ,  $\psi_o$ , and  $\psi_b$  are the matric, gravity, pressure, osmotic, and overburden potentials, respectively.

The soil moisture contents at different matric potentials can be measured in the laboratory with the aid of tension cups for low tensions and with pressure cell extractors for higher tensions.

A tension cup (see Fig. 3.1) is a cup with a sealed porous plate inside, on top of which the sample is placed. The pore sizes in the ceramic plate are such that the tensions at which measurements are made do not exceed the air-entry value of the pores. In other words, all pores of the ceramic plate will remain filled with water. In the neck of the cup, a water-filled flexible tube is inserted to vary the distance between the porous plate and the point of outflow of the tube. Hydraulic equilibrium is reached when no flow of water in the liquid phase occurs. Hydraulic equilibrium between soil water in a sample placed on the porous plate and the

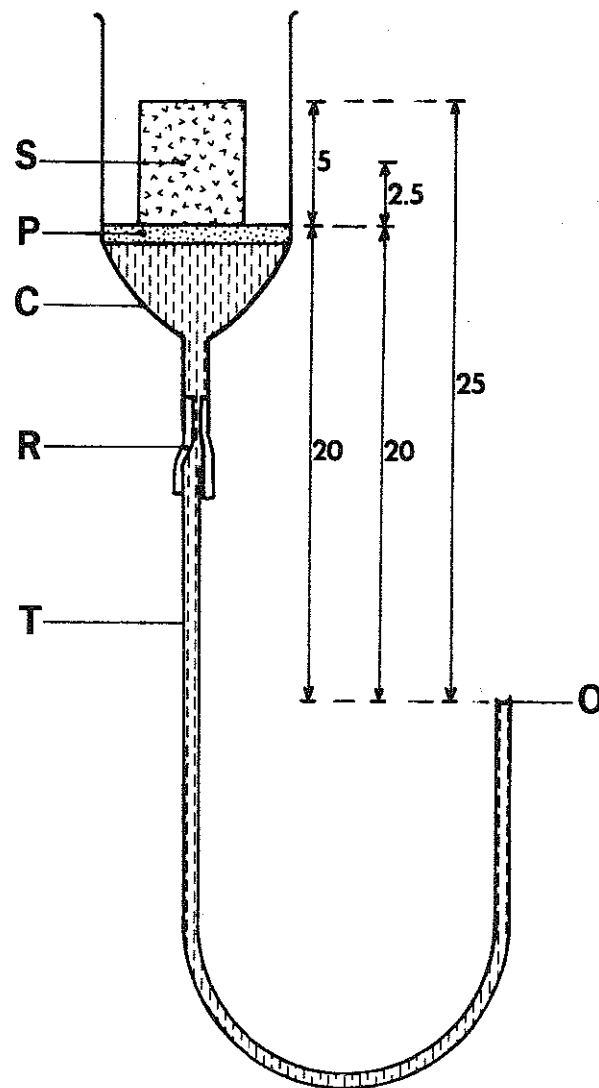


Fig. 3.1. Tension-cup assembly for moisture retention measurements between 0-100 mbar tension. C = cup, P = sealed porous ceramic plate, S = soil sample, O = point of outflow, R = thick-wall rubber, T = Tygon tubing (7/16" OD). Dimensions are in centimeters.

water under the plate occurs when their total potentials equalize:

$\psi_{\text{Total, sample}} = \psi_{\text{Total, cup}}$ . This equilibrium is described by:  
 $(\psi_g + \psi_m)_{\text{soil}} = (\psi_g + \psi_p)_{\text{cup}}$ . Because  $\psi_g$  has the same value at both sides of the equation, the matric potential in the soil sample is equal to the difference in hydraulic head (cm H<sub>2</sub>O) between the sample on top of the plate and the point of outflow of the flexible tube. Equilibrium conditions can be described for different levels in the core, assuming that the distance between the top of the porous plate and the point of outflow is 20 cm and the height of the core is 5 cm. The equilibrium situation in the soil near the porous disk then can be described with

$$\psi_g + \psi_m(\text{soil}) = \psi_g + \psi_p(\text{water});$$

$$20 \text{ cm} + \psi_m = 20 \text{ cm} - 20 \text{ cm}^1);$$

which gives

$$\underline{\psi_m = -20 \text{ cm H}_2\text{O}.$$

At the top of the core we find

$$\psi_g + \psi_m(\text{soil}) = \psi_g + \psi_p(\text{water});$$

$$25 \text{ cm} + \psi_m = 25 \text{ cm} - 25 \text{ cm};$$

which gives

$$\underline{\psi_m = -25 \text{ cm H}_2\text{O}^1).$$

In other words, matric potentials in the core on the ceramic plate at equilibrium change from -20 cm to -25 cm from bottom to top. The average measured matric potential in the condition illustrated in Fig. 3.1 is therefore -22.5 cm water. The difference in hydraulic head thus has to be measured from the center of the core to the point of outflow of the flexible tubing. The relative error involved with this procedure decreases with decreasing potential and as the height

---

<sup>1</sup> Point of outflow is reference level.

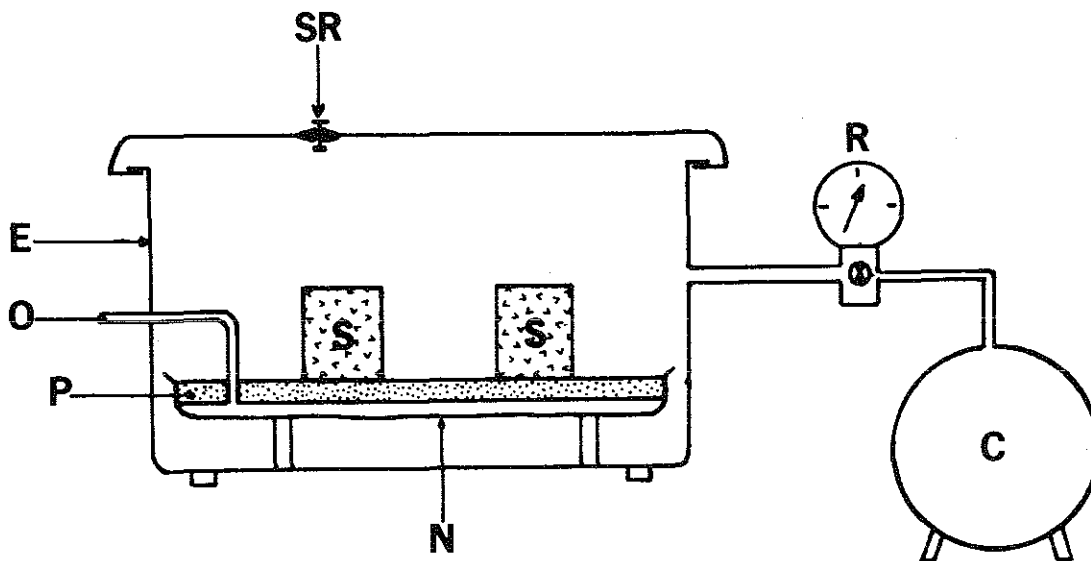


Fig. 3.2. Schematic laboratory setup of a pressure-plate extractor for moisture retention measurements in the range 0.1-15 bar. C = compressor, R = pressure regulator, E = extractor, P = porous ceramic plate, N = neoprene diaphragm, O = outflow tube, SR = safety pressure release valve, S = soil sample.

of the core decreases. For example, application of a water column of 20 cm ( $\psi_p = -22.5 \text{ cm H}_2\text{O}$ <sup>2</sup>) to a 5 cm high core gives a relative error of  $22.5 \pm 2.5$ , which is 11.1%. However, application of a 100 cm long water column ( $\psi_p = -102.5 \text{ cm H}_2\text{O}$ ) results in an error of only 2.4%. Use of large diameter cores with small height is preferable if detailed measurements are to be made at potentials close to saturation.

Instead of the matric potential, often the term tension is used. Tension is defined as being equal in magnitude but opposite in sign to the matric potential.

Different matric potentials may be applied with the tension-cup assembly by varying the distance between the porous plate and the point of outflow by lowering and raising this outflow point. The tension cup is suitable for moisture retention measurements in a range between 0-100 mbar tension.

Higher tensions generally are applied in a pressure-plate extractor (see Fig. 3.2). The saturated sample is placed under pressure on a porous plate or membrane, in which all pores are filled, and remain filled, with water. Soil water is allowed to flow to the outside of the extractor (via membrane and outflow tube), where atmospheric pressure exists. Hydraulic equilibrium of the pressure-plate extractor system can be described by:  $(\psi_g + \psi_m + \psi_p)_{\text{inside}} = \psi_{g,\text{outside}}$ . Because  $\psi_g$  has the same value outside as well as inside the extractor, the tension in a soil sample equals the applied pressure. The pressure-plate extractor is suitable to determine moisture contents corresponding with potentials up to -20 bar.

Soil water is considered the water that can be removed from the soil at a temperature of 105°C; e.g., crystalline water is not thought of as being soil water.

Section 3.1 describes procedures of soil sampling and estimation of moisture retention characteristics in the tension range 0-0.01 bar, 0.01-1 bar, and 1-20 bar, respectively.

---

<sup>2</sup>Hydraulic-head difference between center of core and the point of outflow.

### 3.1.2. Methods

3.1.2.1. *Sampling and pretreatment of samples.* Samples are obtained in the field with the double-cylinder, hammer-driven core sampler (Blake, 1965, p. 376) in small cylindrical rings (5 cm high with a diameter of 7.5 cm) with known volume. The soil samples are carefully cut off at the edges of the rings. One end of the ring is covered with cheesecloth taped into place with water-resistant tape.<sup>3</sup>

The soil in the ring is slowly saturated at a tension of approximately 20 cm for at least one day. This is achieved by placing the cores with the covered side down on moist sponges in a plastic container which has about 1 cm of water at the bottom. Then the soil is completely saturated by slowly raising the water level to the upper brim of the core. Saturation should be maintained for at least one day before making measurements.

#### 3.1.2.2. *Measurements in the 0-100 mbar range (desorption).*

The standard procedure for measuring moisture retention characteristics (desorption) was to place the saturated cores inside the tension cups (see Fig. 3.1), in which a thin layer of fine sand was placed to ensure good contact between the sample and the porous plate in the cup (Bouma, 1973). Different tensions were created at the level of the disk by lowering and raising the point of outflow of the water-filled flexible tube below the cup. When equilibrium was reached (the time at which the water stopped flowing) the sample was taken out and weighed, to estimate the water content at the applied tension. Problems in this method are 1) the repeated removal of the sample when measuring at succeeding tensions, which does not favor a good, continuous contact between sample and plate, and 2) the water loss through evaporation from the sample and the porous disk. A new volumetric method was developed in which a closed system is used, limiting water loss through evaporation and eliminating the repeated removal of the sample from the porous disk.

The revised tension-cup assembly (see Fig. 3.3) is basically the same setup as Fig. 3.1. It is described in Sec. 3.1.1 and was used by Vomocil (1965) for measuring porosity. Modifications are 1) the

<sup>3</sup>

ACME waterproof adhesive tape, ACME Cotton Products Co., Inc., Valley Stream, N.Y. 11582.

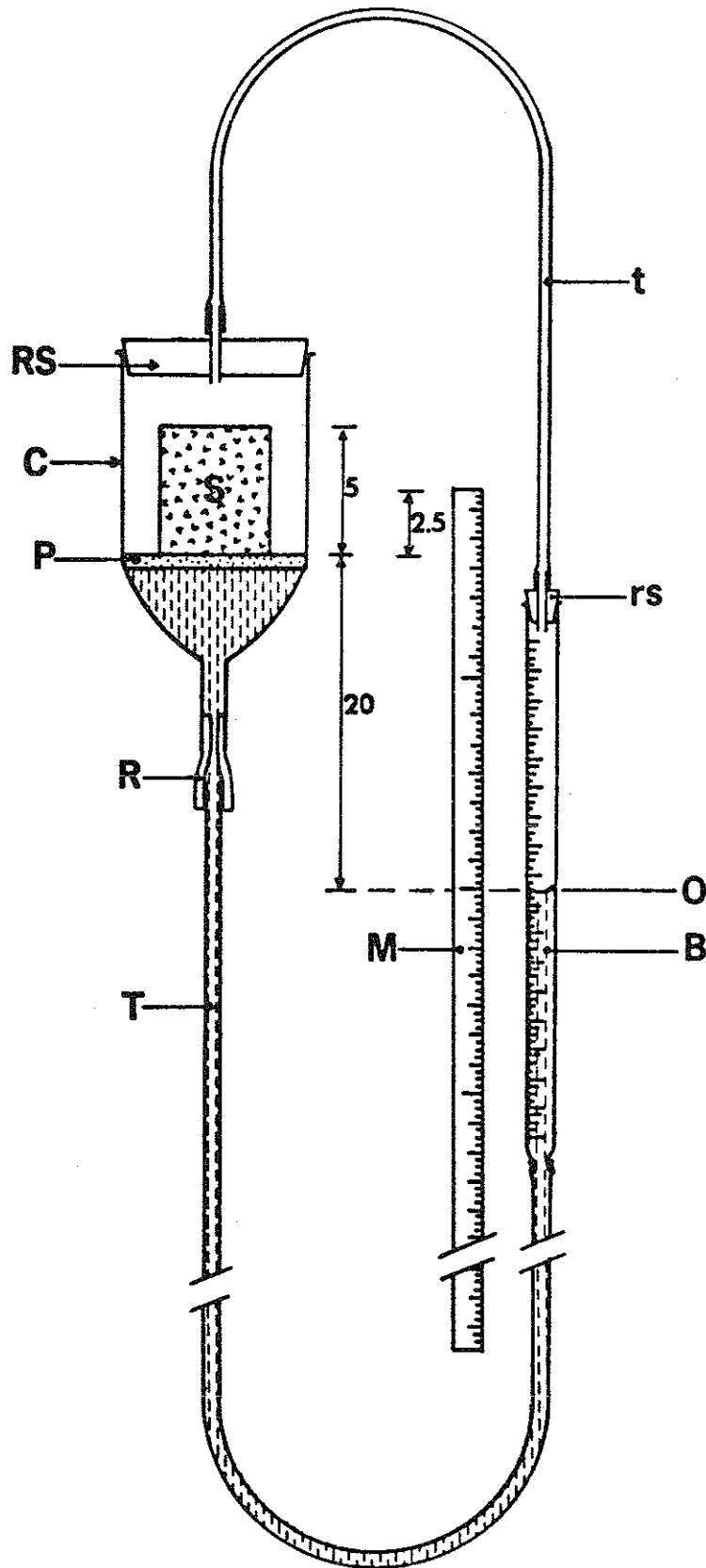


Fig. 3.3. Modified tension-cup assembly for volumetric moisture retention measurements between 0-100 mbar tension. C = cup, P = sealed porous ceramic plate, S = soil sample, B = adjustable burette, O = constant water level at equilibrium, M = meterstick, R = thick-wall rubber, T = Tygon tubing (7/16" OD), t = Tygon tubing (5/16" OD), RS = rubber stopper size #15, rs = rubber stopper size #00. Dimensions are in centimeters.

application of a graduated 50 ml adjustable burette for measuring outflow from the soil sample on the ceramic plate, 2) the application of a specified amount of very fine sand between core and plate to ensure good contact, and 3) an enclosing of the system with stoppers connected by flexible tubing to ensure lack of evaporation.

Estimation of the change in water content of the sample on the plate at different tensions is obtained by the change in volumetric reading of the burette when creating intermittent differences in hydraulic head (tensions) between the center of the core and the water level in the burette.

A laboratory setup for the modified tension-cup assembly is described first, followed by a description of the procedure for estimation of the retention characteristics between 0 and 100 mbar.

*Laboratory setup for the modified tension-cup assembly.* The laboratory setup is shown in Fig. 3.4. The tension-cup assemblies are essentially the same as described in Sec. 3.1.2.2 (Fig. 3.3). Following is a description of how the tension-cup assemblies and a manifold for mounting the sets to the wall are made. The length of the manifold depends on how many tension cups are desirable to use on the same manifold. Use of 4 cups per manifold (length 125 cm) gives a convenient unit. A board (height 120 cm) of 1.5 cm thick plywood is attached to the wall. Mounted on the board are blocks (10 x 10 cm) of 2 cm thick plywood, in which holes with a diameter of 2.5 cm are drilled. The hole is centered 5.5 cm from the board. The blocks are mounted 15 cm from the top edge of the board at distances of 20 cm from each other. Two-inch screw hooks are screwed into the board 10 cm straight above the sides of the blocks.

At least 2.5 cm from the blocks, two parallel wooden strips are mounted. The strips are 2.5 x 2 cm small beams from which the inside is V-shaped; that is the strip is 1.5 cm wide at the board and 2.5 cm wide 2 cm from the board. The strips are placed 7 cm apart on the board. Between these strips a block (2 cm thick) is fitted with dimensions slightly less than the strips allow, to ensure an easy vertical movement of the block. A hole is drilled in the block, in which a 2.5 cm long thumbscrew is fitted, which makes it possible to tighten the block between the strips. On the top of the block,

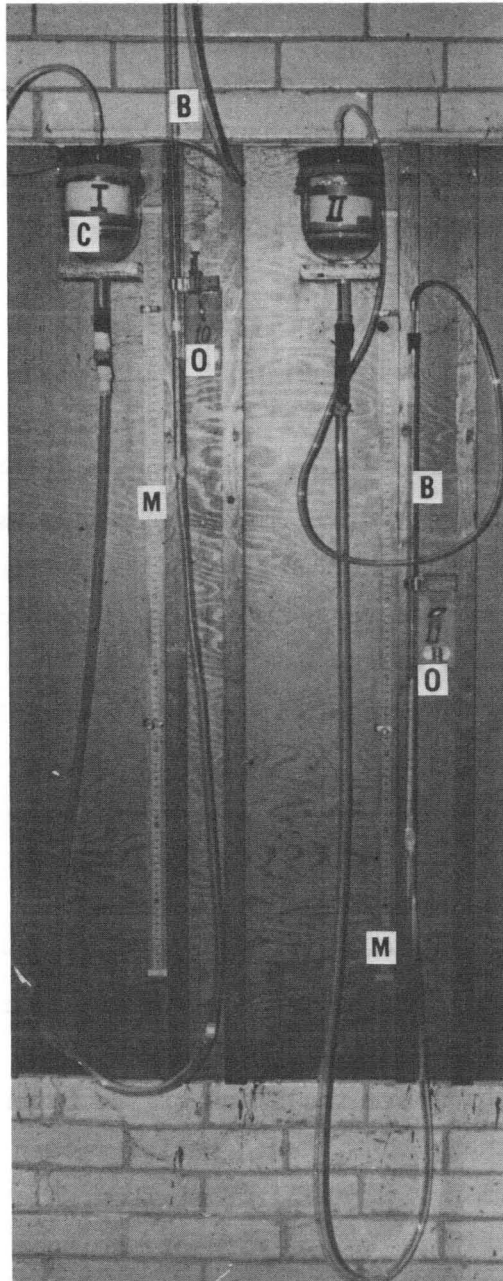


Fig. 3.4. Laboratory setup for low tension moisture retention measurements. C = cup, B = adjustable burette, M = meterstick, O = constant water level at equilibrium.

between the strips, another small block (2 x 4 x 6 cm) is mounted. On the left side of this block a finger clamp is mounted to hold the 50 ml pinchcock burette (see figure 3.4).

Two screw clamps (Hoffman type, open side, for 5/8" OD tubing) are mounted on the board at 2.5 cm on the left side of the wooden strips. The screw clamps are clamped on the board under a metal strip about 3 cm long with screw holes at the ends. The metal, and thus the screw clamp, is screwed onto the board. A meterstick, with the zero centimeter point up, is put between the clamps, which are tightened.

A 600 ml Büchner funnel with fritted disc (Pyrex H36060, ASTM 4-5.5 F) is placed in the 10 x 10 cm block and secured by a rubber band (Arco open ring, size 105) between the two screw hooks.

A piece of 190 cm Tygon tubing (7/16" OD, 5/6" ID) is glued over the bottom end of a 50 ml pinchcock burette with Silastic sealant.<sup>4</sup> The other end of the Tygon tubing is covered on the outside with Silastic sealant and then inserted for about 4 cm in a 10 cm piece of black thick-wall rubber (5/8" OD, 3/8" ID). The outside top of the black rubber is covered with Silastic sealant and then inserted in the neck of the Büchner funnel. Use plenty of sealant; an abundance can be wiped off, but insufficient sealant causes leaking, which in turn gives wrong measurements. Allow the sealant to dry for at least a week to assure maximum adhesive strength.

Small pieces of soft-glass tubing (5 mm OD) are placed in both ends of a piece of 120 cm Tygon tubing (5/16" OD, 3/16" ID). One end of the glass tubing is then inserted in a hole drilled in a #00 rubber stopper. A rubber stopper (#15) is halved in thickness and a hole is drilled in which the other 5 mm glass rod is fitted.

After the sealant has hardened for a sufficient length of time the system is carefully filled with distilled water. Be sure that all the air is driven out, since air bubbles adversely influence the measurements.

The #15 rubber stopper is placed on the Büchner funnel and the small #00 rubber stopper is put on top of the burette. The rubber stoppers may be slightly roughened with fine sandpaper if they slide back over the smooth glass edge.

<sup>4</sup>Silastic, 732 RTV, Dow Corning Corp.

*Procedure.* Exactly 20.0 gr of very fine sand (50-105 microns) is placed on the porous disk. Add distilled water until the water level is about 0.5 cm above the porous disk. Using a small spatula, spread the sand carefully over the disk area in order to drive out any air bubbles. Make sure there is more sand in the center of the disk than on the edges. Wash the spatula and the walls of the cup with distilled water to make sure that all the sand is on the porous disk.

The saturated soil core now is taken from the sponges, slightly dried with Kleenex and weighed to record the saturated weight ( $W_1$ ). The core then is lowered into the cup with the aid of a pair of crucible tongs. The core is carefully wiggled to ensure good contact between sample, sand, and porous disk. The cup is closed with the #15 rubber stopper. The zero point of the vertical meterstick is adjusted to a level corresponding with the center of the core (in general, at 2.5 cm above the surface of the porous disk, depending on the height of the core). The burette is lowered until the water meniscus is parallel with the lower side of the porous disk. Keep adjusting intermittently until all the water in the cup has disappeared and the level in the burette is constant (usually in about one hour). The burette now is almost filled with water. Empty the burette until a level between 50 and 45 ml is reached. Close the stopper on top of the burette and adjust the level until parallel with the underside of the porous disk. It is best to leave the sample overnight to ensure complete equilibrium. The next morning the level is again adjusted (if necessary) until constant with the bottom side of the porous disk. The level in the burette is recorded, after which the burette is lowered until the meniscus is at the 20 cm tension level, or whatever tension has to be applied. The burette is adjusted intermittently until the meniscus is constant at the 20 cm level (this usually takes about 2 days). The level is recorded and the burette is lowered until the next tension level to be applied. The process of adjusting until constant, etc., is repeated.

The difference between two burette readings at two intermittent tension levels implies a determination of the volume of water that left the core between the two applied potential levels.

The number of tension intervals at which the soil moisture contents are measured depends on the accuracy needed for the retention curve.

Intervals of 20 cm are recommended for accurate estimation of the wet end of the retention curve (0-100 cm tension). If a less accurate estimation is appropriate, measurements at 33, 66, and 100 cm tension may be sufficient.

If the burette is filled or is expected to flow over the zero gradation point of the burette, the following procedure is recommended: Record the constant meniscus level at a certain tension. Empty the burette until the 50 to 45 ml level and adjust the burette until the meniscus is again constant at the same tension. Record this level and follow the previously described general procedure.

After the 100 cm tension level has reached equilibrium, the meniscus position is recorded. The system then is opened by removing the #15 rubber stopper. The sample is lifted up with the crucible tongs and the bottom of the sample is carefully cleaned with a bristle tube brush. When the fine sand is removed from ring and cheesecloth the core is reweighed.

The 20.0 gr of very fine sand used to ensure good contact between the porous plate and core has its own moisture retention characteristics. In order to correct for water losses from the sand in the applied tension range, at least one sample with sand only should be run simultaneously with the soil samples. This blank must consist of 20.0 gr of the same very fine sand used under the soil samples.

After the cores have been weighed at the 100 cm tension level, they can be resaturated for moisture retention measurements in the 1/3 to 1 bar pressure-plate extractor (see Sec. 3.1.2.3) or they can be used for the bulk density estimation (see Sec. 3.1.2.5).

*3.1.2.3. Soil moisture retention measurements (desorption) in the 0.1-1 bar range.* Matric potentials between -0.1 to -1 bar are obtained in pressure extractors (pressure cooker type). Section 3.1.1 shows that a matric potential in a soil sample can be created by applying a certain pressure to the sample. Samples are placed on pressure-plate cells in a pressure chamber (see Fig. 3.2). The soil



Fig. 3.5. Laboratory setup of a series of pressure extractors for moisture retention measurements between 0.1-15 bar pressure. A = pressure extractor for measurements in the range 0.1-1 bar, B = extractor for measurements up till 15 bar pressure. C = compressor, P = pressure plate cell, M = manifold for pressure regulating for pressure extractors.

water of the sample is allowed to flow out under pressure through the saturated ceramic pressure-plate cell. A pressure-plate cell consists of a ceramic plate which is sealed on one side by a thin neoprene diaphragm. An internal screen keeps the diaphragm from close contact with the plate and provides a passage for the flow of water. An outlet stem running through the ceramic plate connects this passage with an outflow-tube assembly to the outside of the extractor. The pore size of the plate is such that 1) the air-entry value of the pores is not to be exceeded in the range of the applied pressures and 2) the pores are large enough to provide a reasonably fast time of reaching equilibrium (usually 2 to 3 days, depending on the kind of samples). The soil samples are placed on the ceramic pressure-plate cell. A certain pressure (corresponding with the desired matric potential) is applied and the samples are allowed to reach equilibrium. Depending on the desired accuracy of the retention curve in the 0.1 to 1 bar range, several pressures may be applied. For general purposes, measurements of moisture contents corresponding with pressures of 1/3 bar (4.4 psi) and 1 bar (14.5 psi) will be sufficient. A possible laboratory setup of a series of pressure extractors is shown in Fig. 3.5.

*Procedure.* Three types of soil material may be considered in the measurements: a) undisturbed ring samples, b) soil clods, and c) disturbed soil material.

In the case of undisturbed ring samples, the samples are saturated as described in Sec. 3.1.2.1. A thin layer of a 1:1 mixture of very fine sand (50-105  $\mu$ ) and silt (< 50  $\mu$ ) is spread over the ceramic pressure-plate cell, which has an excess of water standing on the plate. Locally, the sand and silt is sprinkled a little bit thicker. The saturated ring samples are placed on these thicker places and wiggled to ensure a good contact between ceramic plate and soil sample.

Soil clods (natural aggregates) are brought at a potential of about -20 mbar (see Sec. 3.1.2.1.). One side of the clods then is flattened with a knife and the clods are placed directly on the ceramic plate, smooth side down. The aggregates are wiggled to ensure good contact between plate and clods.

When moisture contents at certain matric potentials of the basic soil material are of interest, thus discarding the influence of natural pores and channels, soil material that have been passed through a 2 mm round-hole sieve can be used. About 25 gr of soil is placed in soil sample retaining rings.

Make sure that the sample in the rings represents the soil and that a good contact between plate and sample is established. The ring samples are leveled and allowed to stand at least 16 hours with an excess of water on the plate.

When moisture equilibrium studies are being run, it is desirable to keep the sample heights small in order to keep the time to reach equilibrium reasonable. The time required to reach equilibrium varies with the square of the sample height.

After the samples are placed on the ceramic plate and the outflow connections are checked, the lid of the extractor is closed and the desired pressure is applied. Once equilibrium is reached, which is characterized when no flow through the outside outflow tube is observed, the outflow tubes are clamped off and the pressure is released. The extractor is opened and the samples are transferred into aluminum weighing pans (weight  $W_2$ ) and weighed ( $W_3$ ). Samples, together with the weighing pans, are dried at  $105^{\circ}\text{C}$  for 24 hours and, after cooling in a desiccator, reweighed ( $W_4$ ).

The total weight ( $W_5$ ) of ring and sample is recorded after each run when undisturbed ring samples are used, and the cores are then returned onto the sand- and silt-covered saturated plate, which has water standing on it. Higher pressures than previously may be applied, and the whole process of reaching equilibrium, opening the extractor, etc., is repeated.

*3.1.2.4. Soil moisture measurements (desorption) at potentials lower than -1 bar.* Matric potentials lower than -1 bar can also be obtained in pressure extractors. The extractors are basically the same as the previous described pressure-cooker type. Differences are 1) the extractors are made stronger to withstand the higher pressures applied and 2) the ceramic pressure-plate cells have finer pores. Because higher pressures are applied than described in Secs. 3.1.2.2 and

3.1.2.3 only the extreme fine pores and channels of the soil are filled with water. It is sufficient to use disturbed soil material as described in Sec. 3.1.2.3 when measuring at pressures higher than 1 bar or pastes of the soil material when estimating moisture contents at pressures higher than 5 bar (72.6 psi). Pastes of the soil material (< 2 mm) can be made by adding water and mixing until the soil has a consistency just over the liquid limit. The pastes are carefully transferred into sample retaining rings placed on the ceramic pressure plate. Make sure that the pastes are homogeneous and that a good contact between plate and pastes is ensured. Procedures of handling and processing soil samples at pressures higher than 1 bar are as described in Sec. 3.1.2.3. For soil retention curves, a potential of -15 bar is considered the lower limit because this potential is generally accepted as the limit of plant growth. The Soilmoisture Equipment Company carries a complete line of soil moisture extractors suitable for measurements in the ranges of 0.1-1 bar, 1-5 bar, 5-15 bar, and higher.<sup>5</sup>

3.1.2.5. *Estimation of the bulk density of undisturbed ring samples.* The soil cores are placed, after the previous described estimation of water losses from the soil at different tensions, in tops or bottoms of glass petri dishes and put in the oven at 105°C. After at least 24 hours the cores are removed from the oven and allowed to cool in a desiccator. When cooled, each core is weighed ( $W_6$ ), after which the soil is removed from the ring and the combined weight of the clean ring, tape, and cheesecloth is recorded ( $W_7$ ).

The removed soil may be used for particle density estimation.

### 3.1.3. Calculations

3.1.3.1. *Calculations of moisture contents at corresponding tensions between 0-100 mbar.* The measured saturated moisture content is calculated as follows:

$$\theta_{w,sat} = \frac{W_1 - W_6}{W_6 - W_7} \times 100\% \quad (1)$$

<sup>5</sup>P.O. Box 30025, Santa Barbara, CA 93105.

where  $W_1$  is the total weight of the water saturated core, plus ring, tape, and cheesecloth;  $W_6$  is the total core weight after drying at  $105^\circ\text{C}$ ; and  $W_7$  is the weight of the ring, tape, and cheesecloth. The soil moisture content is now expressed in percentage on weight basis (gr/gr).

Multiplying the weight-based percentages by the bulk density (see Sec. 2.2.1) gives the more commonly used percentage by volume ( $\text{cm}^3/\text{cm}^3$ ).

Subsequent moisture contents at the different applied tensions can be calculated by subtracting the measured water-loss values from  $W_1$ , assuming that the specific gravity of water is  $1 \text{ gr}/\text{cm}^3$ . Corrections must be made for the loss of water from the sand. The accuracy of the procedure can be obtained by subtracting the core weight at 100 cm tension from the saturated weight ( $W_1$ ). This difference must more or less equalize the value obtained by subtracting the meniscus level at 100 cm tension from the level at 0 cm tension, minus the correction for the very fine sand. Laboratory data are supplied in Table 3.1. For an easier understanding of the calculation procedures an example is given.

Table 3.1. Laboratory retention data for core samples from a loam  
(IIB3 of the Batavia silt loam).

Saturated weight core ( $W_1$ ): 850.12 gr

Burette readings:

Applied tension	Reading core	Reading blank
0 cm $H_2O$	43.9 ml	22.6 ml
20 cm $H_2O$	37.3 ml	24.4 ml
40 cm $H_2O$	32.3 ml	22.3 ml
60 cm $H_2O$	29.3 ml	22.2 ml
80 cm $H_2O$	27.1 ml	21.8 ml
100 cm $H_2O$	24.9 ml	20.6 ml

Core weight at 100 cm tension: 832.20 gr

Core weight at 1/3 bar tension ( $W_5$ ): 818.71 gr

Core weight at 1 bar tension ( $W_5$ ): 817.41 gr

Core weight oven dry ( $W_6$ ): 747.94 gr

Weight ring, tape, and cheesecloth ( $W_7$ ): 337.29 gr

Dimensions ring: height, 5.7 cm, diameter, 7.6 cm

Particle density: 2.69 gr/cm<sup>3</sup>

Measurements at 5 bar pressure

weight aluminum weighing pan ( $W_2$ ): 1.36 gr

weight wet sample and weighing pan ( $W_3$ ): 20.21 gr

weight oven dry sample and weighing pan ( $W_4$ ): 17.46 gr

Measurements at 15 bar pressure

weight aluminum weighing pan ( $W_2$ ): 1.36 gr

weight wet sample and weighing pan ( $W_3$ ): 38.41 gr

weight oven dry sample and weighing pan ( $W_4$ ): 25.37 gr

*Example.* The water loss from the soil the very fine sand is calculated from the burette readings and is shown in columns II and III below.

I applied tension	II core	III Blank	IV corrected
20 cm H <sub>2</sub> O	6.6 ml	0.2 ml	6.4 ml
40 cm H <sub>2</sub> O	5.0 ml	0.1 ml	4.9 ml
60 cm H <sub>2</sub> O	3.0 ml	0.1 ml	2.9 ml
80 cm H <sub>2</sub> O	2.2 ml	0.4 ml	1.8 ml
100 cm H <sub>2</sub> O	2.2 ml	1.2 ml	1.0 ml
Total	19.0 ml	2.0 ml	17.0 ml

By subtracting the values for the fine sand from the water losses of the core, the corrected water-loss values can be obtained (column IV). Equation (1) gives the measured moisture content at saturation on a weight basis:

$$\theta_{w,sat} = \frac{W_1 - W_6}{W_6 - W_7} \times 100\%.$$

Substitution of the data supplied in Table 3.1 gives

$$\theta_{w,sat} = \frac{850.12 - 747.94}{747.94 - 337.29} \times 100\% = 24.88\%.$$

Multiplication of  $\theta_{w,sat}$  with the bulk density (see Sec. 2.2.1) gives  $\theta_{v,sat}$

$$\theta_{v,sat} = \theta_{w,sat} \times \text{BD} = 24.88 \times 1.59 = \underline{39.6\%}.$$

The moisture content at 20 cm H<sub>2</sub>O tension can be obtained by subtracting the corrected water-loss value (see Table 3.1) at 20 cm

tension from the saturated core weight ( $W_1$ ) and substitution of the obtained value in equation (1):

$$\begin{aligned} W_{1.20 \text{ cm}} &= W_1 - \text{corrected water-loss value at 20 cm tension} \\ &= 850.12 - 6.4 = 843.72 \text{ gr.} \end{aligned}$$

Substitution in equation (1) gives

$$\theta_{w, 20 \text{ cm}} = \frac{W_{1.20 \text{ cm}} - W_6}{W_6 - W_7} \times 100\% = 23.32\%$$

$$\theta_{v, 20 \text{ cm}} = 23.32 \times 1.59 = \underline{37.1\%}.$$

Calculation of the moisture contents at 40, 60, 80, and 100 cm are calculated similarly and are

$$\underline{\theta_{v, 40 \text{ cm}} = 35.2\%}$$

$$\underline{\theta_{v, 80 \text{ cm}} = 33.4\%}$$

$$\underline{\theta_{v, 60 \text{ cm}} = 34.1\%}$$

$$\underline{\theta_{v, 100 \text{ cm}} = 33.0\%}$$

The accuracy can be calculated as follows: Estimate the core weight at 100 cm tension, as indicated by burette readings:

$$W_1 - (\text{total corrected water loss}) = 850.12 - 17.0 = 833.12 \text{ gr.}$$

Table 3.1 gives the actual measured core weight at 100 cm tension (832.20 gr). The difference of 0.92 gr between actual and estimated core weight at 100 cm tension is due to the fact that the assumed zero burette level is not really the zero tension level for the core, but rather at 2.5 cm from the center of the core.

The difference of 0.92 gr  $H_2O$  can be substituted in equation (1):

$$\theta_{w, 0-100 \text{ cm}} = \frac{0.92}{W_2 - W_3} \times 100\% = 0.22\% \quad (1)$$

which, in turn, gives  $\theta_{v, 0-100 \text{ cm}} = 0.22 \times 1.59 = 0.4\%$ . A value of 0.4% is within the accuracy limits of the method and thus negligible.

The data may be presented in table form, but are more commonly shown on graphs. For lower tensions, moisture contents and their corresponding tensions may be presented as shown in Fig. 3.6. The complete retention curve is commonly presented as shown in Fig. 3.7 on 5 cycle semilogarithmic graph paper.

3.1.3.2. *Calculation of moisture contents at pressures between 0.1 and 15 bar.* The moisture contents for disturbed soil material and soil clods are calculated using the equation

$$\theta_w = \frac{W_3 - W_4}{W_4 - W_2} \times 100\% \quad (2)$$

in which  $W_2$  is the weight of the aluminum weighing pan,  $W_3$  is the weight of the moist soil plus weighing pan, and  $W_4$  is the weight of the soil and weighing pan after drying.  $\theta_w$  is expressed in percentage by weight (% gr/gr). In the case of the soil clod,  $\theta_w$  may be multiplied by the bulk density to get  $\theta_v$ , the more commonly used percentage by volume (%  $\text{cm}^3/\text{cm}^3$ ). When undisturbed ring samples are used, the moisture contents can be calculated using the equation

$$\theta_w = \frac{W_5 - W_6}{W_6 - W_7} \times 100\% \quad (3)$$

in which  $W_6$  is the total core weight after drying at  $105^\circ\text{C}$ ;  $W_7$  is the weight of the ring, tape, and cheesecloth; and  $W_5$  is the total weight of the core before drying. Multiplying the weight-based percentages by the bulk density gives  $\theta_v$ , the percentage by volume (%  $\text{cm}^3/\text{cm}^3$ ).

*Example.* Moisture contents of undisturbed ring samples at tensions of 1/3 and 1 bar are calculated with equation (3).

Substitution of the data supplied in Table 3.1 gives

$$\theta_{w, 1/3 \text{ bar}} = \frac{W_5 - W_6}{W_6 - W_7} \times 100\% = \frac{818.71 - 747.94}{747.94 - 337.29} \times 100\% = 17.23\%.$$



Fig. 3.6. Moisture retention curve for a loam (IIB3 of Batavia silt loam) for the 0-100 mbar tension range.

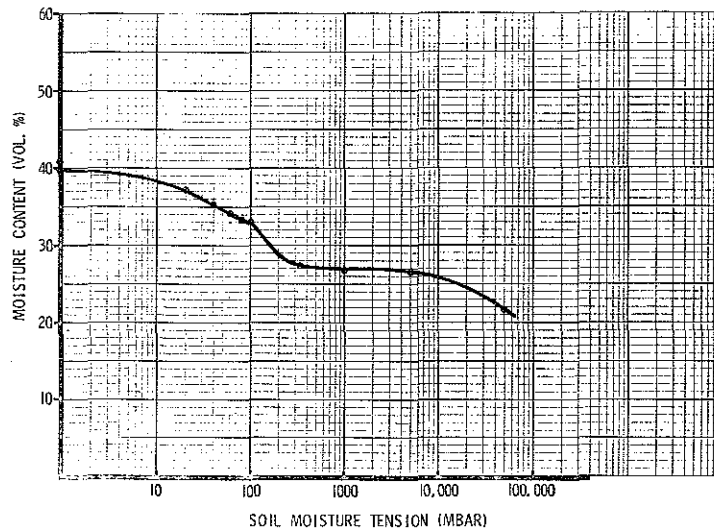


Fig. 3.7. Moisture retention curve for a loam (IIB3 of Batavia silt loam) for the 0-15 bar tension range.

The moisture content at 1/3 bar tension on a volume basis is then calculated as follows:

$$\theta_{v, 1/3 \text{ bar}} = \theta_{w, 1/3 \text{ bar}} \times \text{BD} = 17.23 \times 1.59 = 27.4\%$$

Estimation of the moisture content at 1 bar is similar to the 1/3 bar calculation and gives:  $\theta_{v, 1 \text{ bar}} = 26.9\%$ . Moisture contents at 5 and 15 bar are obtained with equation (2). Substitution of the data gives for 5 bar

$$\theta_{w, 5 \text{ bar}} = \frac{W_3 - W_4}{W_4 - W_2} \times 100\% = \frac{20.21 - 17.46}{17.46 - 1.36} \times 100\% = 26.6\%.$$

Substitution of the data for the 15 bar system gives:

$$\theta_{w, 15 \text{ bar}} = 21.8\%$$

### 3.1.3.3. Estimation of the calculated saturated moisture content.

If the particle density ( $\rho$ ) has been determined, the saturated moisture content may be obtained as follows:

$$\theta_{v, (\text{sat}, \text{calc})} = \left(1 - \frac{\text{BD}}{\rho}\right) \times 100\% \quad (4)$$

where BD is bulk density and  $\rho$  is particle density.  $\theta_{v, (\text{sat}, \text{calc})}$  is often called the porosity and refers to the maximum space available for soil water and soil air in a particular soil. The calculated saturated moisture content is very often somewhat higher than the measured moisture content (see Sec. 3.1.3.1) due to air-inclusions during saturation. A very slow saturation (see Sec. 3.1.2.1) often prevents a too large discrepancy between calculated and measured saturated moisture content.

*Example.* Substitution of the data from Table 3.1 in equation (4) gives

$$\theta_{v, (\text{sat}, \text{calc})} = \left(1 - \frac{\text{BD}}{\rho}\right) \times 100\% = \left(1 - \frac{1.59}{2.59}\right) \times 100\% = 40.9\%.$$

Comparison of  $\theta_v$ , (sat, calc) with  $\theta_v$ , (sat) = 39.6% (see Sec. 3.1.3.1) shows a good agreement.

3.1.3.4. *Bulk density.* Bulk density is calculated as follows:

$$BD = \frac{W_6 - W_7}{\pi r^2 \times h} \quad (5)$$

where  $W_6$  is the total core weight after drying at 105°C;  $W_7$  is the weight of the ring, tape, and cheesecloth;  $r$  is the radius of the sampling ring; and  $h$  is the height of the sampling ring. The bulk density is expressed in  $\text{gr/cm}^3$  and refers to the weight of soil mass per unit volume.

*Example.* Substitution of the data from Table 3.1 in equation (5) gives

$$BD = \frac{W_6 - W_7}{\pi r^2 \times h} = \frac{747.94 - 337.39}{3.14(1/2 \times 7.6)^2 \times 5.7} = 1.59 \text{ gr/cm}^3.$$

Bulk-density values usually range from about 1.85  $\text{gr/cm}^3$  for densely packed soils to 1.20  $\text{gr/cm}^3$  for organic soils.

#### 3.1.4. Literature cited

- Blake, G. R. 1965. Particle density. Amer. Soc. Agron. Monograph 9:371-373.
- Bouma, J. 1973. Guide to the study of water movement in soil pedons above the water table. Geol. and Nat. Hist. Surv., Univ. of Wis., Madison, Wisconsin.
- Richards, L. A. 1965. Physical condition of water in soil. Amer. Soc. Agron. Monograph 9:128-152.
- Richards, S. J. 1965. Soil suction measurements with tensiometers. Amer. Soc. Agron. Monograph 9:153-163.
- Vomocil, J. A. 1965. Porosity. Amer. Soc. Agron. Monograph 9:299-314.

3.2. In situ measurement of saturated hydraulic conductivity:  
the Bouwer double-tube method

3.2.1. Introduction

This method is a standard procedure for measuring hydraulic conductivity of saturated soil, well above the groundwater table (Boersma, 1965 *in* Methods of soil analysis, Part 1, p. 234). With the double-tube method, two concentric tubes are inserted into an auger hole and covered by a lid with a standpipe for each tube (Fig. 3.9). Water levels are maintained at the top of the standpipes to create a zone of positive water pressures in the soil below the bottom of the hole. The hydraulic conductivity (K) of this zone is evaluated from the reduction in the rate of flow from the inner tube into the soil when the water pressure inside the inner tube is allowed to become less than that in the outer tube. This is done by stopping the water supply to the inner tube (closing valve a) and measuring the rate of fall of the water level in the standpipe on the inner tube while keeping the standpipe on the outer tube full to the top. This rate of fall is less than that obtained in a subsequent measurement in which the water level in the outer tube standpipe is allowed to fall at the same rate (by manipulating valve b) as that in the inner tube standpipe. The difference between the two rates of fall is the basis of the calculation of K.

3.2.2. Procedures

The different stages of the method will now be explained in more detail with reference to the numbers on the included pictures (Fig. 3.8). A large auger, with a diameter of 10 inches (1) is used to make a cylindrical hole (2) to the desired depth. A bottom scraper (3) is used to obtain a flat surface at the bottom. Loose soil is removed from the hole. Before using the hole cleaner (4) the outer tube (8) is forced down in the hole. It is often necessary to widen the hole locally to make this possible. This is done with a scraper not pictured here. When the outer tube is found to fit well it is temporarily removed again. The hole cleaner (4) is gently forced into the soil at the bottom of the hole. If the soil is dry, premoistening of it may be necessary. The thin metal fins of the hole cleaner should penetrate

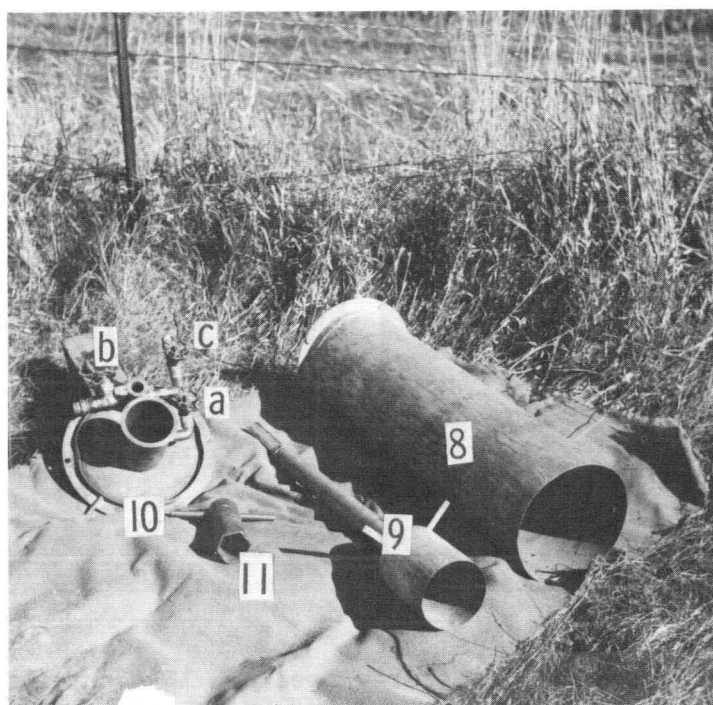
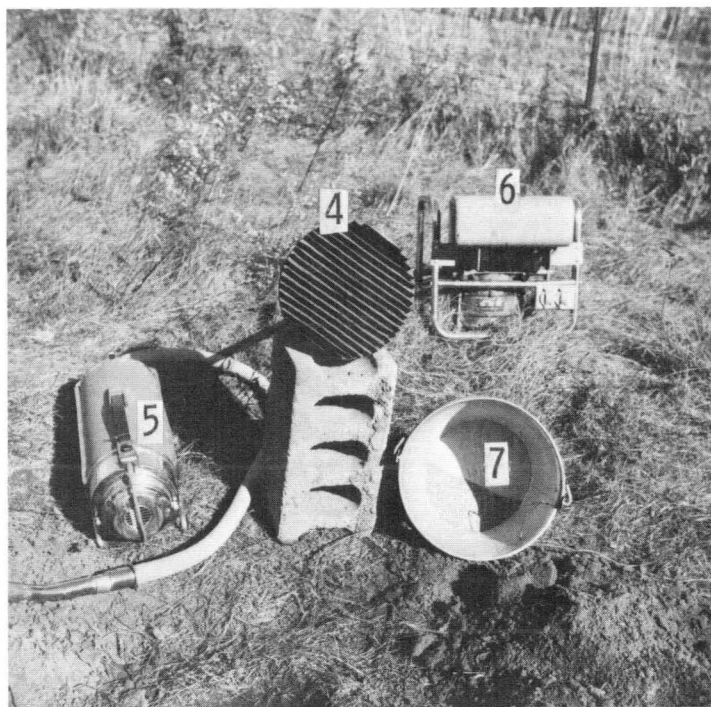
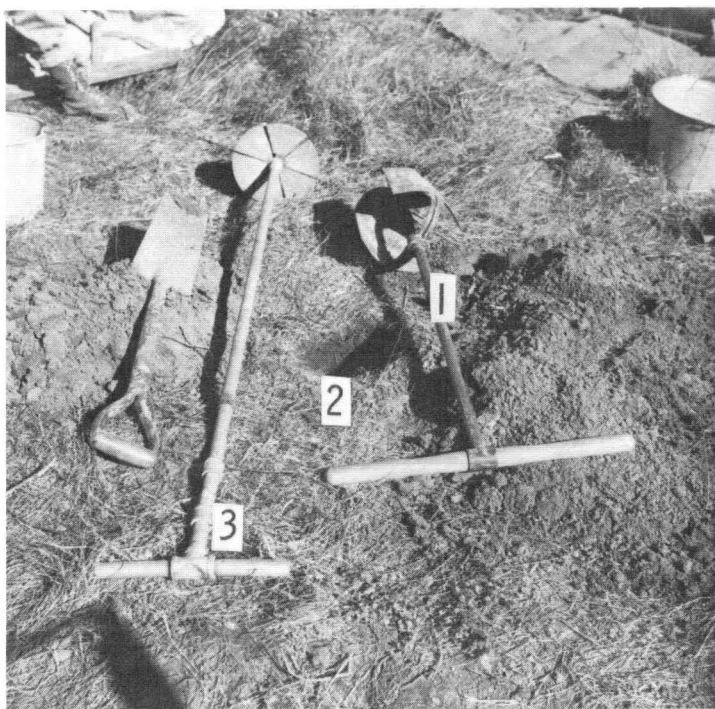


Fig. 3.8. Measurement of the hydraulic conductivity with the Bower double-tube apparatus. 1 = soil auger, 2 = test hole, 3 = bottom scraper, 4 = hole cleaner, 5 = vacuum cleaner, 6 = generator, 7 = bucket with sand, 8 = outer tube, 9 = inner tube, 10 = top plate, 11 = wrench to attach top plate to inner tube.

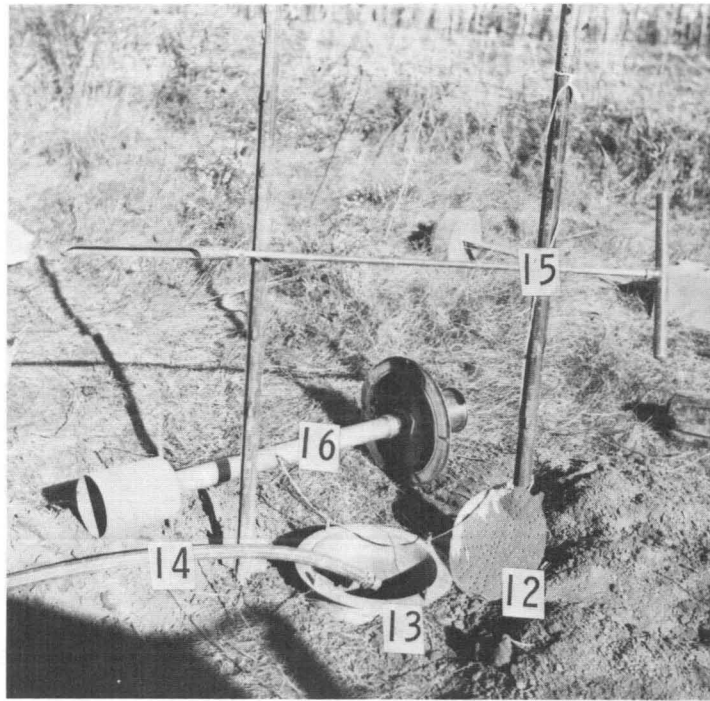


Fig. 3.8. continued. 12 = energy breaker, 13 = outer tube in test hole, 14 = water hose, 15 = reference rod, 16 = assembled inner tube and top plate, 17 = OTS-full measurement, 18 = equal level measurement.

about 2 cm into the soil. Next, the hole cleaner is pulled out of the hole with an upward corkscrew movement that prevents smearing the soil surface, as would happen if the cleaner were turned without being pulled up at the same time. The detached mass of soil is upended for observation of the natural, broken surface of soil held between the fins. A corresponding natural, broken-soil surface is left at the bottom of the hole.

The outer tube (8) is forced down as evenly as possible about 5 cm into the soil at the bottom of the hole (13). This may require careful blows of a sledgehammer on a wooden crosspiece. Control of the distance is by measurement from a fixed horizontal reference rod (15). Loose soil fragments are removed from the bottom of the hole with a vacuum cleaner (5) powered by a portable electric generator (6). This bottom surface is then covered with a thin (1 cm) layer of coarse sand (7), on top of which a baffle is laid (12), with attached strings looped over the top of the tube. The outer tube is slowly filled with water (14). The energy breaker and sand layer protect the natural soil surface from erosion by the turbulent water. Then the inner tube (9) and the top plate (10), which has two basal standpipes leading to the inner tube and outer tube, respectively, and three valves (a, b and c)<sup>6</sup> are assembled into one fixed unit (16). A special wrench (11) is used to tighten a ring with a washer inside the inner well of the top plate (10). This binds the inner tube to its standpipe.

The distance of the bottom of the inner tube from the top plate should be so spaced that the bottom of the inner tube will be only a few cm above the sand when the assembly (16) is set into and attached to the outer tube. The hose (14) is then attached adjacent

---

<sup>6</sup>

The functions of the three valves are explained as follows: Starting with the valves closed, they can be manipulated in the course of the experiment to control the flow of water. Opening valve c allows water to flow into the outer tube basal standpipe, which is situated between valve c and valve b. Opening valve b bleeds water from the outer tube standpipe, which can be isolated from the water supply by closing valve c, and from the inner tube standpipe by closing valve a.

to valve c on the top plate (1). When the outer tube is brim full and water starts streaming between the loose top plate and the upper rim of the outer tube, the bolts are tightly screwed, closing down on the gasket. This procedure flushes out air, avoiding its entrapment on the underside of the top plate. Valve a is now opened to admit water to the inner tube basal standpipe. Then the connection between the top plate and the inner tube is loosened again. The inner tube slides downwards to the soil surface. The sliding distance should not exceed a few cm, in order to avoid turbulence that might disturb the soil surface. The inner tube is pushed down about 2 cm into the soil. In the meantime, water is continuously entering the system in such a quantity as to keep both tubes filled all the time. Overflow water that spills onto the top plate from the outer tube basal standpipe (near valve b) is drained off the top plate through a brass tube and hose extension into a bucket nearby. The depth of penetration of the inner tube is accurately measured, using the reference level (15). Next, the plastic standpipes for the inner and outer tubes are fastened to the two openings in the top plate. For slow infiltrations a smaller inner tube standpipe (ITS) is used ( $R = 0.6$  cm); for larger infiltrations a larger one is used ( $R = 1.85$  cm). Valve c is then opened enough to ensure a slight overflow at the top of the standpipes.

Two types of readings are made, usually starting one hour after application of the water: 1) The outer tube standpipe (OTS) full measurement (17). Valve a is kept closed, as is, of course, valve b. 2) The equal-level measurement (18). Valve a is closed and valve b is opened, but with obstruction by the fingers at the open end of the pipe, in such a way as to synchronize the drop of the water level in the OTS with that in the ITS. Eight stopwatches are started simultaneously at the beginning of a reading. One watch at a time is stopped as the water level in the ITS reaches a mark on the tube. The marks are spaced 5 cm apart, over a total distance of 60 cm. Elapsed time is recorded in tenths of a second. The readings over a distance of 40 cm should yield a difference of at least 6 seconds between two measurements, that is, between one OTS-full measurement

and the average value of the preceeding and the next equal-level measurements. If the time difference is less than 6 seconds, measurement should be extended to, say, 60 cm and readings made within the lower 40 cm interval thereof. The measurements are to be repeated at regular time intervals until the ratio  $\Delta t/t^2$  eq. level becomes constant (Bouwer, 1962). Here,  $\Delta t$  is the time difference between the OTS-full and the average value of equal-level measurements before and after this OTS-full measurement.

A constant ratio may occur after a period varying from one to four hours. The constant ratio is supposed to indicate sufficient saturation of the soil below the tubes. The intervals between successive measurements should be approximately ten times as long as the time required for each separate reading, or 15 minutes (Baumgart, 1967), whichever is shorter, to allow reestablishment of equilibrium. The two final curves obtained (Fig. 3.9) differ because of flow of water from the outer tube into the inner during the OTS-full measurement.

K is calculated according to the equation

$$K = [R_v^2 / (F_f \cdot R_c)] \cdot (\Delta H / \int H dt)$$

where: H = difference in hydraulic head H between both curves at any time t

$\int H dt$  = surface below OTS curve (to be determined graphically)

$F_f$  = flow factor, to be read from tables, expressing the influences of the dimensions of the system and the depth D to a layer with much smaller or higher permeability. When D is several times larger than the diameter of the inner tube ( $R_c$ ), a general set of curves may be used to estimate  $F_f$  (see Bouwer, 1961). The flow factor deviates usually only slightly from unity.

A more convenient method of calculation was suggested by Bouwer (1962) using the ratio  $2\Delta t/t^2$  eq. level instead of  $\Delta H / \int H dt$ .

The ratios obtained for the final set of data are extrapolated to zero to correct for the decrease in infiltration that occurs during the equal-level reading, due to the gradual decrease of hydraulic head (see example of data sheet and calculation in Table 3.2). The calculation of K values, according to this procedure, may be difficult sometimes because of the rather inaccurate procedure of extrapolation (see left part of Fig. 3.10). Problems can be reduced when the total drop H of the water level in the inner tube standpipe (ITS) is varied for different measurements, so as to create a difference between the equal-level and OTS-full times of approximately 8 seconds. For example, in soils with a high infiltration, it may be necessary to extend the measurement to H = 80 cm, instead of the usual 40 cm. Baumgart (1967) made a study of the Bouwer method and suggests a somewhat modified procedure of calculation based on the Bouwer calculation with an available  $H_b$  value.

$H_b$  is the difference in cm between the top of the outer tube standpipe (OTS) and the water level at balanced flow conditions, when  $Q_I = Q_H$ , where  $Q_I$  is the flow leaving through the bottom of the inner tube due to intake and  $Q_H =$  flow, entering through the bottom of the inner tube due to a difference H between the water levels in inner and outer tube. Then

$$K = \frac{2 \cdot 3R_v^2}{R_c F_f t} \cdot \log \frac{H_o - H_b}{H_t - H_b} \quad (\text{Bouwer, 1961})$$

where  $R_v$  = radius of inner tube standpipe,  $R_c$  = radius of inner tube,  $F_f$  = flow factor, t = elapsed time, H = distance of water level in the inner tube below water level in the outer tube  $H_b = H$  at balanced flow. This equation can only be applied when  $H_b$  can be measured. Mostly, this is not the case and then the OTS-full and equal-level measurements are made as discussed previously. Baumgart (1967) suggests that this formula be used in all cases, and to estimate  $H_b$  values until the plotted values of t and  $\log H_o - H_b / H_t - H_b$  are on a straight line. With some practice, this can be done rather easily and quickly (see right part of Fig. 3.10) (from: Baumgart, 1967). K values calculated by this procedure compared well, with those obtained

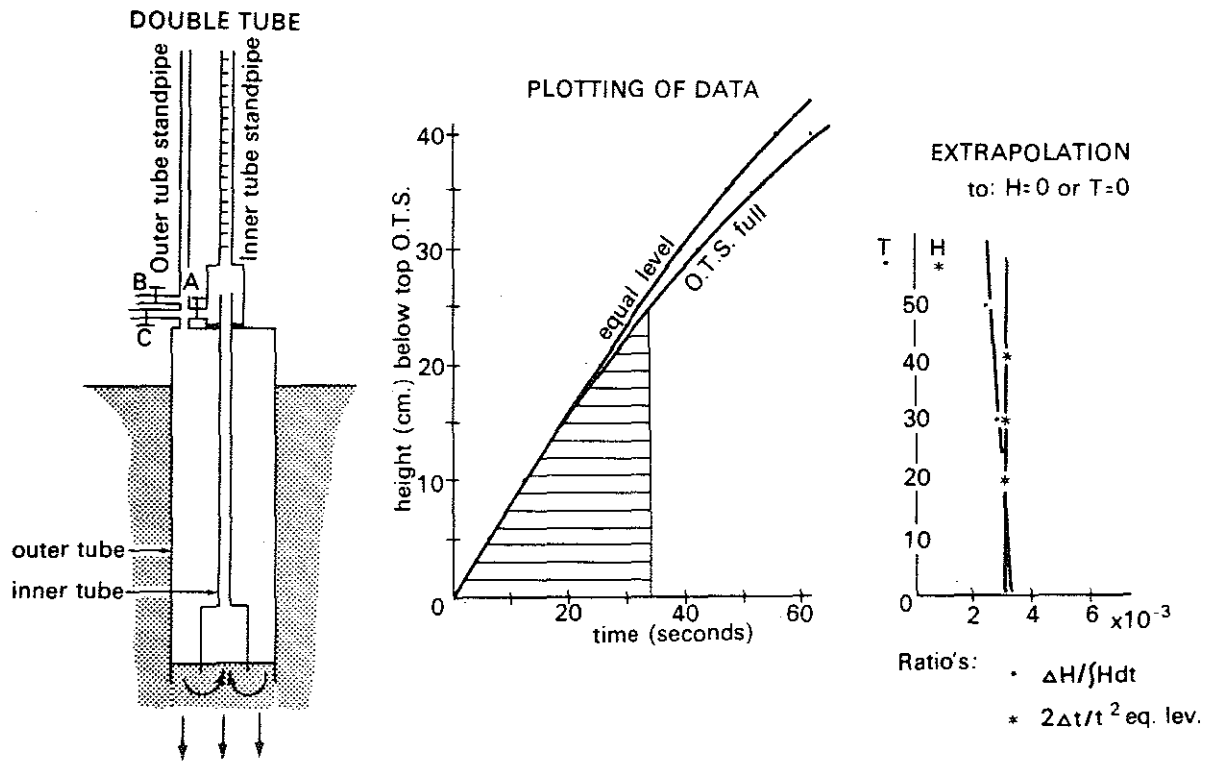


Fig. 3.9. The double-tube method for measurement of  $K_{sat}$  *in situ* cross section of the apparatus and plotting of experimental data.

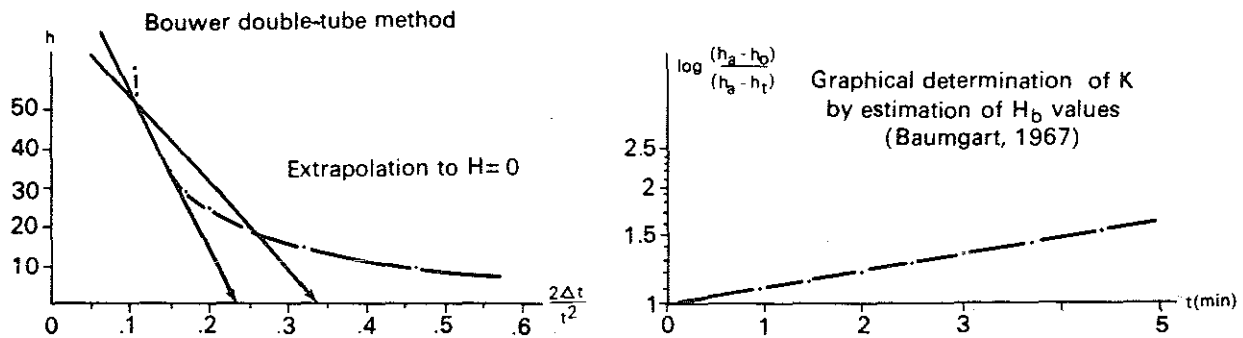


Fig. 3.10. Extrapolation procedure and graphical determination of  $K_{sat}$  using field data of the double-tube method (after Baumgart, 1967).

Table 3.2. Calculations of the double-tube method for determining  $K_{sat}$  in situ.

General data:

Date: Aug. 5, 1969. Soil profile: Plano silt loam, B<sub>2</sub> 55 cm depth. Time water started: noon.  
 Temp. water: 20°C. Tube radii: outer tube = 12.5 cm, inner tube ( $R_c$ ) = 6.2 cm,  $R_v = 0.6$  cm ·  $d = 2.6$  cm. 51

Measurements:

t	1:45 PM	1:55	2:05	2:15	2:25	2:35	2:45	2:55	3:05	3:15	3:25	3:35	3:45	3:55
H	OTS	Eq.1	OTS	Eq.										
0														
5	3.9	4.4	4.3	4.6	4.2	4.7	4.2	5.2	5.4	5.6	6.2	6.2	6.0	6.2
10	7.7	7.9	8.8	9.0	8.9	10.0	9.2	9.8	10.4	11.0	11.8	12.2	12.4	12.0
15	12.0	11.6	13.0	13.0	13.4	14.7	13.8	15.0	16.2	16.8	18.2	18.4	19.0	18.2
20	16.6	15.5	18.2	17.7	18.6	20.0	19.0	20.4	22.0	23.0	24.8	25.6	26.2	25.0
25	20.8	20.0	23.9	23.0	24.0	26.0	24.5	26.0	28.4	28.9	32.5	32.2	33.8	31.9
30	25.8	24.2	28.8	27.6	29.8	31.6	30.0	31.8	35.2	35.2	39.8	39.4	41.8	39.2
35	31.7	28.8	34.4	33.0	35.9	37.4	37.0	37.6	42.6	42.0	48.4	47.0	50.8	47.0
40	37.0	34.2	41.2	38.6	42.6	44.2	45.0	44.4	50.0	49.4	58.0	55.0	61.0	55.1

Ratio's  $\frac{\Delta t}{t^2 \text{ eq. lev.}}$  : 0.00305 (1:55-2:15); 0.0007 (2:15-2:35); 0.00032 (2:35-2:55); 0.00014 (2:55-3:15);  
 0.00020 (3:15-3:35) and 0.00020 (3:35-3:55). (constant!)

Calculation of K based on:

OTS: 3:45 PM

Eq.: level: average of 3:35 and 3:55

t	$\Delta H$	Hdt	Ratio	H	$2\Delta t$	$t^2 \text{ eq. lev.}$	Ratio
30	1.0	352.5	$2.84 \times 10^{-3}$	20	1.8	625	$2.9 \times 10^{-3}$
40	1.8	610.0	$2.95 \times 10^{-3}$	30	5.0	1544	$3.2 \times 10^{-3}$
50	2.2	975.0	$2.25 \times 10^{-3}$	40	12	3025	$3.9 \times 10^{-3}$

Ratio extrapolated to  $t = 0$  :  $3.0 \times 10^{-3}$  (Fig. 3.9).      Ratio extrapolated to  $H = 0$ ;  $3.0 \times 10^{-3}$  (Fig. 3.9).

The ratio  $\frac{R_c}{d}$  (=2.38) was used to determine the flow factor  $F_f$  from a diagram of Bouwer (1961).

$F_f = 1.1$  Then:

$$K = \frac{R_v^2}{F_f \cdot R_c} \cdot \frac{\Delta H}{Hdt} = 13 \text{ cm/day, or } K = \frac{R_v^2}{F_f \cdot R_c} \cdot \frac{2\Delta t}{t^2 \text{ eq. lev.}} = 13 \text{ cm/day.}$$

with the OTS-full, equal-level procedure. Application of this calculation method is recommended because it saves time and is applicable to any type of test result.

### 3.2.3. Literature cited

Baumgart, H. E. 1967. Die Bestimmung der Wasserleitfähigkeit  $k_f$  von Boden mit tief liegender Grundwasseroberfläche. Mitteilungen aus dem Institut für Wasserwirtschaft und Wasserwirtschaftlichen Wasserbau der Technischen Hochschule Hannover. 275 p.

Bouwer, H. 1961. A double-tube method for measuring hydraulic conductivity of soil *in situ* above a water table. Soil Sci. Soc. Amer. Proc. 25:334-339.

Bouwer, H. 1962. Field determination of hydraulic conductivity above a water table with the double-tube method. Soil Sci. Soc. Amer. Proc. 26:330-335.

Bouwer, H. and H. C. Rice. 1964. Simplified procedure for calculation of hydraulic conductivity with the double-tube method. Soil Sci. Soc. Amer. Proc. 28:133-134.

Bouwer, H. and H. C. Rice. 1967. Modified tube diameters for the double tube apparatus. Soil Sci. Soc. Amer. Proc. 31:437-439.

### 3.2.4. Alternative procedures

The double-tube method is rather time consuming and hundreds of gallons of water may be needed to make a single test. This aspect has offered practical problems and forms one reason why our research has tried to define more simple procedures. A second, more important, reason is based on features of the test itself. The measured K value reflects both vertical and horizontal K values, as previously discussed. Profiles with large, vertically continuous worm channels may have high infiltration rates, certainly when they are formed in silty deposits overlying sandy outwash with deep groundwater tables. Saturated K values measured in the silt with the double tube do not reflect this high vertical conductivity because vertical worm channels do not allow lateral flow from the outer into the inner tube. Some misleading measurements have therefore been made. Current research tries to define optimum sample sizes for cores for different soil materials, to be used for  $K_{sat}$  measurements, if possible, *in situ*,

following work reported by Anderson and Bouma (1973).<sup>7</sup> Field experiments are conducted now by F. G. Baker using excavated soil columns (prepared for the crust test procedure, Sec. 3.2) for *in situ*  $K_{sat}$  measurements. The double-tube method is still very valuable in many soils with relatively homogeneous structures without many large, vertically continuous worm channels.

Another method for measurement of  $K_{sat}$  *in situ* has been developed by Bouwer using an air-entry permeameter.<sup>8</sup> This method has not been tested in Wisconsin but very promising results have recently been reported by Dr. R. B. Grossman, SCS-USDA, Lincoln, Nebraska.

### 3.3. A detailed description of the crust-test procedure for measuring hydraulic conductivities of unsaturated soil *in situ*

#### 3.3.1. Introduction

The crust-test procedure is used to measure hydraulic conductivities (K values) of unsaturated soil *in situ*. The method consists of a series of infiltration runs--each of which yields one point on the hydraulic conductivity curve. Curves usually cover K values in a moisture-tension range between 10 and 90 cm. Each run is made in a soil pit, using an excavated cylindrical column with a height and diameter of approximately 25 cm (10"). The equilibrium infiltration rate through a gypsum-sand crust applied on top of the column in a cylinder infiltrometer is measured, as is the corresponding subcrust tension. Separate runs are made through three or four gypsum-sand crusts, following a sequence from high to low crust resistances. Crusts with a high resistance yield a low infiltration rate (which corresponds with a K value when the hydraulic gradient below the crust is 1 cm/cm) at a relatively low moisture content and a relatively high soil moisture tension.

<sup>7</sup>Anderson, J. L. and J. Bouma. 1973. Relationships between saturated hydraulic conductivity and morphometric data of an argillic horizon. Soil Sci. Soc. Amer. Proc. 37:408-413.

<sup>8</sup>Bouwer, H. 1966. Rapid field measurement of air entry value and hydraulic conductivity of soil as significant parameters in flow system analysis. Water Resources Research, Vol. 2, No. 4:729-738.

A profile description is made before applying the test to determine characteristic depth ranges, usually corresponding with major horizon boundaries, within which separate columns should be excavated. Technical details of the method will be discussed in the following sections.

### 3.3.2. Installation procedures

A horizontal plane is prepared at the desired level at the test site by using a putty knife and a carpenter's level (Fig. 3.11, 1). A cylindrical column of soil, at least 25 cm high, with a diameter of 25 cm, is carved out from the test level downward, taking care to chip or pick the soil away from the column as the desired form is approached, so as to prevent undue disturbance of the column itself (Fig. 3.11, 2+3). A ring infiltrometer, 25 cm in diameter and 10 cm high, with a 2.5 cm wide brim at the top, is fitted onto the column (Fig. 3.11, 4). The level soil surface inside the infiltrometer should be approximately 1 1/2 cm (1/2 inch) below its brim to avoid an excessively large space between the soil surface and the infiltrometer-cover, which is applied later. The sides of the column are then sealed with aluminum foil to avoid evaporation losses and soil is packed around it (Fig. 3.11,5). Complete sealing is not necessary because water will not flow from the column under unsaturated conditions. A half-inch thick acrylic plastic cover with a diameter of 30 cm (12") and with a sponge-rubber gasket glued to it is bolted to the top of the infiltrometer with ring nuts (Fig. 3.11, 6). An intake port and air-bleeder valve are provided in the cover. The infiltrometer with the acrylic cover should be placed under a very slight slope with the highest point at the location of the air bleeder, to allow air to escape during filling of the infiltrometer. The direction of the slope can be determined with a small carpenter's level placed on top of the acrylic cover. The cover is removed after the cylinder is positioned, to allow placement of the crusts. Thin pencil-size, mercury-type tensiometers attached to 1/8" plastic tubing (Fig. 3.11, 7-8) are implanted from the sides to a point 1 cm below the crust in the center of the column and 3 cm deeper. Two types of tensiometers can be used to measure tensions inside the column (Fig. 3.12). One

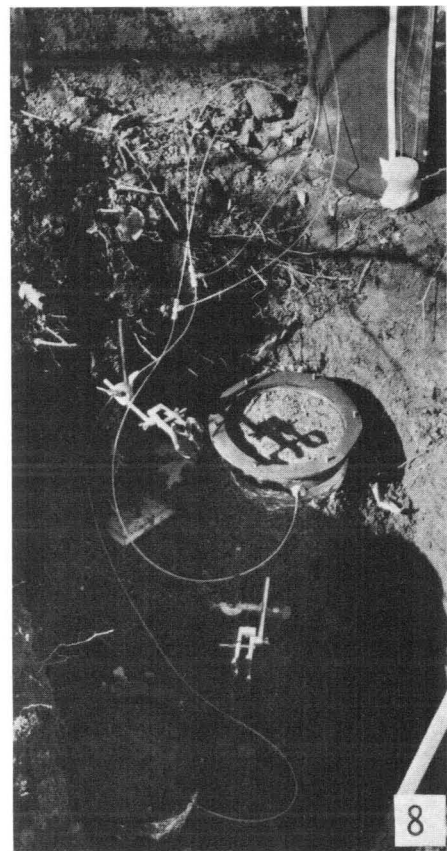
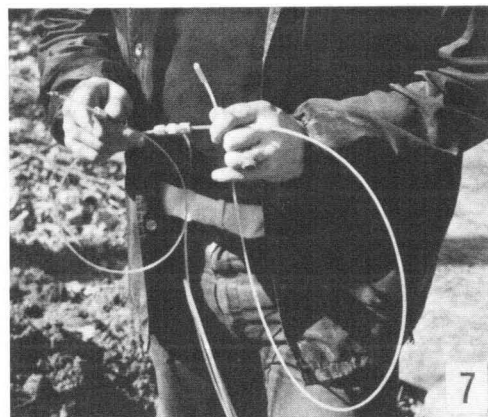
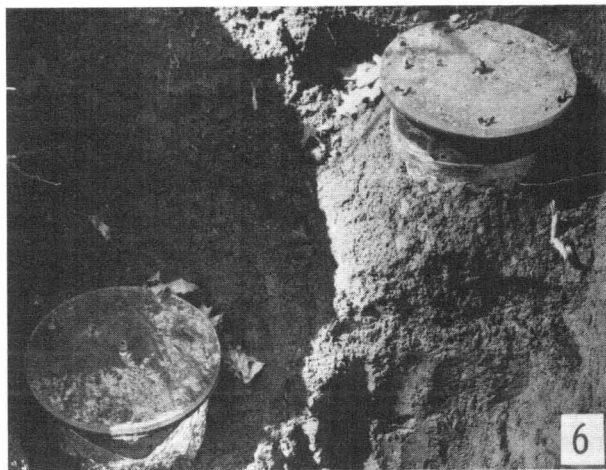
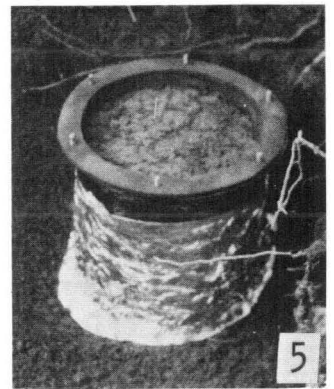
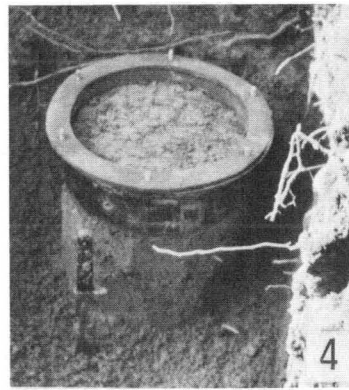
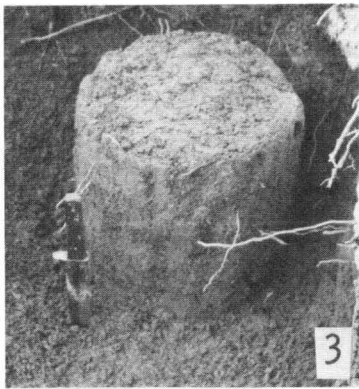
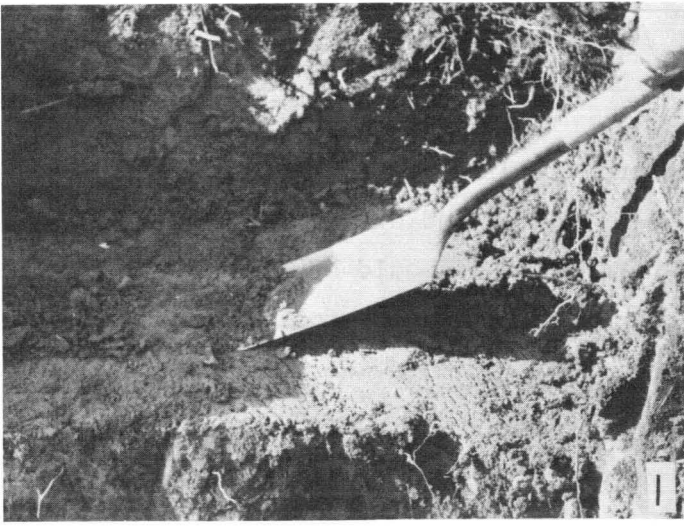


Fig. 3.11. Installation of crust test procedure.

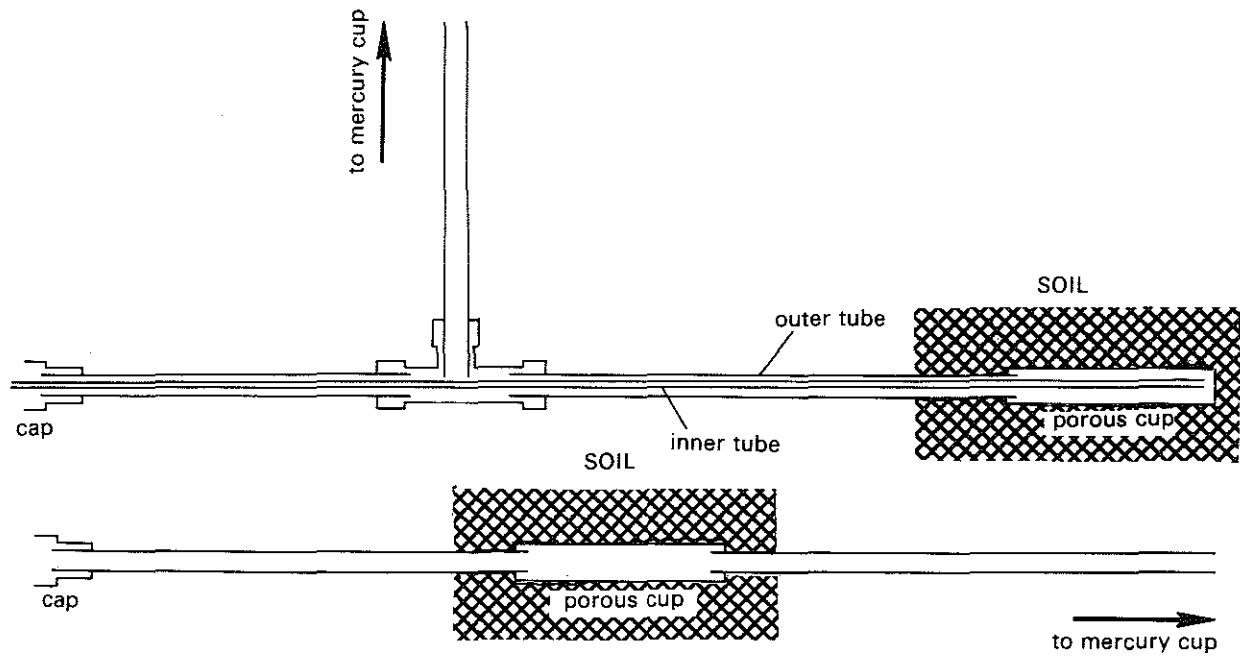


Fig. 3.12. Two types of tensiometers used to measure soil moisture tensions around operating seepage beds and in soil columns for the crust-test procedure.

type (lower picture in Fig. 3.12) is a simple flow-through system consisting of 1/8" tubing which is sealed onto both ends of a porous cup. One end of the tubing is in a container filled with mercury, the other is capped. Fill the tensiometer with de-aired water,<sup>9</sup> using a syringe that fits on the 1/8" tubing. Once the tube is filled with water and air has been removed from the tubing (to be observed when air bubbles stop rising through the mercury), the open end is closed with a cap. The rise of mercury in the tube is a measure for the total moisture potential in the soil in contact with the porous cup. Installation of this type of tensiometer in the cylinder is difficult because a small cylindrical cavity is needed through the entire column before the tubing and cup can be installed. Carefully positioned holes in the steel infiltrometer ring and use of a small auger with a slightly smaller diameter than the porous cup to prepare a tight-fitting cavity are needed. The other type of tensiometer (upper picture in Fig. 3.12) uses a small 1/16" tube inside a 1/8" tube, the latter with a porous cup at one end and a removable cap at the other. The inner 1/16" tube extends from the capped end of the outer tube to the sealed end of the porous cup. A three-way union tee is used to add a third 1/8" tube segment leading to the mercury container. Filling of this tensiometer is achieved by applying de-aired water to the 1/16" inside tube with a syringe. This water will fill the other larger tubes, starting at the closed tensiometer cup, pushing air out of the 1/8" tubing in the direction of the cap and of the mercury container. The cap is closed when all air bubbles have disappeared from the 1/8" tubing. Use of transparent tubing is necessary to allow observation of air bubbles. This type of tensiometer does not need a pre-made cavity all the way through the column. A small, 12-cm-long hole with a diameter slightly smaller than the porous cup can be made into the column with a small auger. Filling of these tensiometers usually takes longer than filling the other type. The pressure applied to the syringe is directly

---

<sup>9</sup>De-aired water is readily prepared by stirring distilled water on a magnetic stirrer while applying a vacuum to the container with a pump or aspirator. When few or no bubbles rise to the surface, the water is ready for use. This usually takes about one hour. De-aired water should be transported in completely filled bottles to avoid re-aeration during transportation.

transferred to the porous cup and a considerable volume of water may be pressed from the cup into the surrounding soil before all tubes are filled with water. This is not a good procedure because of its effect on the original moisture tension of the soil. Long periods of time may be needed to re-establish the original moisture tension. An alternative procedure is as follows: the porous cup is placed in a cup of water rather than in the soil. The uncapped tube of the tensiometer is placed in the mercury container and the tubes are filled as described earlier. The cup is then removed from the cup with water, dried with a piece of cloth, and placed in the pre-constructed cavity in the column. Recent test results have indicated that only one tensiometer at a depth of 3 cm below the crust will suffice. A measurement of soil moisture tension in the column should be obtained before crusts are applied to determine the possible range of K values that can be measured. For example, if natural tensions are only 20 cm, it would be useless to apply crusts that would induce higher tensions (lower soil moisture potentials!) into initially, relatively dry soil. Exposure of the column to the air is useful to lower the moisture content and increase tensions by evaporation. Drying may take much time, though, and the best sequence of measurements is to start with a heavy crust (100% gypsum) (low moisture content below crust, and high tension) and follow with crusts of progressively decreasing gypsum contents (yielding higher moisture contents below the crust and lower tensions).

In the first experiments with the crust-test procedure, various puddled soil materials were used for crusts (Bouma, et al., 1971). Additional field experience, however, showed that some of these crusts (in particular the ones with a relatively low resistance) were rather unstable and easily disturbed, due to continuous swelling of the clay particles. A different procedure was therefore developed in later experiments, using dry gypsum powder<sup>10</sup> thoroughly mixed with varying quantities of a medium sand. After sufficient wetting and continuous mixing, a thick paste is obtained. Then this

---

<sup>10</sup>Ultracal -30 and Hydrocal, both products of U.S. Gypsum, have been used successfully.

material is quickly transferred to the prepared soil surface in the column and is applied on top with a carpenter's knife as a continuous crust to the wall of the cylinder to avoid boundary flow. Crusts of this type harden within about 30 minutes, thereby providing a stable porous medium with a fixed conductivity value. Crust resistance can be varied by changing the relative quantities of gypsum and sand. Crusts composed of gypsum only have the highest resistance. For example: A subcrust tension of 52 cm was induced in a sand column capped with a 5 mm thick gypsum crust with 3 mm water on top. This crust had a  $K_{sat}$  value of 0.007 mm/day. Another crust, formed from a pre-wetted mixture composed of 14% gypsum and 86% sand by volume as measured in the field using a graduated cylinder, induced a subcrust tension of only 11 mbar.  $K_{sat}$  of this crust was 8.3 cm/day. The higher  $K_{sat}$  value is due to the occurrence of larger pores between the sand grains (Bouma and Denning, 1972).

A series of crusts is applied to the same column for succeeding runs. A common series of four crusts would be composed of 100%, 50%, 20%, and 12% gypsum by volume, respectively. A graduated cylinder with a content of 1000 cc is used (20% gypsum crust material = 200 cc gypsum powder and 800 cc sand) to obtain an adequate amount of crust material. Relative volumes of gypsum can be changed as needed to obtain data points in the desired range. Each infiltration run through a particular crust yields one point of a curve of hydraulic conductivity versus soil tension (see Fig. 3.13).

### 3.3.3. Measurement procedure

A measurement is initiated by ponding water on top of the crust to a level slightly higher than the top level of the cylinder. Water applied this way does not have to be applied through the burette and this procedure saves time. The cover is then bolted to the cylinder. The sponge-rubber gasket between cover and cylinder should be flat and should cover clean surfaces before the cover is applied to avoid leakage. A piece of 1/4" semirigid tubing, attached to a water-filled burette, is then attached to the intake port in the cover. The 1/4" tubing connecting burette and cylinder should be completely

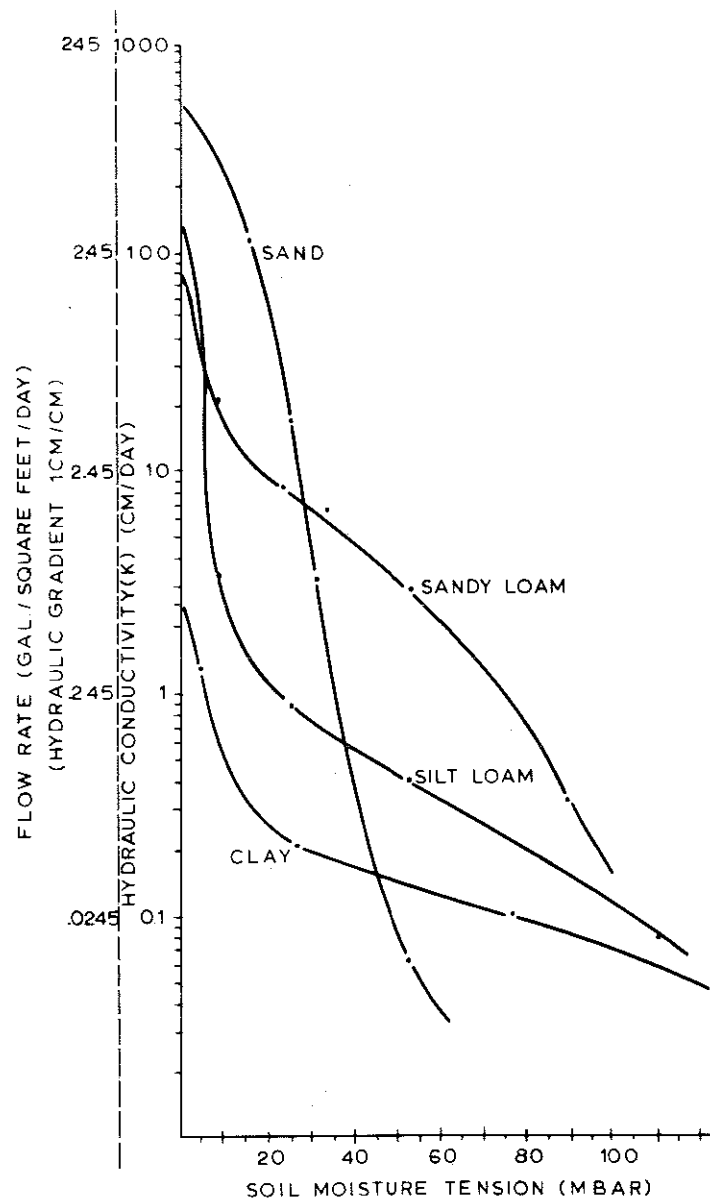


Fig. 3.13. Hydraulic conductivity (K) as a function of soil moisture tension measured *in situ* with the crust-test procedure.

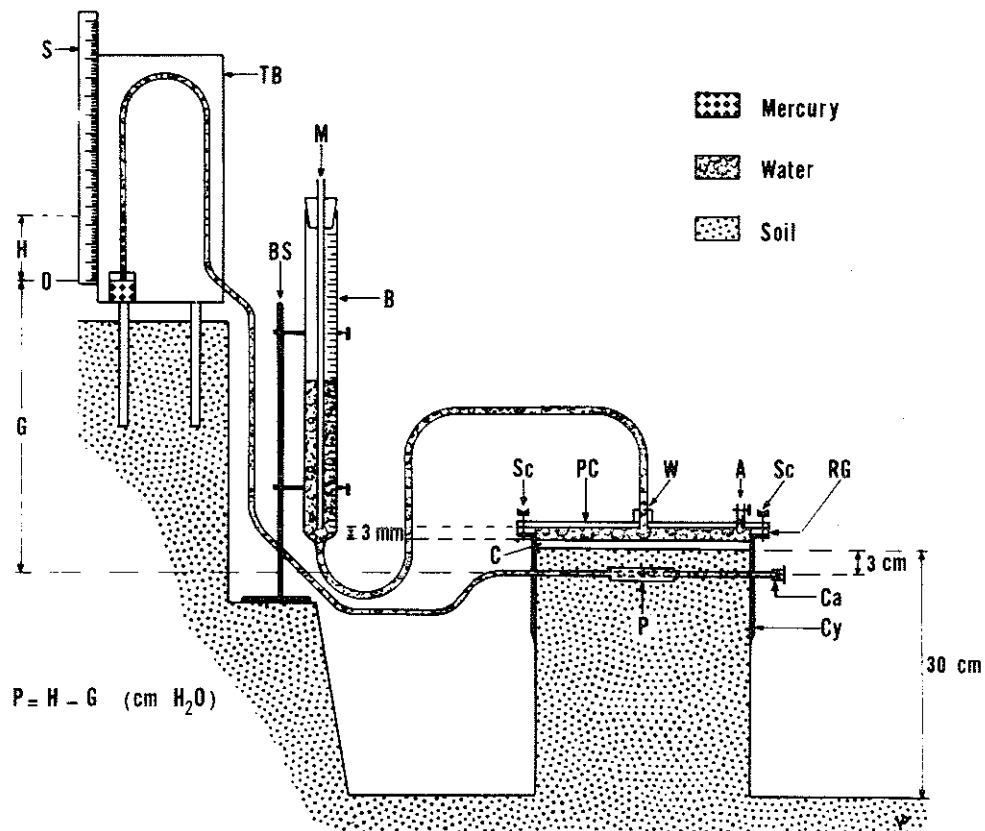


Fig. 3.14. Schematic diagram of the crust-test procedure. TB = manometer board, S = scale, B = burette, BS = burette stand, M = marriot device, Cy = metal cylinder, C = crust, PC = plastic cover, Sc = wing nut, W = water inlet, A = air bleeder, RG = rubber gasket, Ca = cap, P = porous cup, O = zero mercury level, H = height mercury level above zero level, G = distance between porous cup level and zero mercury level.

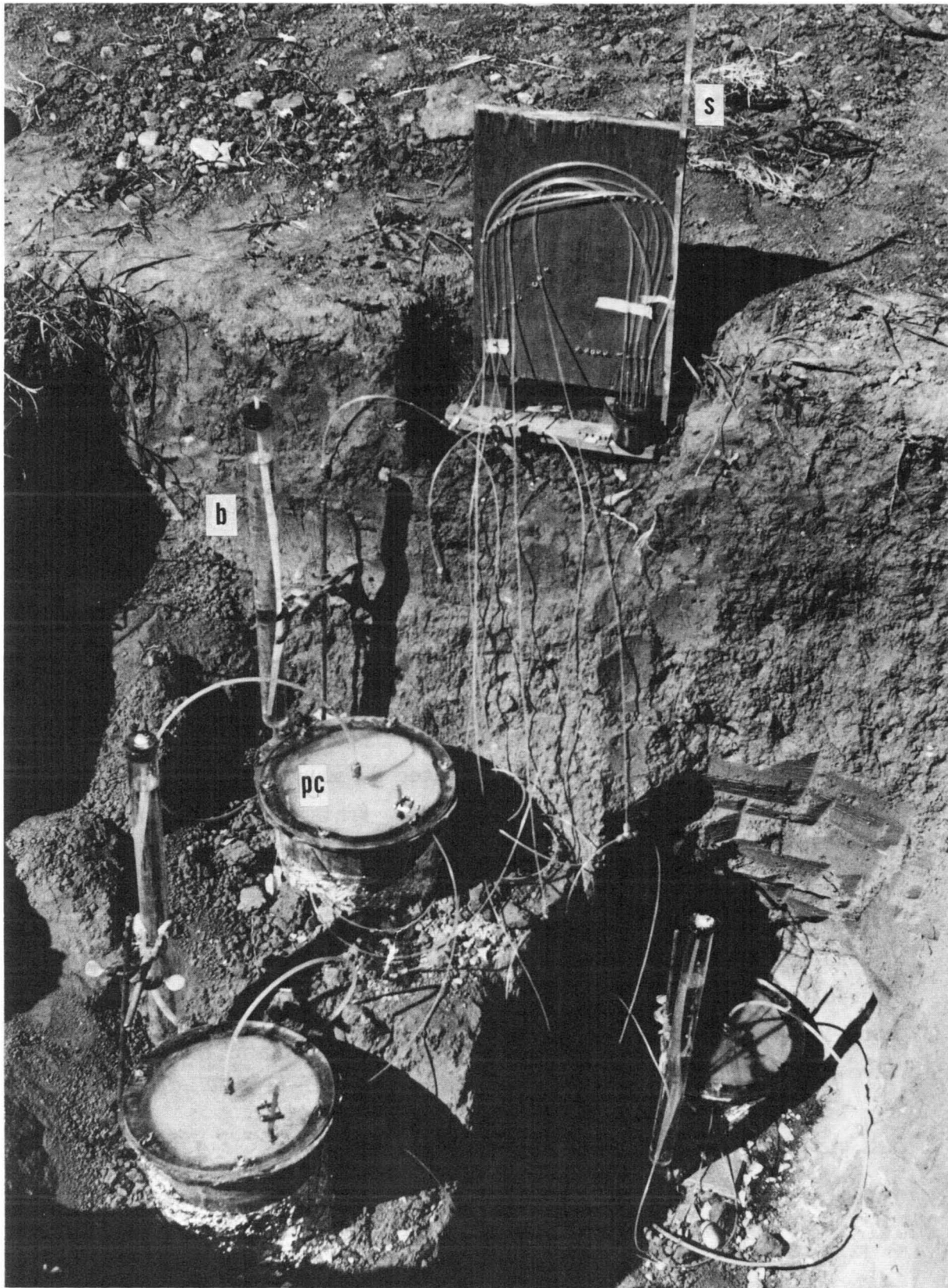


Fig. 3.15. Field measurement of unsaturated hydraulic conductivity *in situ* with the crust-test procedure. Inflow into the soil through the crust on top of the column is measured with a burette (B) discharging into the water-filled space between the crust and the acrylic plastic cover (PC). Soil moisture tensions derived from the mercury rise in 1/8-inch plastic tubes along calibrated scales (S) are measured in the columns.

full of water to avoid irregular flow rates. Air can be removed from the 1/4" tubing by turning the unattached burette upside down after closing it at the top and by patting against the tubing.

The air-bleeder valve should be open during filling until the small space between the crust (C) and the cover of the cylinder (PC in Fig. 3.14) is full of water. A Mariotte device, in a burette (B), maintains a constant pressure of about 3 mm water over the crust (Fig. 3.14). The infiltration rate into the soil, corresponding to the rate of movement of the water level in the burette, is recorded as soon as the tensiometers show that equilibrium has been reached. Soil moisture tensions are measured in the columns and are derived from the mercury rise in 1/8 inch plastic tubes along calibrated scales (S) (Figs. 3.14 and 3.15).

The calibrated scales indicate the total potential of the soil water (Fig. 3.14) and soil moisture tensions can be obtained by subtracting the gravitational potential (see Sec. 2.2).

The infiltration rate, when constant for a period of at least one hour, is taken to be the unsaturated K value at the subcrust tension when the tension gradient is zero (this means only gravitational flow occurs:  $v/i = 1$ ). In some cases, a tension gradient remains at steady-state conditions. Hydraulic conductivity is then calculated according to  $K = v/i$ , where  $v$  = infiltration rate and  $i$  = hydraulic gradient below the crust (in such a case 1). However, the hydraulic gradient is usually close to unity and use of one tensiometer at 3 cm depth below the crust suffices to obtain a representative tension corresponding with a unit hydraulic gradient.

#### 3.3.4. Literature cited

- Bouma, J., D. I. Hillel, F. D. Hole and C. R. Amerman. 1971. Field measurement of hydraulic conductivity by infiltration through artificial crusts. *Soil Sci. Soc. Amer. Proc.* 35:362-364.
- Bouma, J. and J. L. Denning. 1972. Field Measurement of Unsaturated Hydraulic Conductivity by Infiltration through Gypsum Crusts. *Soil Sci. Soc. Amer. Proc.* 36:846-847
- Hillel, D. and W. R. Gardner. 1969. Steady infiltration into crust-topped profiles. *Soil Sci.* 107:137-142.

Hillel, D. and W. R. Gardner. 1970a. Transient infiltration into crust-topped profiles. Soil Sci. 109:69-76.

Hillel, D. and W. R. Gardner. 1970b. Measurement of unsaturated conductivity and diffusivity by infiltration through an impeding layer. Soil Sci. 109:149-153.

## Appendix

This list of materials is included as a service to the reader and does not necessarily represent any expression of preference for these specific items, which were the ones used in our studies.

### Tensiometers

Porous cups. 8" long segments to be cut to desired lengths. (OD = .22" wall thickness .040") multitube filter elements with pore sizes of .29 micron, type MT-FEF. Sold by Selas Flotronics-Fluid Processing, Dresher, PA 19025; General address: Spring House, PA 19477.

Flexible 1/8" plastic tubing. Nylo-seal, semirigid nylon II tubing. Serial No. 22-SH, colorless and transparent. Sold by Imperial Eastman Co., 6300 W. Howard Street, Chicago, IL 60648.

Epoxy, to attach cups to tubing, can be bought in any hardware store.

Union tee's, caps, and ferrules used for tensiometers were obtained from Badger Valve and Tube Fitting Corp., 1504 Underwood Ave., Wauwatosa, WI 53213. These items are available from other manufacturers. The different serial numbers are not listed here. The company catalog can provide this information.

Cylinders used in this study were custom-built in the UW machine shop.

The sponge rubber between cylinder and acrylic covers was obtained from McMaster-Carr, PO Box 4355, Chicago, IL 60600. Brand name: Neoprene.

3.4. A detailed description of the instantaneous-profile method for measuring hydraulic conductivities of unsaturated soil *in situ*

by F. G. Baker

3.4.1. Introduction

In the instantaneous-profile method a fallow plot of soil is artificially wetted to saturation. The plot is then covered to prevent evapotranspiration, and internal drainage occurs. By the use of tensiometers, placed at depths corresponding to the lower part of major horizons, soil moisture tensions are measured. Moisture contents at these depths are also determined simultaneously. These two characteristics are measured frequently, starting at saturation, which represents time zero.

From these data, the hydraulic gradient ( $\frac{\partial H}{\partial Z}$ ) and the change in moisture content over time ( $\frac{\partial \theta}{\partial t}$ ) can be obtained and subsequently the hydraulic conductivity can be calculated.

3.4.2. Theory

Taking the general equation of vertical hydraulic flow in a soil profile

$$\frac{\partial \theta}{\partial t} = \frac{\partial}{\partial Z} [K(\theta) \frac{\partial H}{\partial Z}] \quad (1)$$

where  $\theta$  = volumetric moisture content,  $H$  = hydraulic head ( $H = \psi + Z$ ),  $K(\theta)$  = hydraulic conductivity at moisture content  $\theta$ ,  $Z$  is depth (positive downward), and  $t$  = time.

By integration and rearrangement, we find

$$\int_0^Z \frac{\partial \theta}{\partial t} dZ = K(\theta) \frac{\partial H}{\partial Z} \text{ or } K(\theta) = \frac{\partial \theta / \partial t}{\partial H / \partial Z} \cdot Z \quad (2)$$

In multilayered profile the factor  $\frac{\partial \theta}{\partial t} \cdot Z$  becomes the sum of

$$\left(\frac{\partial \theta}{\partial t}\right)_1 \cdot Z_1 + \left(\frac{\partial \theta}{\partial t}\right)_2 \cdot (Z_2 - Z_1) + \left(\frac{\partial \theta}{\partial t}\right)_3 \cdot (Z_3 - Z_2), \text{ etc... } (3)$$

where  $Z_1$ ,  $Z_2$ ,  $Z_3$  are the depths of the lower boundaries of the respective soil horizons 1, 2, 3, in order of depth and the quantities involving  $Z$  are respective horizon thicknesses. The individual  $(\frac{\partial \theta}{\partial t})$  factors correspond to the respective horizons, as indicated. The factor  $\frac{\partial H}{\partial Z}$  can be derived and  $K(\theta)$  calculated.

Soil moisture content can be plotted versus time (zero time is when the profile is saturated and drainage begins) and the slope of the resulting curve gives  $\frac{\partial \theta}{\partial t}$  for any particular time. The curve is usually in the form of a hyperbolic function, as shown in Fig. 3.16.

The hydraulic gradient  $(\frac{\partial H}{\partial Z})$  of an internally draining, initially wetted profile is often unity. The exact value is the slope of the line created by plotting hydraulic head ( $H = \psi + Z$ ) versus the depth  $A$  to the tensiometer cup where the head is measured (Fig. 3.17). This slope does vary with time, and the slope must therefore be determined for each time of observation at which  $K$  is calculated (Fig. 3.17). This will be discussed in greater detail in the specific example in a following section.

### 3.4.3. Site selection and preparation

A nearly level site is selected for the experiment so that water may be ponded more or less uniformly over the entire area. To retain the water, a simple earthen dike can be constructed surrounding the plot. A water depth of about 2 or 3 cm over all portions of the pond is desired, but may be difficult to achieve. On slopes of low grade, uniform distribution of water is not a problem, but on steeper slopes uneven infiltration and subsurface flow can occur. Fig. 3.18a illustrates the desired flow pattern in the experimental plot. Water infiltrating over the entire area of the plot moves generally downward under the influence of gravity. Because the soil surrounding the plot is drier than the soil directly under the pond, lateral movement of water can be expected to occur. This drier surrounding soil exerts a tension on the water inside the experimental volume, pulling it away from the center of the plot. This effect is greatest at the boundaries of the area and decreases toward the center. As the flow lines indicate, flow is nearly vertical below the center of the plot. Here, approximate one-dimensional flow is achieved. All the details of plot preparation are designed to maintain vertical

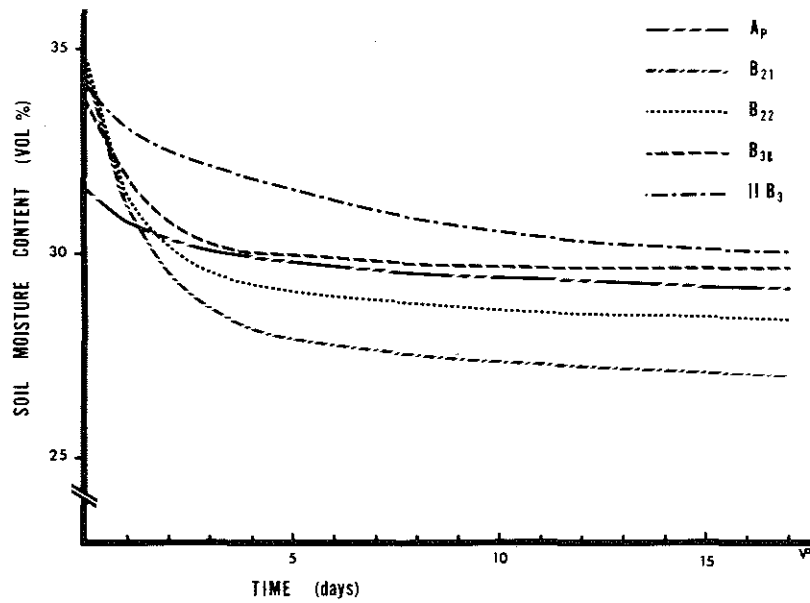


Fig. 3.16. Moisture content as a function of time during drainage of an initially saturated profile (used for calculations of the instantaneous-profile method).

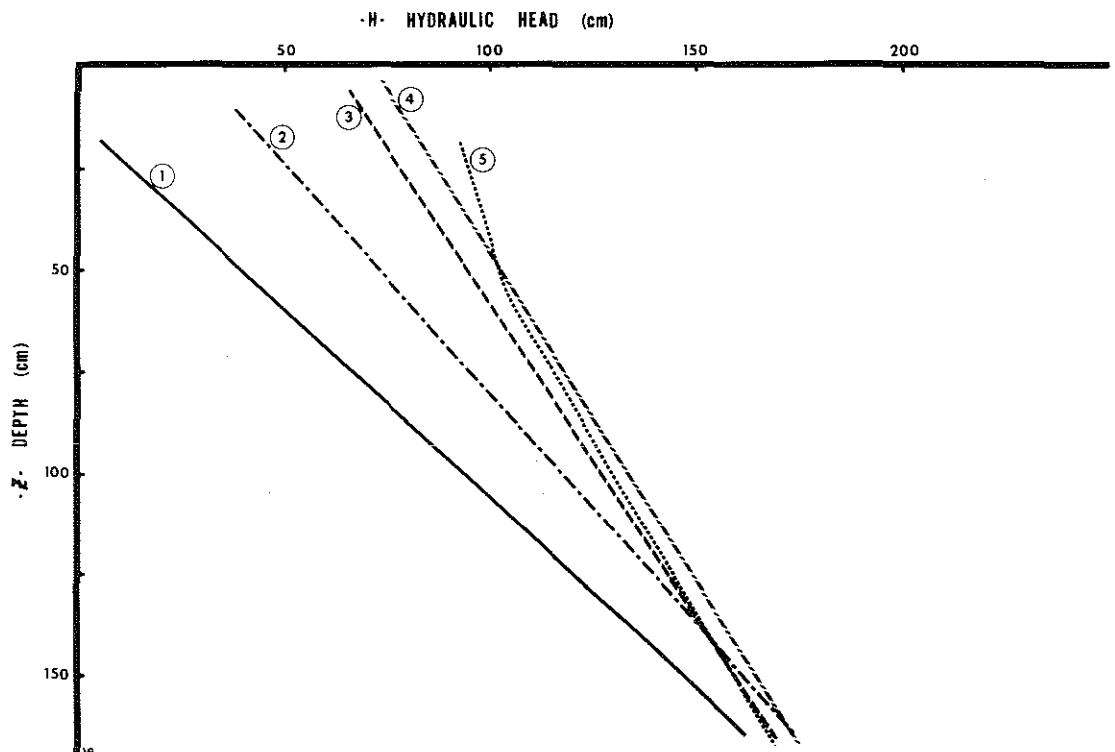


Fig. 3.17. Total potential as a function of depth and time during drainage of an initially saturated profile.

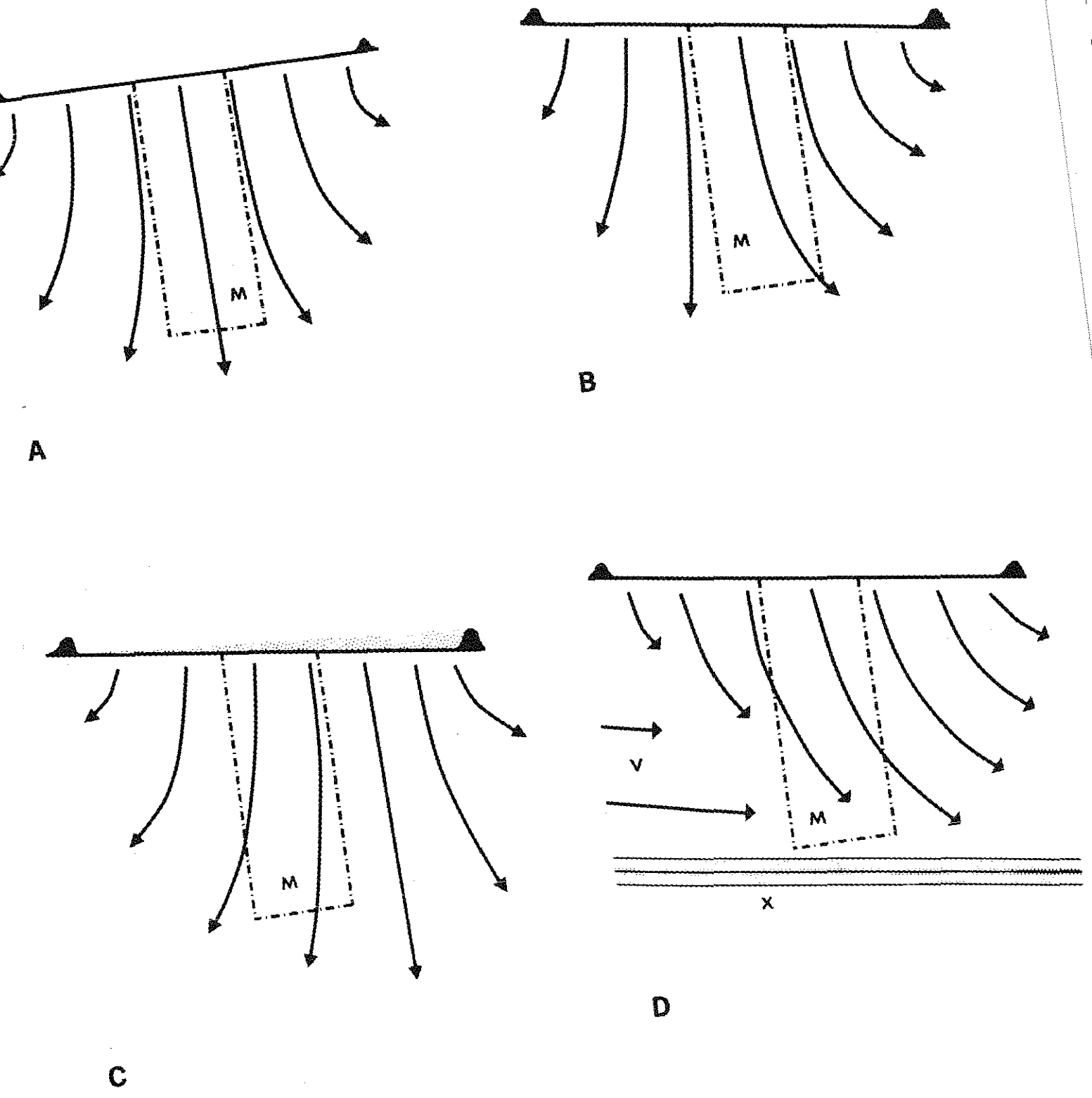


Fig. 3.18. Diagrams illustrating possible flow patterns occurring when saturating soil for the instantaneous-profile method.

drainage at this point, isolating this zone from the effects of lateral flow and from changes of soil moisture content due to external factors such as evapotranspiration and precipitation. Fig. 3.18b illustrates the effect of slope on water movement for a plot where uniform infiltration occurs (as in the case of a sprinkle infiltration system).

Vertical flow is seen to be shifted somewhat from the center of the plot and lateral flow is seen to be greatest on the downslope side of the plot and least on the upslope side. In such a case, knowing where vertical flow occurs may become a problem. The location and orientation of instruments is dependent on this knowledge. On low slopes ( $< 3\%$ ) this problem is very small, assuming uniform infiltration over the entire area.

One of the largest problems on slopes is achieving uniform infiltration. Often the surface is such that water will be a few inches deeper on the lower portion of the plot than on the upslope portion of the area. Fig. 3.18c indicates this situation. There is not only a problem with distributing the water over the surface but also the difference in hydraulic head will cause flow rates to vary from upper to lower sections. The length of the flow lines in the figure represents the relative magnitude of flow rates. Notice that vertical flow is found downslope from the center of the experimental area.

It can be seen from these examples that the ideal case will rarely be encountered in the field experiment. A sloping site will cause nonvertical flow under the center of the plot and uniform distribution of water will become difficult to achieve.

Other problems may arise due to flow of external moisture from upslope through the soil of the plot. Fig. 3.18d exemplifies this situation. This directional flow is most significant at saturation when downslope movement due to gravity is the dominant force involved. Saturation may occur in the form of a real water table or of a "perched" water table where water is temporarily ponded above slowly permeable horizons or strata. Water contained in this manner by a less conductive horizon below may well cause saturation in the horizon above the less pervious layer, and flow downslope may occur. If this occurs upslope from the experimental plot, external water may be

introduced at one or more levels in the pedon, setting up a complex drainage pattern which may change the gradients drastically. Data obtained under such conditions can be extremely difficult to interpret.

A related situation is encountered when the site of the experiment is located in a depression, where not only surface water but also subsurface moisture flow is concentrated due to downslope gravity movement.

In homogeneous media, such as some sands, a nearly uniform gradient is found during drainage. In multilayered soils where horizons have different hydraulic conductivities, a nonuniform gradient develops. Impeding horizons and other features will prevent free drainage from occurring within the experimental volume of soil. Soil moisture tensions above such an impeding layer may approach or reach zero (approaching saturation) while the tension beneath the layer can be lower (lower moisture content). Such a layer can then behave as an impeding crust, preventing saturation from occurring in horizons below itself. Therefore, a part of a given multilayered soil may not reach saturation, and  $K$  values close to saturation for the unsaturated horizons cannot be determined by a free-drainage method such as this. Examples of some soil features that can act as impeding layers are a plow sole, an argillic horizon, and pans.

Fig. 3.19 presents the tensions recorded as time progressed after the wetting of a plot of soil in the Grays silt loam. The tensions dropped to very low levels in the upper horizons. The IIC horizon is composed of sandy till. The overlying horizons have developed in loess, so there is a dramatic textural difference at the interface of these materials. Because the sand has many larger pores and a higher conductivity, it is able to conduct this water away at a relatively lower tension than the overlying silt loam. The tension in the sand never rose above -32 cm water.

Once a site has been selected, the area must be prepared for the experiment. These efforts are designed to isolate the plot from its surrounding environment and to ensure that the plot is a closed system.

The size of the plot used may depend on the moisture condition of the surrounding soil. For example, when a very dry soil surrounds the plot, lateral movement from the plot to the surrounding environment can be great. This may lead to exaggerated drainage rates, as recorded by the instruments located at the center of the plot. Because the lateral movement of moisture is not uniform over the depth of the profile and is usually greatest for the uppermost horizon, the head gradient ( $\frac{\partial H}{\partial Z}$ ) can be exaggerated. If the plot is surrounded by very moist soil, drainage will take place very slowly. Moisture may enter the system from the surrounding soil and the length of time required to achieve a certain tension in the plot may be very long. This may be because there is no place for the moisture to drain to, due to a moisture regime that rarely achieves a low enough tension, or due to a high water table which interferes with the head gradient because of its capillary fringe.

A circular plot of a diameter of 3 meters has been used successfully (Davidson, et al., 1971), but under extreme conditions of drying in the surrounding soil, this may be an inadequate volume to allow undisturbed internal drainage at the center of the site (Vepraskas, et al., 1974). In such a case, the diameter of the plot may be expanded to ensure unaffected drainage at the center. On the other hand, in some environments a smaller plot may be sufficient to eliminate boundary effects over a low-tension range.

The site is selected and the necessary area is estimated. Vegetation is either entirely or partially removed. Cutting vegetation off at ground level is more effective than pulling or hoeing it, as this will not disturb the infiltration surface. Plant removal is relatively simple in open fields but on wooded sites where shrub and tree roots permeate the soil, little can be done without destroying these plants. The root systems of trees on a hot summer day can noticeably affect the moisture content of a profile, thus interfering with the experiment. Selection of a site at a location farther from trees may bias the experiment somewhat but the results will be more representative of the actual conductivities of the soil at that point. Also, if the roots of the plants remain, revegetation is faster and the soil is less subject to erosion.

Walking on the plot should be held to a minimum when the plot is dry and should be eliminated entirely if the soil is moist or wet. This precaution is necessary to prevent puddling of the soil surface. Placing a sheet of plywood on the plot or extending planks across it supported with blocks at the boundary are two simple methods to keep traffic off the soil.

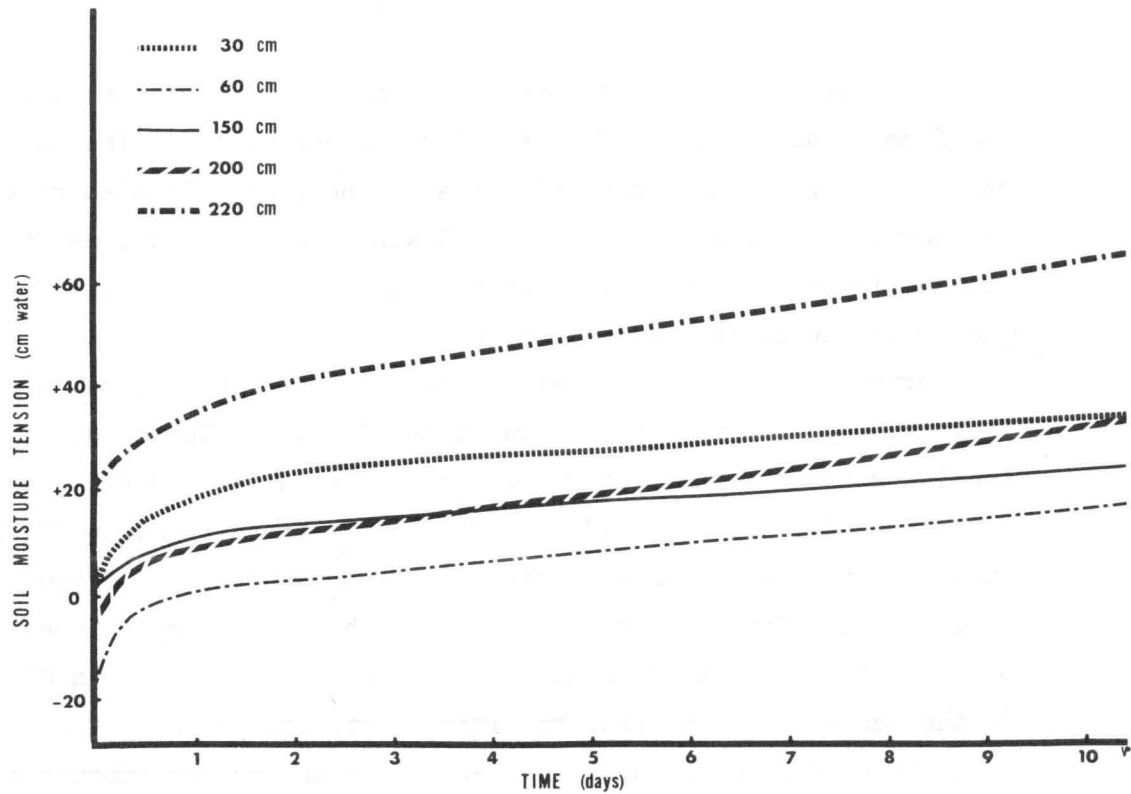


Fig. 3.19. Soil moisture tensions as a function of time, starting at saturation in major horizons of a Grays silt loam.



Fig. 3.20. Picture of prepared plot for the instantaneous-profile method with the first plastic sheet in position.

An earthen dike about 7 cm high can be constructed easily with sod from outside the boundaries. The purpose of this dike is to allow ponding of water over the area of the plot. It also prevents any downslope surface runoff from flowing over the plot, rewetting it, and interfering with the experiment. Fig. 3.20 shows a prepared plot with the earthen dike in place.

After the profile has been wetted, it must be isolated from such factors as precipitation and evapotranspiration. These can be controlled with two sheets of plastic sheeting large enough to easily cover the plot. One should be sufficiently broad to allow it to be supported at the center with the sides sloping out beyond the boundary of the plot. The smaller of the sheets should be simply spread out over the freshly wetted area. Cut a hole about one foot in diameter in the center of it so that the instruments can protrude for convenient maintenance and recording. The earth between the instruments can then be covered over with aluminum foil or small plastic sheets. If the plastic sheet is nontransparent, preferably black colored, sunlight will not easily penetrate to the soil surface and plant growth will be severely retarded. With a transparent sheet, plants will grow up quickly allowing transpiration to occur with removal of moisture from the soil. The sheets are held down at the edges with weights or stakes. The larger plastic sheet is used as a tent to shed precipitation. It is supported at the center of the plot by a post about 1 meter high, on the top of which is a circular wooden disk about 25 cm in diameter. The disk should not have rough edges that would tear the plastic. The circular design distributes the weight of the plastic uniformly and prevents punctures. The sides of the sheet are weighted or staked out beyond the plot boundaries. Plastic does stretch, and so a tightly fitted tent is difficult to achieve. Water does accumulate on the sheet at the sides, but is easily removed after each rain. A tougher material such as canvas or nylon cloth could be used to completely shed the rain. These materials have the advantage that they can be staked out at the sides and need not be weighted down, so they are easier to draw back for periodic readings of the instruments. Fig. 3.20 shows a prepared plot with the first plastic sheet in position and 3.21 with the second plastic sheet in position.

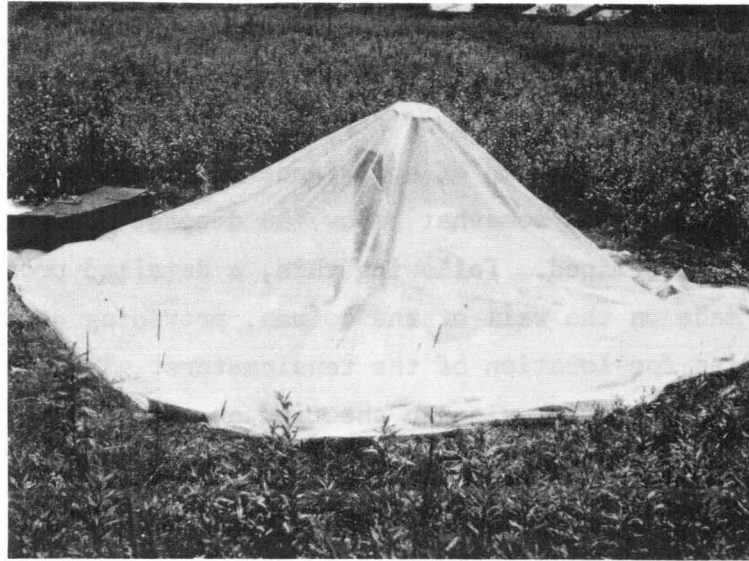


Fig. 3.21. Picture of prepared plots with the second plastic sheet (b) in position.

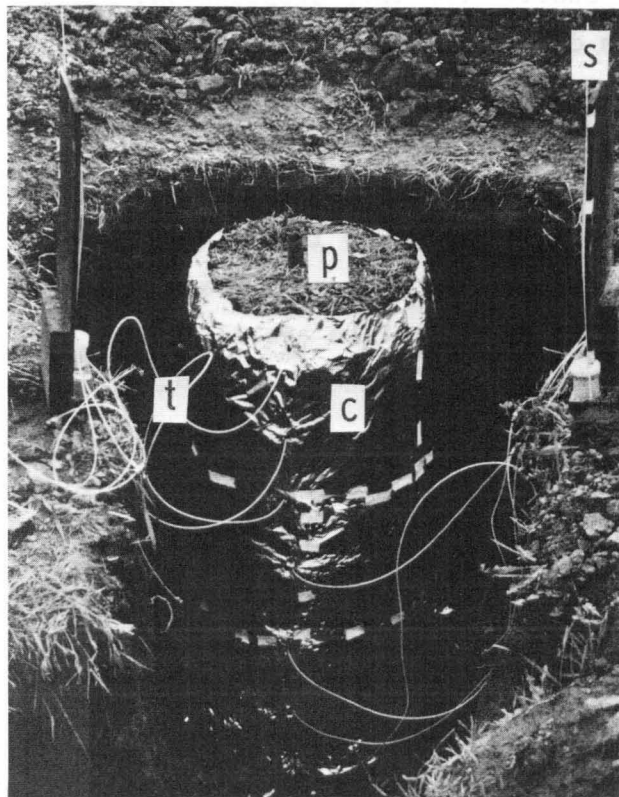


Fig. 3.22. Large excavated column for running the instantaneous-profile method on sites where the regular procedure cannot be applied. p = metal pipe for neutron probe; c = soil column; t = tensiometers and s = tensiometer boards with calibrated scales for reading moisture tensions.

Alternate forms of plot preparation are possible. One involves more digging but provides better control over environmental factors. This requires the digging of a ringlike trench around a 1 meter diameter undisturbed column of soil (Anderson and Bouma, 1973). The trench is made to a depth somewhat below the deepest horizon whose conductivity is to be determined. Following this, a detailed profile description can be made on the wall of the column, providing accurate horizon boundaries for location of the tensiometers. The sides of the column must be covered with plastic sheeting or aluminum foil to prevent evaporation.<sup>11</sup> The surface is prepared as described previously, and a ring or dike is constructed to retain the ponded water on the top for wetting. Fig. 3.22 shows a prepared column arrangement.

This arrangement has the distinct advantage that tensiometers can be implanted from the sides and many of the problems of vertical placement can be eliminated, such as the need to seal the cavity around the tensiometer shaft. For this application, small 1/4"-diameter tensiometers, as described for the crust-test method, can be used. The neutron moisture probe is a convenient tool for moisture-content measurement here.

One of the main advantages of the column method is that one-dimensional flow is maintained. There is no lateral interference with drainage or downslope moisture flow. Internal drainage proceeds uninterrupted. Effects of neighboring vegetation are eliminated and problems associated with slope are greatly reduced. However, the procedure is elaborate and costly.

#### 3.4.4. Instrumentation

Accurate soil-moisture-tension and soil-moisture-content measurements are necessary for the implementation of this technique. The careful placement of tensiometers in specific horizons of the profile and the sealing of these tensiometers in place will be discussed here, followed by a discussion of methods of moisture-content determination. Before this, it is important to point out that an accurate profile description of the soil at or adjacent to the site is essential for the determination of depths of placement of

---

<sup>11</sup>

Spraying the walls with paint or some water-repellent compound may also be effective.

tensiometers and for the useful interpretation of results. This technique can be applied very well to major horizons, but may not be specific enough for smaller soil features, such as some subhorizons.

Normally, the depth of tensiometer placement is meant to coincide with the lower boundary of the horizon to be studied. Placement a few centimeters above this boundary is perhaps more realistic since the tensiometer doesn't read pinpoint tensions, but measures the tension of the small volume surrounding the cup. It is the difference in tension across the layer which is needed to find the conductivity of that layer. This is the head gradient. So if only one horizon is to be studied, a tensiometer is needed at both the top and bottom of that particular horizon to define that gradient (see Fig. 3.23).

#### 3.4.5. Tensiometry

Tensiometers with porous cups measuring 1.9 cm OD and 5 cm long, attached to clear plastic tubing of 2.0 cm OD, and cut to various lengths were used by the author.<sup>12</sup> These were placed in the soil by the following methods.

Using a screw auger, a hole is bored of slightly larger diameter than the tensiometer itself. This hole is made 5 cm less than the depth of desired tension measurement. A push auger of a smaller diameter than that of the tensiometer may be used to extend the depth of the hole, or if the soil is moist enough, the tensiometer may be pushed into final position. This last technique will disrupt some structure and may cause rather severe puddling surrounding the cup.

A cavity along the side of the tensiometer may conduct water to the vicinity of the cup leading to tension measurements not representative of that horizon. For this reason, the space surrounding the tensiometer must be filled or sealed.

To seal the auger hole around the tensiometer, a liquid slurry is poured into the empty hole in such a way as not to trap air at some point along the cavity. This is accomplished by pouring the slurry

---

<sup>12</sup>See Appendix A for a list of equipment and manufacturers' names and addresses.

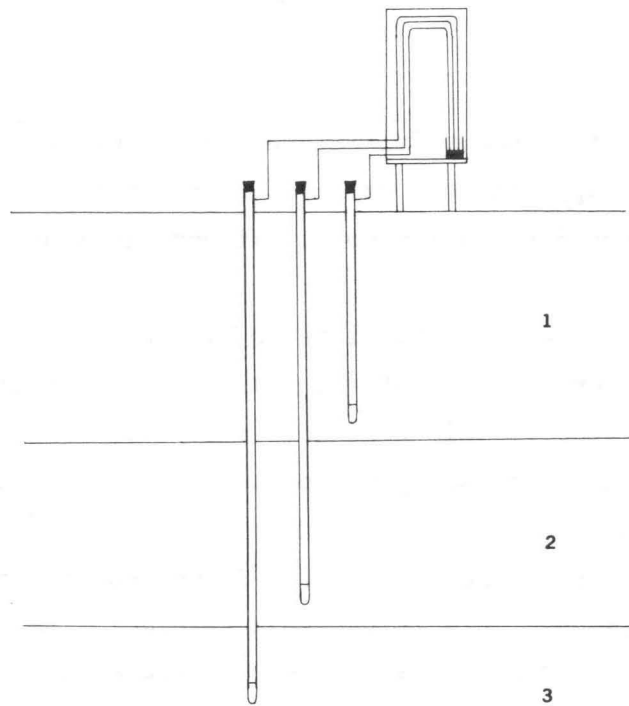


Fig. 3.23. Schematic diagram showing appropriate locations of tensiometers in a soil profile with three horizons.

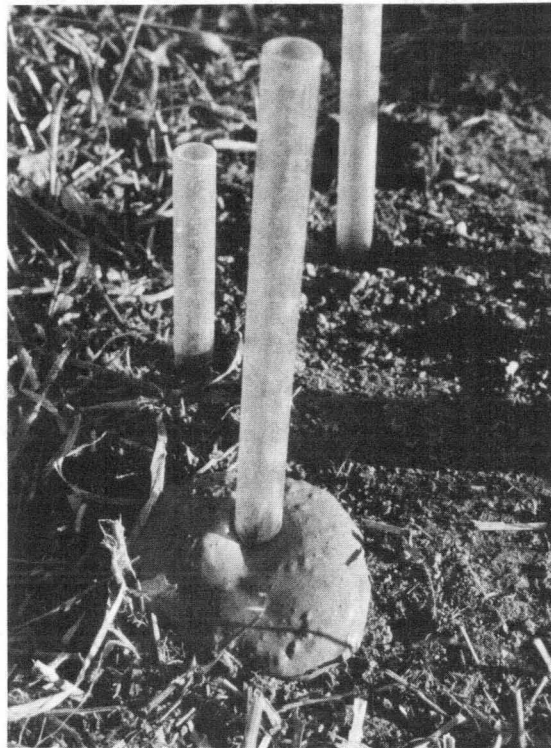


Fig. 3.24. Installed vertical tensiometer with slurry forced out at the surface to form a cap over the hole.

just to one side of the hole so that it will flow as a stream down onw wall of the hole and thus not prevent the escape of air from below. Once the hole is filled, the tensiometer is pushed into the slurry forcing it out at the surface to form a cap over the hole (see Fig. 3.24). If some air has been trapped, it will also rise to the surface. The displacement causes the slurry to be forced into holes and cracks along the walls of the auger hole, reducing the possibility of lateral water movement. In a dry soil with well-developed structure, slurry may be forced back along interpedal voids or into biopores for a distance of a few centimeters from the tensiometer. If this were to happen to any great extent, the natural moisture flow associated with these voids would be affected. Where the cup of the tensiometer reaches the bottom of the hole, it must be forced into place to provide good contact between the cup and the soil. Some smearing along the sides of the cup are inevitable, but smearing should be held to a minimum, if possible. Fig. 3.25 illustrates the good contact between the cup and soil and the sealing along the length of the tensiometer.

The slurry is prepared from soil of a texture equal to or slightly heavier than the texture of horizons being studied. For instance, a silty clay loam is used for profiles which are largely of silt loam texture. This material is placed in a shallow basin and small aliquots of water are added, with mixing, until a viscous liquid results. Time must be allowed for the swelling of clays. The material must be mixed thoroughly and any aggregates or clods should be broken down. An electric hand mixer of the type used for mixing cake batter in the home may effectively be used for this purpose. The slurry should be a viscous liquid and must flow evenly when poured.

Another method of tensiometer placement requires making a hole to the required depth with a push auger of slightly smaller diameter than that of the tensiometer itself. The tensiometer is then forced into place, assuring good contact with the soil.

Either of these techniques provide good contact between the porcelain cup and the soil. However, the first method assumes that there is a cavity along the tensiometer and procedures are defined to fill it, while the second method relies on the tensiometer being

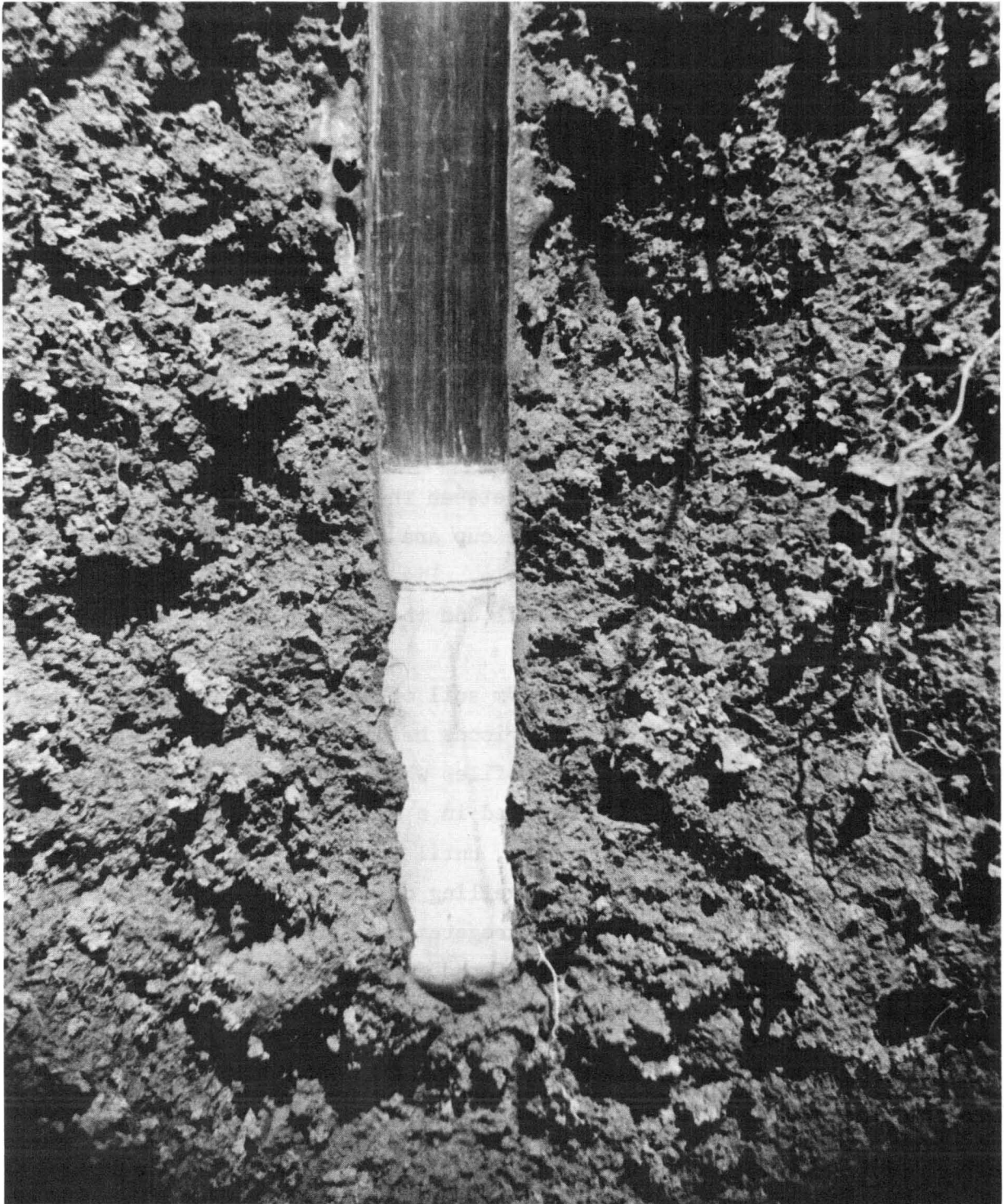


Fig. 3.25. Excavated tensiometer cup showing good contact between soil and porous cup and complete filling of the hole above the cup with slurry.

forced in for the length of the hole to a close fit. It is important that there be no unnatural vertical cavities in the profile, since at saturation such a cavity will act as a short-circuit and conduct water rapidly downward, creating unnatural moisture distribution.

Small holes are bored in the walls of the plastic tube for insertion of an 1/8" flexible tube that connects the plastic tensiometer tube to the mercury cup via a manometer board as shown in Fig. 3.26.<sup>13</sup> The scales for the boards are graduated to read cm of water and can be purchased individually. An adequately large mercury reservoir is selected so that the surface of the mercury in the reservoir does not fluctuate greatly as tensions vary. A top for the mercury reservoir is recommended with holes drilled in the cap to accommodate the 1/8" tubes.<sup>14</sup> The reservoir should be taped or otherwise anchored to the manometer board to avoid spillage.<sup>15</sup>

The tensiometers are filled with de-aired water<sup>16</sup> by pouring the water down the inside of one wall of the plastic tube of the tensiometer until the shaft is completely full. The water is poured gently to avoid dissolving too much air in the water. Next, a 50 or 60 ml plastic syringe with a single-hole rubber stopper (No. 1) fixed on the tip is inserted into the plastic tube (see Fig. 3.27) with the stopper fitting tightly in the plastic tube. By pushing the

---

<sup>13</sup>The nylon tubing provided by the manufacturer was found to weather rapidly, cracking in several weeks time of field use. We have substituted a 1/8" plastic tubing by boring a slightly larger hole in the plastic shaft of the tensiometer. This tubing lasts several times longer and is cheaper. See Appendix A.

<sup>14</sup>30 and 50 dram plastic chemical vials are easily converted to this purpose.

<sup>15</sup>Mercury is a dangerous metal and is very difficult to remove from the environment once spilled, so precautions are needed. There is always the possibility of an animal or children discovering the shiny metal, and extra thought should be given to their protection.

<sup>16</sup>See Section 3.3.2 on crust-test method for preparation of de-aired water.

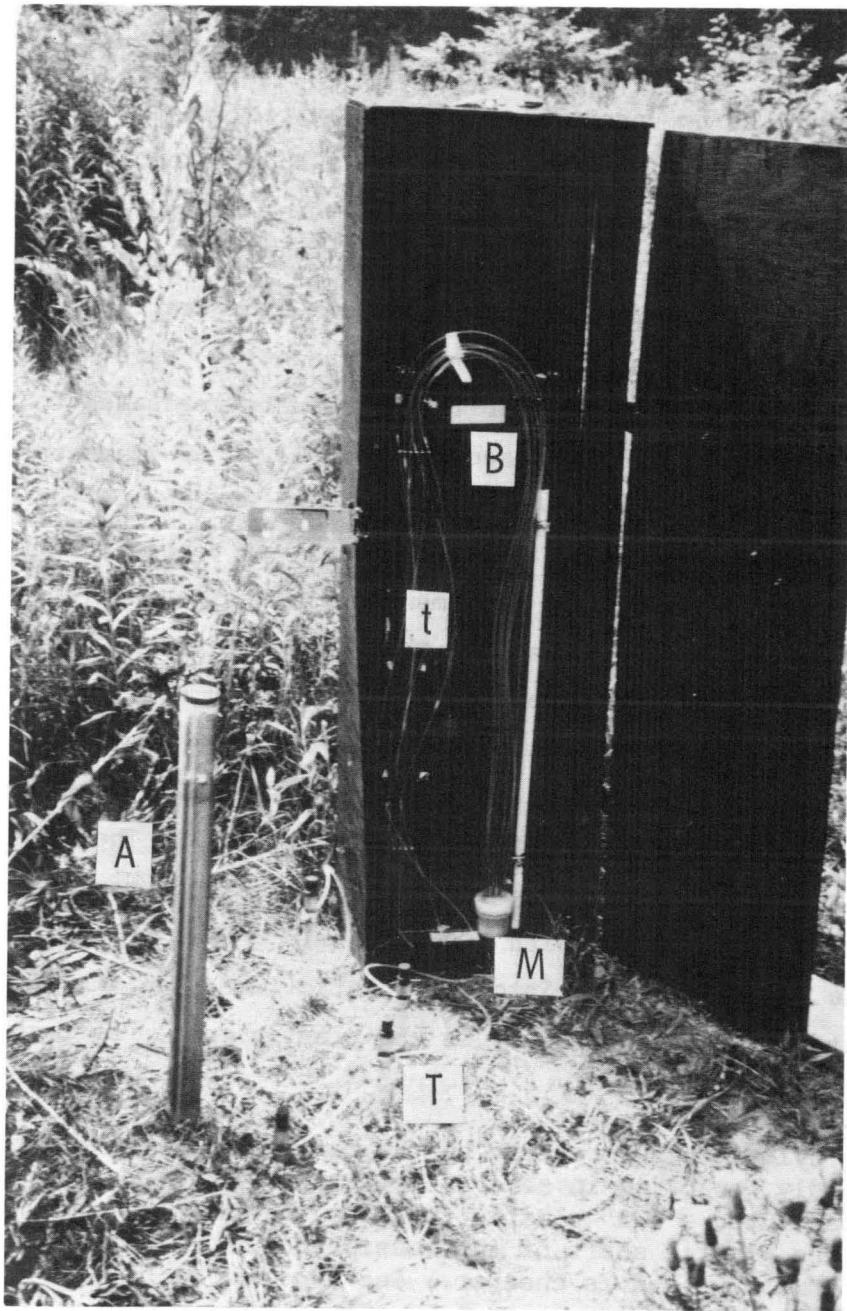


Fig. 3.26. Tensiometer assemblage, showing the connection of the plastic tube (T) with the manometer board (B) and mercury cup (M) through 1/8" flexible tubing (t). The black box with a lock serves as a deterrent to vandalism. The access tube (A) for the neutron probe is next to the tensiometers.

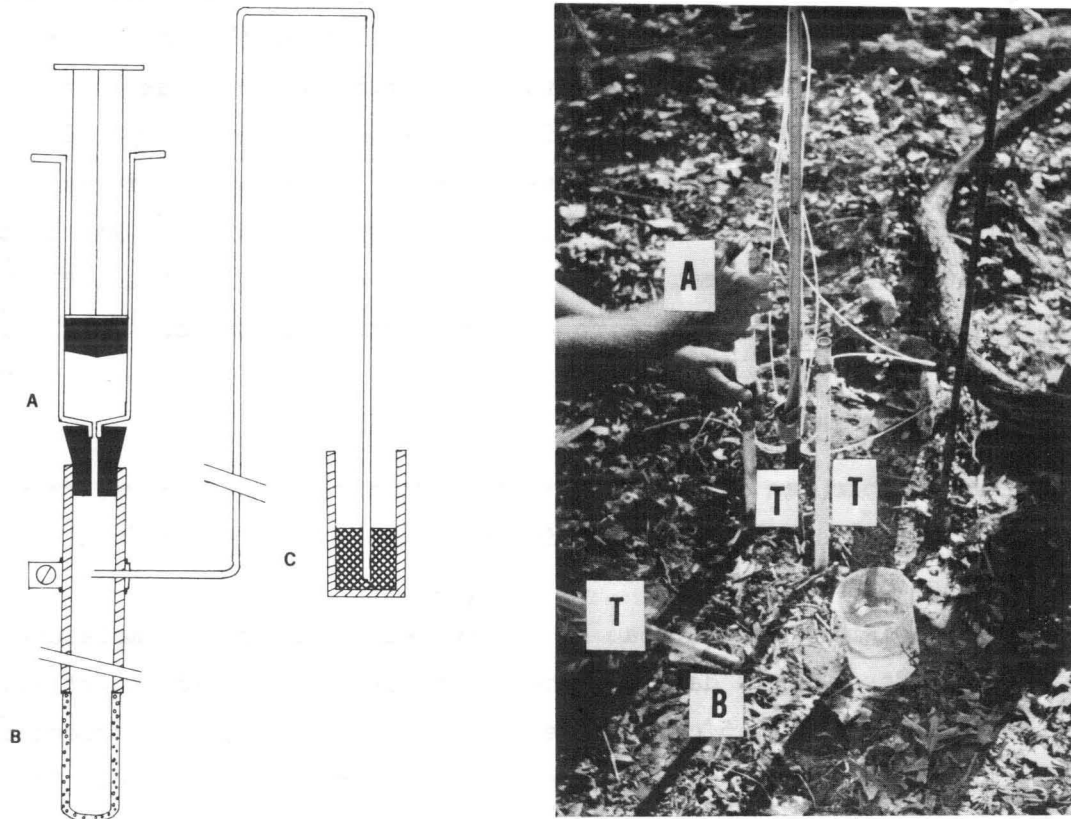


Fig. 3.27. Filling of the 1/8" flexible tubing, using a plastic syringe (A), which connects the water-filled plastic tube (T) and porous cup (B) and the mercury cup (C).

plunger of the syringe forward, water is forced into the system and fills the 1/8" plastic tubing. When water flows out of the top of the mercury reservoir the syringe is removed, the tube filled to overflowing and a solid rubber stopper (No. 1) is used to close the system. With the tensiometers shaft-oriented vertically, any air in the water tends to rise to the top of the shaft under the rubber stopper. Even though de-aired water is used, some air may appear here, particularly at higher tensions. Whenever air accumulates under the stopper it should be removed by filling the tube with more water. Gas in the system can lead to erroneous tension measurement, due to expansion and contraction with temperature variations. If a lot of air is present or if the condition persists for several days, this may indicate a leak in the system, usually a pinhole or crack in the 1/8" tubing or a bad seal of the fine tubing to the tensiometer shaft.

#### 3.4.6. Soil moisture content

Two methods can be used here: 1) indirect values derived from moisture retention cores and 2) direct values derived from *in situ* neutron probe measurements.

Soil moisture content can be determined by the use of moisture retention (desorption) data for the given horizons (Davidson, et al., 1971). Soil cores (7.5 cm diameter, 5 cm high) are taken adjacent to the plot at the depths to which tensiometers are to be placed. The moisture retention curve is derived as described in Sec. 3.1 of this bulletin. The plot is wetted and drainage occurs. In this case, only matric tension is recorded as the experiment progresses. The moisture content of a specific horizon is determined from the moisture retention curve by finding  $\theta$  for the core at the tension recorded in the horizon at that time. The moisture content data is indirectly gained but can be used in the calculation of K. The limitation of this technique is that the soil core may not represent the horizon as a whole. Several cores may be needed for a good average of values. Double tensiometry may also be needed to ensure accuracy.

The neutron probe may also be used for this purpose. The neutron moisture probe consists of a fast neutron source and slow neutron detector. Fast neutrons travel radially into the surrounding soil where, if they strike the hydrogen atom of a water molecule, they

are slowed considerably. The main source of hydrogen in the soil in the form of water, and so, aside from the small background noise of the soil material itself, the number of slow neutrons detected is roughly proportional to the amount of water in the soil (Cannell and Asbell, 1974). A counter attached to the probe converts this information into digital form. With calibration, counts/minute can be translated to % water by volume.

An access tube, 1-5/8" OD thin-walled metal conduit, is placed in a hole augered several inches deeper than the deepest horizon at which measurement is desired. The pipe should fit the hole tightly and may need to be driven into place. The hole should not be filled in around the pipe as this may lead to unrepresentative moisture contents. The probe can then be lowered in the access tube to the depth where measurements are required, measured from the soil surface to the neutron source (see instruction manual for Model P-19 Moisture Probe, Nuclear Chicago Corp., 223 W. Erie Street, Chicago, IL.) Note that the size of the roughly spherical volume of soil for which the moisture content is being determined varies with the moisture content of the soil. When the soil is very wet a small volume is required to slow the neutrons and when the soil is very dry a larger volume may be needed to slow the neutrons. This means that in drier soils a larger sample volume is needed and the moisture probe becomes less specific for a single thin subhorizon. So the neutron probe cannot yield the specific information in a dry soil that it can in a wetter soil. If a measurement is taken near a horizon boundary, the resulting moisture content may be somewhere between that of each horizon.

Gravimetric determinations of the soil moisture content can be used. A limitation of the technique is that a large number of samples would need to be taken during the course of the experiment and variability across the plot may lead to slight variations of the data. The change in water content over time will be recognized as  $\frac{\partial \theta}{\partial t}$ .

#### 3.4.7. Experimental procedure

Now that the plot has been prepared and the instruments are in place, the plot can be wetted. Often it will be necessary to wet the plot a day or two before the start of the actual measurements. This allows time for the swelling of clays and adsorption of water by the peds. Wetting can be accomplished by running a hose from a nearby house or by the use of trailer-mounted, large-capacity water tanks. Impact of the water on the plot surface should be dissipated to avoid disturbing the surface and suspending soil material which in turn may cause clogging of some pores. Water is ponded on the surface to assure uniform infiltration. Application of water continues until they remain constant. At this point the wetting process ends, and as soon as water is no longer visible on the surface the first measurements are taken at time zero and the plot is covered with plastic sheeting as previously described. Subsequent measurements are taken every hour or two for the first several hours. The time intervals may be extended as the rates of change decrease, until at about a week's time, measurements are taken every second day. The frequency of measurement depends on the rate of change of the gradients.

In some cases a tensiometer may show positive tensions. If these are of low magnitude they may be due to temporary ponding of water on a less permeable feature or horizon. In such a case a detailed soil profile description can be useful in determining the cause for this behavior. Another possible cause of positive tensions is a large cavity adjacent to the cup of the tensiometer. This may be due to some large natural void (i.e., worm burrow or root channel) near the cup or due to an inadequate seal. Use of duplicate tensiometers decreases the probability of such an occurrence.

If a tensiometer does yield sizeable positive matric tensions that do not decrease rapidly during the first few hours, the wetting procedure may need to be repeated, after resealing that tensiometer. If the questionable tensiometer shows a decreasing tension approaching the expected value, then in many cases the tensions of the first few hours can be approximated by extrapolation back to time zero (but not necessarily to zero tension). This procedure, although less reliable, can save much time and eliminate the need to repeat the whole process.

### 3.4.8. Example calculation

After data have been collected over a period of time, covering the range of soil moisture tensions desired, hydraulic conductivities can be calculated. An example calculation is carried out here based on data gathered for a Batavia silt loam (Mollic Hapludalf). (See Appendix B, profile description). Tensiometers were placed at depths of 30 cm, 55 cm, 81 cm, and 100 cm corresponding to the Ap, B1, B22, and B3 horizons, respectively.

Table 3.3 presents the matric tensions (cm) recorded at each depth as indicated along the top for several times, the latter indicated along the side. At time 0 all tensiometers show positive tensions, indicating ponding of water above the tensiometer cups. Within 0.15 days these heads had been eliminated, except in the very heavy horizons.

Table 3.3 presents soil moisture content ( $\theta$ ) data for the same horizon depths determined at the times that tensions were recorded. Along the right-hand column the average shield reading for that time (in counts per 30 seconds) is indicated. The shield reading represents the number of counts per unit of time (usually one minute or 30 sec.) when the neutron source is withdrawn within its shield. This rate should vary only slightly over time.<sup>17</sup> It is important that the neutron source be withdrawn to exactly the same point in the shield to maintain the same shielding for each reading. The plain numbers are the readings recorded at the depths in the soil. The underlined numbers are the field readings minus the shield factor. These numbers can be converted to % moisture by volume by reading across the standard curve for the probe. This standard curve is presented in Fig. 3.28.<sup>18</sup>

<sup>17</sup>Generally, there is little variation on the shield count and little correction needs to be made. A simple method of reducing variation is to subtract the shield count from the reading of soil moisture content. This must also be done for readings used for the standard curve.

<sup>18</sup>A standard curve must be made for each neutron probe individually. This is achieved by taking readings in horizons of soils at various moisture contents and taking simultaneous gravimetric moisture samples. Then these moisture contents are plotted versus the counts per unit time for each sample as shown in Fig. 3.28.

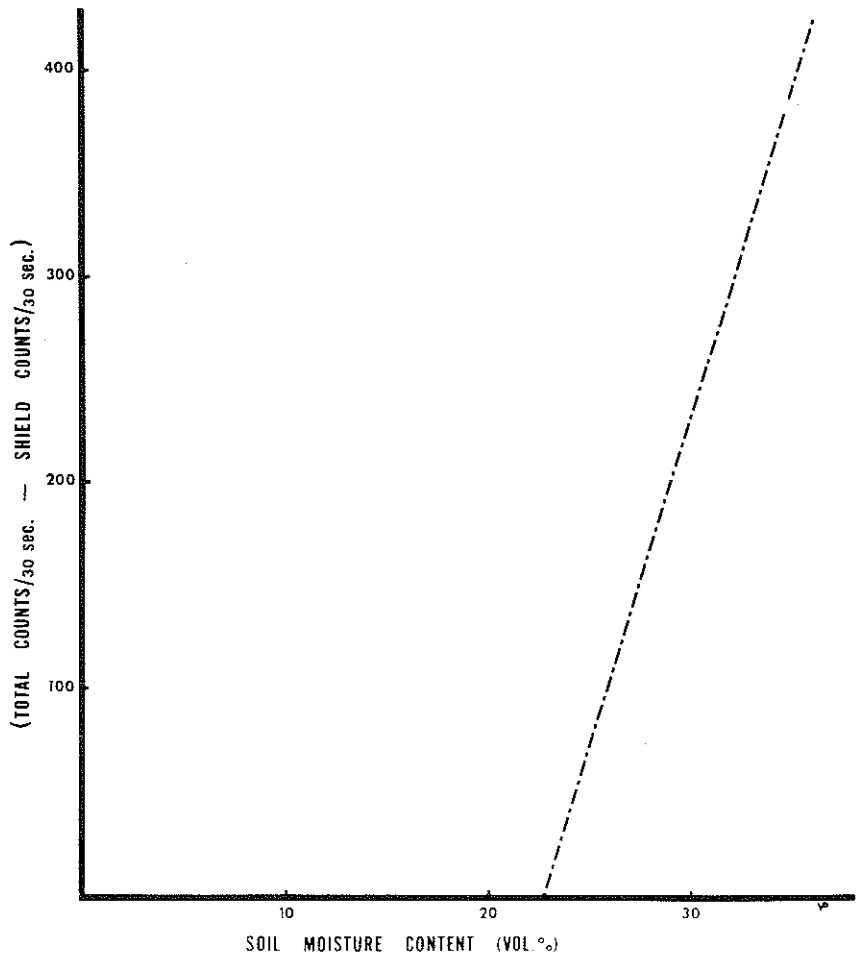


Fig. 3.28. Standard curve for the neutron probe.

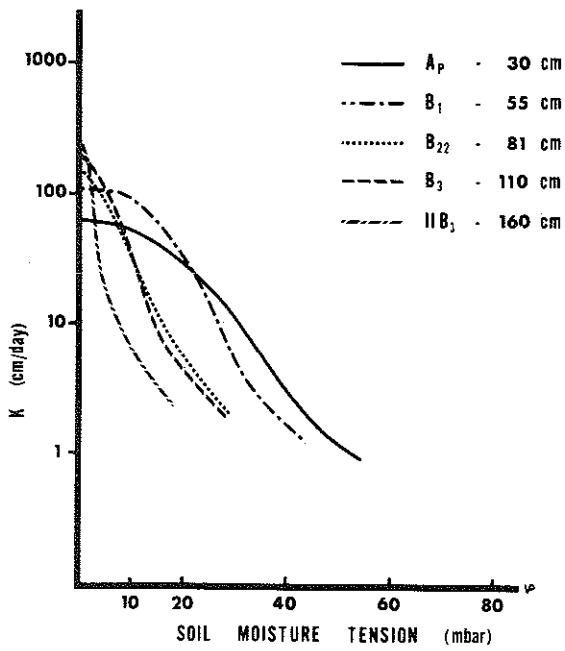


Fig. 3.29. Hydraulic conductivity values determined with the instantaneous-profile method.

These moisture contents (expressed as vol%) are plotted as a function of time of measurement in Fig. 3.16. A curve is plotted this way for each of the horizons studied. From this graph the slope of each curve at the times of measurement are derived. These slopes are the gradient  $\frac{\partial \theta}{\partial t}$  ( $\text{cm}^3/\text{cm}^3/\text{t}$ ) and appear in Table 3.4 (listed by the time and depth).

Hydraulic head is the recorded matric tension at a particular depth and time, plus the gravity head affecting that depth. The gravity head is the depth to the middle of the tensiometer cup down from the ground surface. This should not be equated with the total tension displayed on the manometer board as an additional few centimeters are included in this for the height of the mercury level above the ground surface. Fig. 3.17 is the result of plotting hydraulic head (H) versus the depth (Z) to the horizon sample in cm. For any given time the set of readings will form an approximate line or series of lines whose slope varies as drainage proceeds. This slope represents the desired gradient  $\frac{\partial H}{\partial Z}$ . The gradient can be found for specific times after the beginning of the experiment and is recorded in Table 3.5 for the respective times for each depth. For the cases where a single line is not accurate, two or three slopes may need to be taken, each one specific for the horizon at which it occurs.

Following the example of Hillel, et al., incremental flux is calculated for each horizon and time (Table 3.4) by multiplying the moisture content variation by the thickness (dZ) of the horizon effected. The sum of these increments is the flux q for the depth Z of the deepest horizon. K is calculated by dividing q by  $\frac{\partial H}{\partial Z}$  (Table 3.5) for each time. Also listed on Table 3.5 is the corresponding moisture content  $\theta$  (%) and matric tension  $\psi_m$  (cm) for each time and depth.

Fig. 3.29 presents these K values for each horizon plotted against the matric tension. A logarithm scale is used on the vertical axis to contain the wide range of values achieved over the small range of tensions.

Table 3.3. Soil moisture probe data.

Time (days)	$\psi_m$ (matric tension)					$\theta$ (counts per minute)					av. shield count (30 cts/s)	
	Horizon depth (cm)	Ap 30	Bl 55	B22 81	B3 110	IIB3 160	Ap 30	Bl 55	B22 81	B3 110		IIB3 160
0.0	---	+26	+29	+25	+11	669	693	759	734	616	383	
						<u>286</u>	<u>310</u>	<u>376</u>	<u>851</u>	<u>233</u>		
0.15		-9	-7	0	+15	+2					368	
3.0		-36	-25	-11	+15	+6	641	593	575	646	645	418
							<u>273</u>	<u>225</u>	<u>207</u>	<u>278</u>	<u>277</u>	
6.75		-44	-31	-19	-15	-3	651	582	548	629	730	429
							<u>250</u>	<u>287</u>	<u>263</u>	<u>265</u>	<u>334</u>	
10.0							630	599	560	612	697	443
							<u>187</u>	<u>156</u>	<u>117</u>	<u>169</u>	<u>254</u>	
12.0		-50	-33	-18	-15	-7	666	642	585	668	675	427
							<u>239</u>	<u>215</u>	<u>158</u>	<u>241</u>	<u>248</u>	
17.0							647	557	548	645	631	392
							<u>255</u>	<u>165</u>	<u>156</u>	<u>253</u>	<u>239</u>	
18.0		-57	-38	-21	-18	-6						

Table 3.4. Calculation of soil moisture flux.

Time (days)	Z (cm)	$\frac{\partial \theta}{\partial t}$ (days <sup>-1</sup> )	$(\frac{\partial \theta}{\partial t})dZ$ (cm/day)	$q = \Sigma(\frac{\partial \theta}{\partial t})dZ$ (cm/day)
0.0	30	1.70	51.0	51.0
	55	1.75	43.8	94.8
	81	1.70	44.2	139.0
	110	1.15	33.4	132.4
	160	0.42	21.0	193.4
0.15	30	1.50	45.0	45.0
	55	1.70	42.5	87.5
	81	1.65	42.9	130.4
	110	1.10	31.9	162.3
	160	0.40	20.0	182.3
3.0	30	0.10	3.00	3.00
	55	0.30	7.50	10.50
	81	0.18	4.68	15.18
	110	0.18	5.22	20.40
	160	0.12	6.00	26.40
6.8	30	0.04	1.20	1.20
	55	0.08	2.00	3.20
	81	0.05	1.30	4.50
	110	0.04	1.16	5.66
	160	0.14	7.00	12.66
12.0	30	0.04	1.20	1.20
	55	0.02	0.50	1.70
	81	0.04	1.04	2.74
	110	0.04	1.16	3.90
	160	0.08	4.00	7.90
18.0	30	0.04	1.20	1.20
	55	0.02	0.50	1.70
	81	0.03	0.78	2.48
	110	0.04	1.16	3.64
	160	0.06	3.00	6.64

Table 3.5. Calculation of hydraulic conductivity.

Z (cm)	q (cm/day)	$\frac{\partial H}{\partial Z}$ (cm/cm)	K (cm/day)	$\theta$ (%)	$\psi_m$ (cm water)
30	51.0	1.00	51.0	31.7	---
	45.0	0.86	52.3	31.5	-9
	3.00	0.65	4.62	30.1	-36
	1.20	0.63	1.90	29.7	-44
	1.20	0.53	2.26	29.4	-50
	1.20	0.63	1.90	29.1	-57
55	94.8	1.00	94.8	39.4	+26
	87.5	0.86	101.7	39.0	-7
	10.5	0.65	16.15	28.6	-25
	3.20	0.63	5.08	27.7	-31
	1.70	0.53	3.21	27.3	-33
	1.70	0.63	2.69	26.9	-38
81	139.0	1.00	139.0	34.0	+29
	130.4	0.86	151.6	33.7	0
	15.2	0.65	23.4	29.5	-11
	4.50	0.63	7.14	28.9	-19
	2.74	0.53	5.17	28.5	-18
	2.48	0.63	3.94	28.4	-21
110	172.4	1.00	172.4	33.7	+25
	162.3	0.86	188.7	33.4	+15
	20.4	0.65	31.4	30.3	+5
	5.66	0.63	8.98	29.8	-15
	3.90	0.53	7.36	29.7	-16
	3.64	0.63	5.78	29.7	-18
160	193.4	1.00	193.4	30.0	+11
	182.3	.86	212.0	----	+2
	26.4	.65	40.6	31.4	+9
	12.66	.63	20.10	----	-3
	7.90	.67	11.79	30.5	-7
	6.64	.81	8.19	30.2	-6

### 3.4.9. Literature cited

- Anderson, J. L. and J. Bouma. 1973. Relationships between saturated hydraulic conductivity and morphometric data of an argillic horizon. *Soil Sci. Soc. Amer. Proc.* 37:408-413.
- Baker, F. G., P. L. M. Veneman and J. Bouma. 1974. Limitations of the instantaneous profile method for field measurement of unsaturated hydraulic conductivity. *Soil Sci. Soc. Amer. Proc.* (in press).
- Davidson, J. M., L. R. Stone, D. R. Nielsen, and M. E. LaRue. 1969. Field measurement and use of soil-water properties. *Water Resources Research* 5:1312-1321.
- Hillel, D. I., V. D. Krentos, and Y. Stylianon. 1972. Procedure and test of an internal drainage method for measuring soil hydraulic characteristics *in situ*. *Soil Science* 114:395-400.
- Klute, A. 1972. The determination of the hydraulic conductivity and diffusivity of unsaturated soils. *Soil Science* 113:264-276.
- Preliminary instruction manual for model P-19 moisture probe and model 2800 scaler. 1957. Nuclear Chicago Corp., 223 W. Erie Street., Chicago, IL.
- Vepraskas, M. J., F. G. Baker, and J. Bouma. 1974. Soil mottling and drainage in a Mollic Hapludalf as related to suitability for septic tank construction. *Soil Sci. Soc. Amer. Proc.* 38:497-501.

### Appendix A

A list of equipment essential to the instantaneous-profile method is presented here. Where possible, specific catalog numbers are included with the name and address of a manufacturer. Much of the equipment may be available from other firms, but the equipment used by the authors is from these companies.

### Tensiometers

Tensiometers with 1.9 cm diameter porous cups, 5 cm in length attached to plastic tubes of several lengths.

Cup tube kit. No. 2325. Available from Soil Moisture Equipment Corp., PO Box 30025, Santa Barbara, CA 93105.

Cup tube clamp assembly No. 2326 for attachment and seal of 1/8" plastic tubing into tensiometer tube. Also from Soil Moisture Equipment Corp.

Manometer Scale, Fiberglass, reading 0-850 millibars. No. 2091.  
Also from Soil Moisture Equipment Corp.

3/4" diameter insertion tool (push auger) in three lengths. No. 241.  
Also from Soil Moisture Equipment Corp.

Manometer stands can be easily constructed from wood, using screw eyelets for the support of 1/8" tubing and with a small platform at the bottom to hold mercury reservoir. Multiple manometer kits No. 2310 can also be purchased from Soil Moisture Equipment Corp.

1/8" OD semirigid nylon (thermoplastic) tubing. Available from Imperial Eastman Corp., 6300 West Howard Street, Chicago, IL 60648 (Catalog No. 22-SN).

A Model P-19 Moisture Probe combined with a Model 2800 Scaler, both from Nuclear Chicago Corp. 223 W. Erie St., Chicago, IL, have been used by the authors with satisfactory results.

## Appendix B

### Profile Description of Batavia Silt Loam

The pedon described here is located in the town of Middleton, Dane County, Wisconsin. The site of description lies on a north-facing slope of less than 3%. The initial material is loess over what are believed to be lacustrine deposits from Glacial Lake, Middleton, which in turn overlies glacial till. This profile is not considered typical of the Batavia series in that the subsoil is unusual.

<u>Horizon</u>	<u>Depth (cm)</u>	<u>Description</u>
O1	2-0	Partly decomposed grass litter.
Ap	0-42	Very dark grayish brown (10YR 4/2); silt loam; moderate thick platy structure; very friable; abrupt smooth boundary.
A2	42-51	Dark yellowish brown (10YR 4/4); silt loam; moderate medium platy structure; friable; clear wavy boundary.
B1	51-60	Dark brown (10YR 4/3); sandy loam; weak thick platy parting to weak fine subangular blocky structure; friable; clear wavy boundary.
B21	60-90	Dark brown (10YR 4/3); silty clay loam; weak medium prismatic parting to moderate fine subangular blocky structure; friable; gradual broken boundary.
B22	90-123	Dark yellowish brown (10YR 4/4); silty clay loam; moderate coarse subangular blocky parting to fine subangular blocky structure; firm; distinct many medium ped mangans, distinct few fine manganese nodules and distinct few fine iron nodules; clear broken boundary.
IIB3	123-148	Light brownish gray (2.5Y 6/2) matrix, with distinct common coarse yellowish red (5YR 4/8) bands (< .5 cm in width, possibly varves); clay loam; moderate coarse subangular blocky parting to strong medium subangular blocky structure; firm; diffuse broken boundary.
IIC	139-268	Light brownish gray (2.5Y 6/2) matrix with distinct common coarse yellowish red (5YR 4/8) bands (< .5 cm in width, possibly varves); clay; massive structure; sticky; clear broken boundary.
IIIC	268+	Brownish yellow (10YR 6/8); sand; single-grained structure, loose.

Comments: The lower horizon depths are very variable over the pedon, for example, within 6 ft of the section described the following horizon depths were measured:

Ap	0-42 cm	B22	90-114
A2	42-54 cm	IIIB3	114-144
B1	54-72 cm	IIIC	144+
B21	72-90 cm	The IIC has apparently been incorporated into the IIB3.	

### 3.5. Calculation of hydraulic conductivities from moisture retention data

A detailed description of this method, based on a review and revision of earlier work, is given by Green and Corey (1971). Larger soil pores are progressively emptied with increasing soil moisture tension and since flow rates are strongly correlated with pore sizes (Chapter 2), a relationship between flow rates and moisture tension can be derived in principle for different soil materials using moisture retention characteristics. In addition, a pore interaction model is necessary to express the dominant hydraulic effect of small pores on the rate of flow in a complex heterogeneous pore system. The equation used by Green and Corey (1971) is as follows:

$$K(\theta)_i = (K_s/K_{sc}) \cdot (30\delta^2/\rho g \eta) \cdot (e^p/n^2) \cdot \sum_{j=1}^m [(2j+1-2i)h_j^{-2}]$$

$$i = 1, 2, \dots, m$$

where  $K(\theta)_i$  is the calculated conductivity for a specified water content (given in cm/day);  $\theta$  is water content ( $\text{cm}^3/\text{cm}^3$ );  $i$  = last water content class on the wet end:  $i = 1$  = pore class corresponding with  $\theta_{\text{sat}}$ .  $i = m$  = pore class with lowest water content for which  $K$  is calculated;  $K_s/K_{sc}$  = matching factor (= measured/calculated  $K$ );  $\delta$  = surface tension of water (dynes/cm);  $\rho$  = density of water ( $\text{g}/\text{cm}^3$ );  $g$  = gravitational constant ( $\text{cm}/\text{sec}^2$ );  $\eta$  = viscosity of water ( $\text{g}/\text{cm sec}$ );  $e$  = porosity ( $\text{cm}^3/\text{cm}^3$ );  $p$  = parameter. Here  $p = 2$ ,  $n$  = total number of pore classes between  $\theta = 0$  and  $\theta_{\text{sat}}$ ;  $h_j$  = pressure of a given class of waterfilled pores (cm water).

The need for use of the matching factor ( $K_s/K_{sc}$ ) implies that the method does not directly yield a curve at the correct level of conductivities for each moisture content or tension, but that the slope of the calculated  $K$ -curve is assumed to be correct.

Extensive application of this technique to soils in Wisconsin has shown that results are satisfactory for sands only, which have

pores that can be considered as capillary tubes. However, use of the method for other soils is not recommended because any kind of K curve can be produced by the calculation procedure by varying the values of  $m$  or  $\theta_{sat}$ . Direct measurement of  $K$ , as discussed, seems to be the only realistic procedure.

#### References

- Denning, J. L., J. Bouma, O. Falayi and D. J. vanRooyen. 1974. Calculation of hydraulic conductivities of horizon in some major soils in Wisconsin. *Geoderma* 11:1-16.
- Bouma, J. and J. L. Denning. 1974. A comparison of hydraulic conductivities calculated with morphometric and physical methods. *Soil Sci. Soc. Amer. Proc.* 38:124-127.
- Green, R. E. and Corey, J. C. 1971. Calculation of hydraulic conductivity: a further evaluation of some predictive methods. *Soil Sci. Soc. Am. Proc.*, 35:3-8.

## Chapter 4

## SOME APPLICATIONS OF FLOW THEORY TO SPECIFIC EXAMPLES

These applications assume the availability of  $K$  curves and of moisture retention data (see Chapter 3), and will be concerned with problems of increasing complexity starting with saturated flow.

4.1. One-dimensional steady saturated flow4.1.1. One layer

Fig. 4.1 illustrates flow of water through a soil core under saturated conditions. The soil in the ring has a height of 10 cm, and 1 cm water is ponded on top. Assume that water is leaving this ring at a flow rate of 5 cm/day while the 1 cm head is maintained at the top. The question to be answered is, What is the  $K_{\text{sat}}$  value of the soil in the core? Following Darcy's law ( $V = K \Delta H/L$ ), we need to know  $H$  in order to calculate  $K$ , since  $L = 10$ .  $H$  is composed of  $P$  (pressure potential) and  $Z$  (gravitational potential). It is advantageous to obtain differences in  $P$  and  $Z$  between the top and bottom of the core separately and then add them up:  $(P_T - P_B) + (Z_T - Z_B)$ . The alternative would be to calculate  $\Delta(P + Z)$  separately for the top and for the bottom and then determine the difference  $(P_T + Z_T) - (P_B + Z_B)$ . This approach is without problems for saturated flow, but confusion often results for flow under unsaturated conditions when pressure values are negative. For the simple case discussed, we find  $\Delta P = 1$  cm,  $\Delta Z = +10$ , and thus  $\Delta H = 11$ . (Reference level for  $G$  is at bottom of core and  $P = 0$  at bottom of core because outflow occurs under atmospheric pressure.) It follows that  $K = 5/11 = 4.55$  cm/day. The values for the pressure, and the gravitational and the total potential have been pictured in Fig. 4.1 for different positions inside the core.

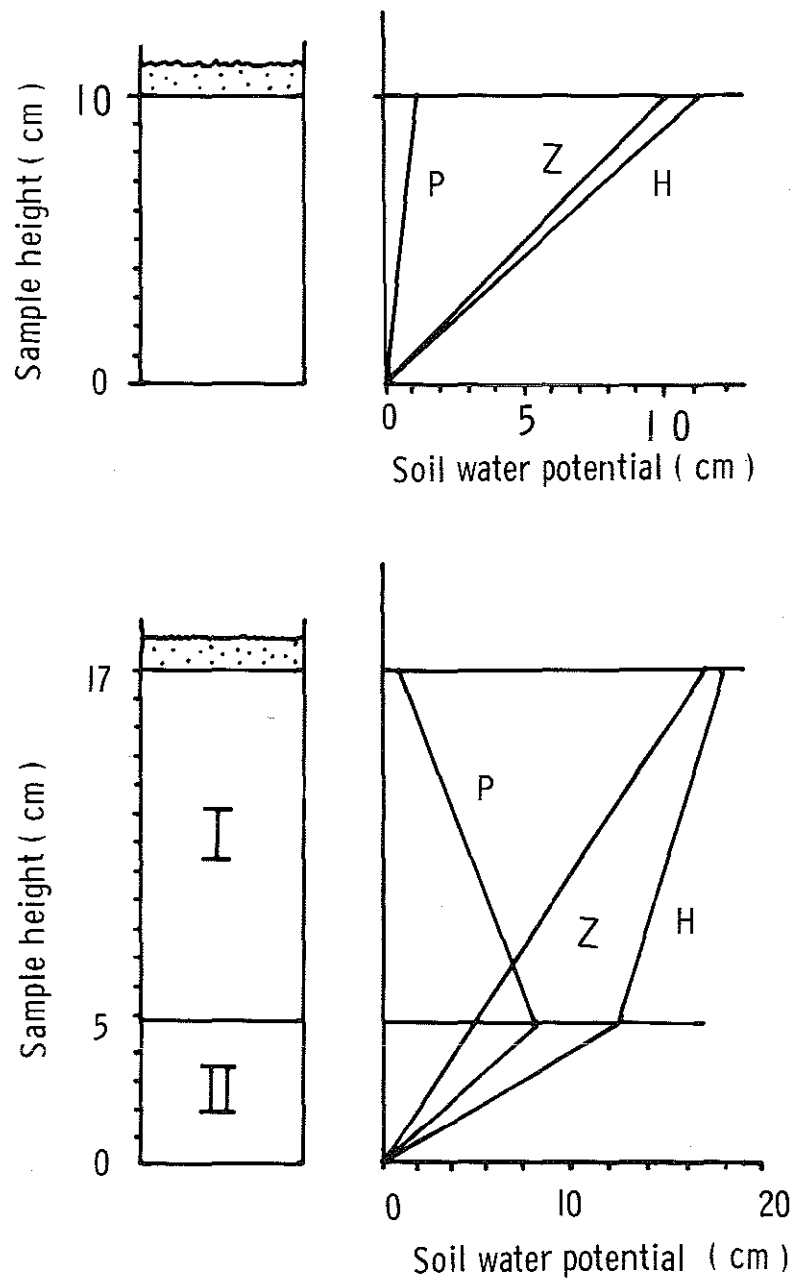


Fig. 4.1. Moisture conditions in cores during steady saturated flow.

#### 4.1.2. Two layers

A slightly more complicated situation is found when steady saturated flow occurs through a soil core that has two layers with different  $K_{\text{sat}}$  values. Fig. 4.1 shows two layers (12 and 5 cm thick) of soil in a core, with one cm of water ponded on top. Assume  $K_{\text{sat}}(\text{I}) = 10 K_{\text{sat}}(\text{II})$ . Question: What are the values for the different potentials in this flow system at steady-flow conditions?

The flow rate can again be expressed as  $V = K \cdot \frac{\Delta H}{L}$ .  $V$  can only be constant if  $\Delta H/L$  varies inversely with  $K$ . This means that the slope of the H-potential line should be ten times as steep in I as in II. We know the two end points of the H-potential line (Top:  $P = +1$ ,  $Z = +17$  if the reference level is taken at the bottom of the 17 cm high core. Therefore:  $H = +18$ . Bottom:  $Z = 0$ ,  $P = 0$ , since outflow occurs). The H-potential line can now be constructed using the proper slopes. The Z-potential line is known, since it varies from zero at the bottom to 17 cm at the top. The P-potential line can be constructed from the other two, subtracting  $Z$  from  $H$ . The P-potential line shows that pressure increases with depth until the interface with layer II is reached.

### 4.2. One-dimensional steady unsaturated flow

#### 4.2.1. One layer

The flow conditions in a homogeneous soil material are very simple and have been discussed in Chapter 2, which dealt with water movement through soils. Any given steady flow rate that is lower than the saturated hydraulic conductivity of a soil material corresponds to a characteristic soil moisture tension because it is related to its particular pore-size distribution. Flow occurs only by forces of gravity expressed by the gravitational potential  $Z$  because the pressure potential  $P$  (or better the matric potential  $M$  because pressures are negative) is constant at all depths under conditions of steady flow. Fig. 4.2 gives the hydraulic conductivity curves for the Ap and the B2 horizon of a Batavia silt loam (Mollic Hapludalf) measured *in situ* with the crust test at the Charmany University of Wisconsin

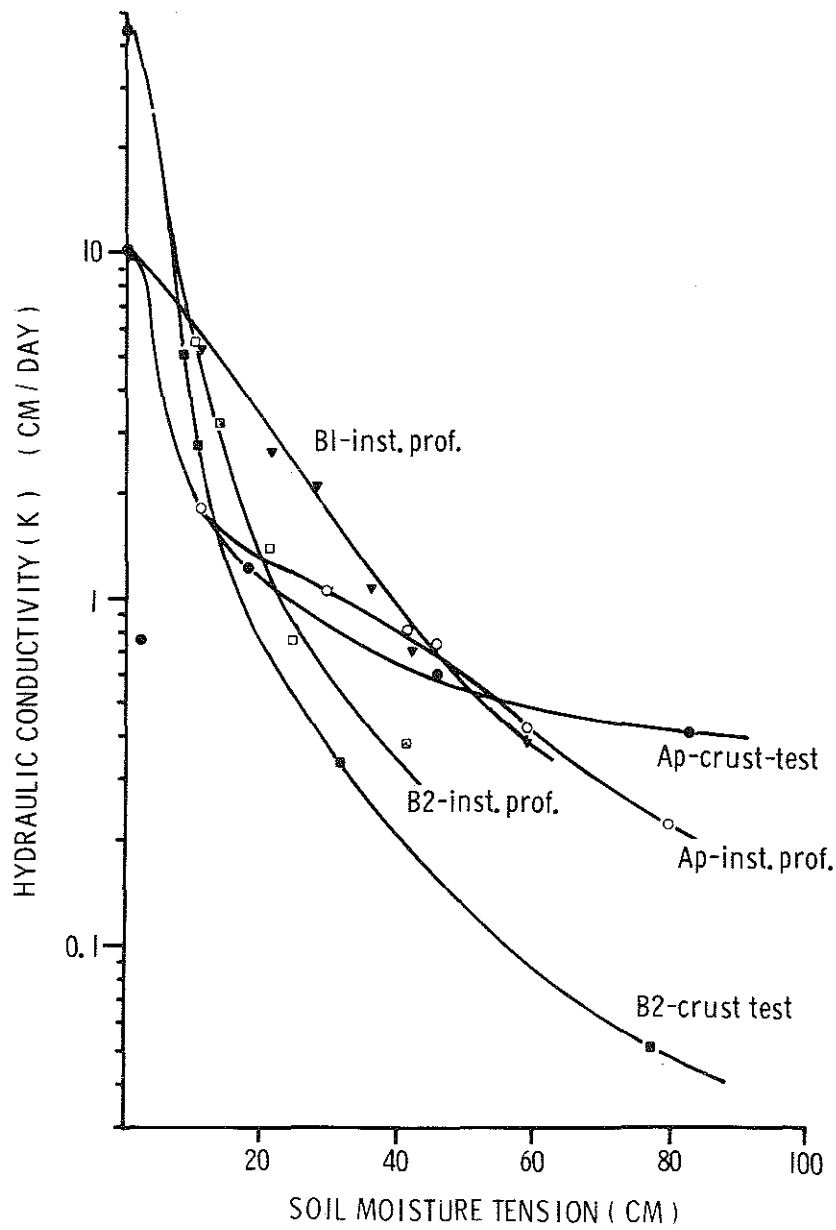


Fig. 4.2. Hydraulic conductivities for the Ap and B2 horizon of the Batavia silt loam determined *in situ* with the crust test. (The figure also includes curves determined with the instantaneous-profile method, see Section 3.4).

Experimental Farm in Madison, Wisconsin. Curves like these make it possible to predict moisture tensions (and corresponding phase distributions if moisture retention data are available) at steady flow rates (unrealistically assuming that the horizons are of semi-infinite depth, see next section). For example, tensions at a steady flow rate of 1 cm/day would be 20 cm in the B2 (B2 crust-test curve) and 30 cm in the Ap (Ap crust-test curve). At 5 mm/day these tensions would be 26 and 58 cm, respectively. Soil horizons, of course, are not semi-infinite and interferences of underlying horizons strongly influence tensions with depth. These effects can be calculated, using an approach summarized in Baver, et al. (1972), p. 358.

#### 4.2.2. Two or more layers

Darcy's law can be written as

$$V = -K\left(1 + \frac{dh}{dz}\right)$$

where  $z$  is the vertical dimension (cm, positive upwards)  $K$  is the hydraulic conductivity (cm/day) and  $h$  is soil moisture potential (cm). This equation can be integrated as follows:

$$Z_n = - \int_0^{h_n} \frac{dh}{1 + \frac{V}{K}}$$

where  $Z_n$  is the height above a horizon boundary (or a water-table level) at which the pressure  $h_n$  is experienced. So by choosing a steady-velocity  $V$  for the flow system and by reading appropriate  $K$  values from the  $K$  curves for the different layers, a complete profile of  $Z$  versus  $h$  may be plotted if a sufficiently high number of different limits  $h_n$  is used. This method will be illustrated by using  $K$  data for the two surface horizons of the Batavia silt loam (Fig. 4.2) (crust-test data).

We assume that the B2 extends very deep and that only flow from the Ap into the deep B2 will be considered.

At a steady flow rate of 4 mm/day, the tension in the B<sub>2</sub> is 30 cm. This tension will occur, therefore, at the boundary of A<sub>p</sub> and B<sub>2</sub>. However, a steady flow rate of 4 mm/day represents a tension of 83 cm in the A<sub>p</sub>. Tensions are always continuous in a soil and an abrupt change from 83 cm to 30 cm tension at the interface of the horizon is therefore not possible. The integration procedure is used now to calculate tensions in the A<sub>p</sub> in the transition zone between 30 and 83 cm. The basic question is as follows: At what height *h* above the boundary does a tension occur of, for example, 40 cm (To construct a tension curve for the transition zone, small intervals must be used.) Thus,  $h_n = 40$  cm,  $V = 0.4$  cm/day, and  $K = 0.7$  cm/day (=K at 40 cm tension in the A<sub>p</sub>, read from Fig. 4.2)  $dh = 40 - 30 = 10$  cm. Since downward flow is considered, *V* has a negative sign. Thus,

$$Z_n = - \int_{30}^{40} \frac{10}{1 - \frac{0.4}{0.7}} \cdot Z_n = 23.3 \text{ cm}$$

Result: At 23.3 cm above the boundary of A<sub>2</sub> and B<sub>2</sub>, a tension of 40 cm occurs at a flow rate of 4 mm/day. The next point could be to calculate a tension of 50 cm as follows:

$$Z_n = - \int_{40}^{50} \frac{10}{1 - \frac{0.4}{0.6}} \cdot Z_n = 28 \text{ cm}$$

which gives a total distance of 51.3 cm. This integration can be continued until a tension of 83 cm is reached, which is the equilibrium tension at the given flow rate.

A part of the complete calculated curve is in Fig. 4.3, where other curves for additional flow rates were also calculated. Note the curve for a flow rate of 2.5 cm/day, when tensions in both horizons are 10 cm. Horizons are often not deep enough to reach equilibrium tensions corresponding with steady flow rates. This is certainly true of the A<sub>p</sub> just discussed. Whatever its depth, theoretical tensions at the soil surface can be estimated (assuming all the time that there is no evaporation) by drawing a horizontal line

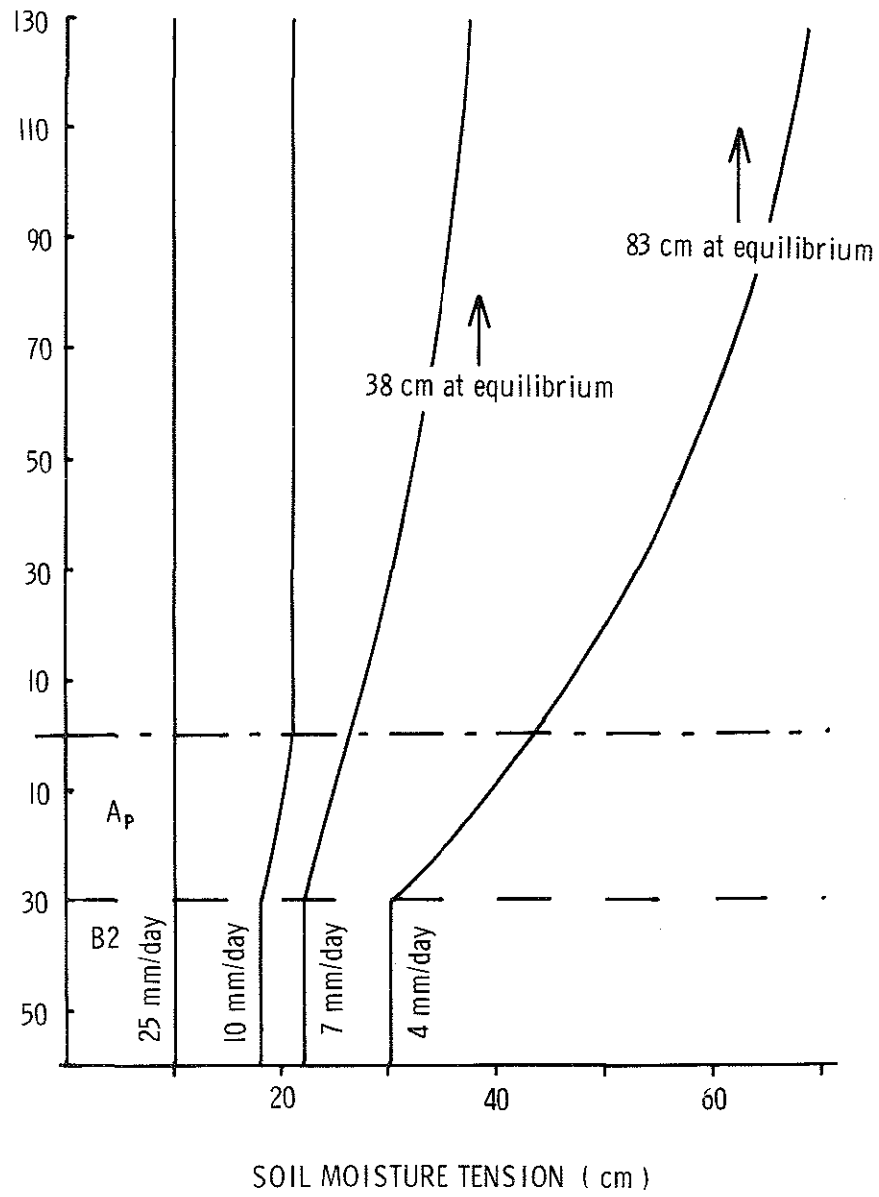


Fig. 4.3. Calculated tension profiles in the Ap and B2 of the Batavia silt loam at four flow rates.

at any desired depth in the Ap and by reading the tensions at that level from the calculated curves.<sup>1</sup>

#### 4.2.3. Flow into crusted soil

A special case of the two-layer flow system occurs when very thin layers with different hydraulic properties occur in a flow system. An example will be discussed concerning thin barriers (crusts) on top of infiltrative surfaces (Hillel, 1971).

Assuming steady infiltration (as will be occurring during the crust-test measurement, discussed in Sec. 3.3) the flux through the crust ( $q_b$ ) should be equal to the flux in the subcrust soil ( $q_s$ ).

$$q_b = q_s \text{ or } K_b \left( \frac{dH}{dZ} \right)_b = K_s \left( \frac{dH}{dZ} \right)_s \quad (1)$$

where  $K_b$  and  $K_s$  are hydraulic conductivities of the barrier and the underlying soil with  $dH/dZ$  the hydraulic head gradient in both materials. The hydraulic head gradient will be approximately unity in the soil at steady infiltration (Baver, et al., 1972). Assuming flow in the soil thus to result only from gravitational forces:

$$q = K_{s(m)} = K_b \cdot \left( \frac{H_o + M + Z_b}{Z_b} \right) \text{ or}$$

$$\frac{K_{s(M)}}{H_o + M + Z_b} = \frac{K_b}{Z_b} = \frac{1}{R_b} \quad (2)$$

where  $K_{s(M)}$  is the unsaturated K value of the soil at a moisture tension of M cm,  $H_o$  is the positive hydraulic head on top of the barrier by ponded liquid,  $Z_b$  is the thickness of the barriers and

---

<sup>1</sup>More examples of this type of analysis can be found in the following publication:

Bouma, J. 1973. Use of Physical Methods to Expand Soil Survey Interpretations of Soil Drainage Conditions. Soil Sci. Soc. Amer. Proc. 37:413-421.

$R_b$  = hydraulic resistance of the barrier,  $R_b$  can be determined from Darcy's law as applied to the barrier:

$$q = K_b \cdot \frac{\Delta H}{Z_b} \text{ or } q = \frac{K_b}{Z_b} \cdot \Delta H = \frac{\Delta H}{R_b} \quad (3)$$

$\Delta H$  can be determined as:  $H_o + M + Z_b$ . When the flux  $q$  is known, from the measured tension and the  $K$  curve,  $R_b$  can be determined from (3).  $K_b$  can be calculated if barrier thickness ( $Z_b$ ) is known; otherwise use of  $R_b$  is most appropriate.

The hydraulic effects of barriers can be predicted using equation (2) when  $K$  curves are available for the soils below the barriers and when  $R_b$  values are known for the barriers themselves.

This is illustrated in Fig. 4.4 where  $K$  curves, measured *in situ* with the crust test (see Sec. 3.3 in this bulletin) are shown for a sand, a sandy loam, a silt loam and a clay. The other curves were derived from equation (2) assuming different  $R_b$  and  $H_o$  values, and a value of 2 cm for  $Z_b$ . The curves are composed of all points where the relationship between  $K_{s(M)}$  and  $M$ , as expressed by equation (2), is valid for the assumptions made. Curves were drawn in Fig. 4.4 for  $R_b = 5, 100$  and  $1,000$  days, combined with  $H_o = 5, 30$  and  $60$  cm (for  $R_b = 1,000$  only  $H_o = 5$ ). Points where both types of curves cross represent the only hydraulic conditions, in terms of tensions below barriers and flow rates, that can be expected at the specified  $H_o$ ,  $Z_b$  and  $R_b$  values. Some conclusions of practical interest can be drawn from Fig. 4.4: (1) infiltration rates decrease and tensions below the barrier increase as the resistance of the barrier increases. The effects are a function of the capillary properties of the underlying soil, as expressed by the  $K$  curve (Chapter 2). For example, a barrier of  $R_b = 5$  days ( $H_o = 5$ ) induces tensions of 35 cm (sandy loam), 28 cm (sand), 13 cm (silt loam) and 3 cm (clay) with corresponding flow rates of 0.14 cm/day; 0.14 cm/day, 0.10 cm/day and 0.05 cm/day, respectively. These data illustrate that a clay can be more permeable than a sand under unsaturated conditions; (2) identical barriers induce different moisture tensions in different soils because

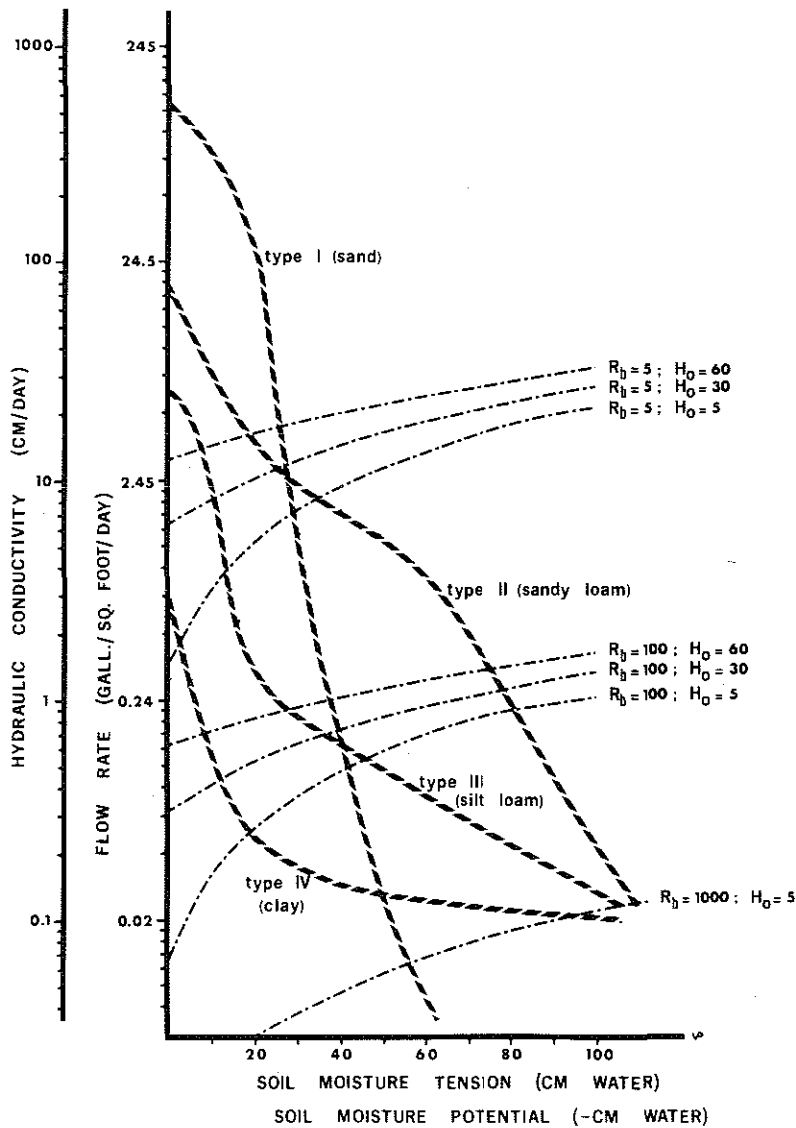


Fig. 4.4. Hydraulic conductivity curves for four major types of soil and curves expressing the hydraulic effects of impeding barriers of different resistances (see text).

their hydraulic effect is not only dependent on their own resistance but also on the capillary properties of the underlying porous medium (see equation 2). For example, a crust with  $R_b = 100$  days,  $H_o = 5$  cm induces tensions of 80 (sandy loam), 45 (silt loam), 40 (sand) and 20 cm (clay). Associated flow rates are 0.9, 0.55, 0.5 and 0.25 cm/day, respectively. The statement: "The ultimate rate of acceptance of the soil is identical to the rate of acceptance of the clogging layer" which is cited frequently is physically incorrect; (3) increasing the hydraulic head on top of a barrier with fixed  $R_b$  increases the flow rate and reduces tensions in the soil. But effects are generally minor. For example, a barrier with  $R_b = 100$  days induces flow rates of 0.5 cm/day ( $H_o = 5$ ), 0.7 cm/day ( $H_o = 30$ ) and 1 cm/day ( $H_o = 60$ ) in sand. Corresponding tensions are 42, 40 and 38 cm, respectively. The effect of increasing the head is a function of the capillary properties of the porous medium and thus, the shape of the K curve (Chapter 2); (4) barriers with a small resistance ( $R_b = 5$  days) will not affect the clay soil (except for  $H_o = 5$  where a tension of 3 cm and a flow rate of 1.8 cm/day is induced). In fact, the  $R_b \rightarrow H_o$  curves reflect hydraulic conditions imposed by the crust and the K curves reflect hydraulic conditions imposed by the soil and the K curves reflect those allowed by the soils. The most limiting of the two (the K curve in the example discussed) determines conditions if the curves don't cross.

#### 4.3. One-dimensional unsteady unsaturated flow

Flow conditions considered so far in this chapter were steady state, which implies that moisture contents and tensions did not change with time and location in the flow system. This condition may occur in the field in deeper soil horizons or during extended infiltration through impeding layers, such as crusts. Generally, though, flow velocities will be constantly changing in the upper soil horizons as periodic rain showers add water to the soil while water is extracted by evapotranspiration and deep drainage. This means that the general flow equation cannot generally be solved analytically. Phillip (1957) developed a mathematical-analytical method to describe horizontal and vertical infiltration of water into soil. Discussions of this procedure are in the literature. When infiltration takes place under shallow

ponding conditions into an initially dry soil, the soil moisture tension gradients in the topsoil are at first much greater than the gravitational gradient, and the initial vertical infiltration rate will be relatively high to decrease with time to a lower rate as the wetting zone increases in depth, thereby reducing the hydraulic gradient. The final infiltration rate at steady state equals the saturated hydraulic conductivity (hydraulic gradient = 1 cm/cm) of the soil when no crusts are present. This final infiltration rate is independent of the initial moisture content of the soil. But the initial infiltration rate is strongly affected by it because this rate is mainly determined by the gradient of the soil moisture tension, which will be lower as the original moisture content is higher. Lower gradients result in lower flow rates, thus giving lower initial infiltration rates when the initial soil moisture content is high. Of great practical interest in areas without irrigation is the problem of infiltration followed by redistribution of limited quantities of water, as may be added to the soil by a single shower. Infiltration of, for example, a few centimeters of water usually proceeds rapidly in most soils, unless strong soil crusting occurs. This water will then flow downward in the soil, wetting the soil first, followed by drying as the wetting front moves downward and no new water is added on top. Physically, these conditions are very difficult to describe because flow rates and tensions change continuously and strong hysteresis processes (Sec. 2.3) are involved because wetting (moisture adsorption) and drying (moisture desorption) occur within a relatively short time span. A complex, numerical computer analysis can be made to analyze the problem for any particular situation with well-defined boundary conditions.

#### 4.3.1. Literature cited

Baver, L. D., W. H. Gardner and W. R. Gardner. 1972. *Soil Physics*. New York: John Wiley, 498 p.

Hillel, D. and W. R. Gardner. Steady infiltration into crust-topped profiles. *Soil Sci.* 107:137-142.

#### 4.4. Some applications of flow theory to soil survey interpretations

Research is in progress in the Soil Survey Division of the Wisconsin Geological and Natural History Survey in cooperation with the Soil Science Department of the College of Agricultural and Life Sciences to apply physical flow theory, as discussed, to soil survey interpretations and soil morphology studies. Following are some publications on this research:

##### Relating hydraulic conductivity to soil structure characteristics

Bouma, J. and F. D. Hole. 1971. Soil structure and hydraulic conductivity of adjacent virgin and cultivated pedons at two sites: A Typic Argiudoll (silt loam) and a Typic Eutrochrept (clay). Soil Sci. Soc. Amer. Proc. 35:316-319.

Bouma, J. and J. L. Anderson. 1973. Relationships between soil structure characteristics and hydraulic conductivity. In R. R. Bruce, ed., Field Soil Water Regime, SSSA Special Publ. No. 5, Chapter 5, pp. 77-105.

Anderson, J. L. and J. Bouma. 1973. Relationships between saturated hydraulic conductivity and morphometric data of an argillic horizon. Soil Sci. Soc. Amer. Proc. 37:408-413.

Bouma, J. 1973. Use of physical methods to expand soil survey interpretations of soil drainage conditions. Soil Sci. Soc. Amer. Proc. 37:413-421.

Bouma, J. and J. L. Denning. 1974. A comparison of hydraulic conductivities calculated with morphometric and physical methods. Soil Sci. Soc. Amer. Proc. 38:124-127.

Denning, J. L., J. Bouma, O. Falayi, and D. J. vanRooyen. 1974. Calculation of hydraulic conductivities of horizons in some major soils in Wisconsin. Geoderma 11:1-16.

Bouma, J., D. J. vanRooyen, and F. D. Hole. 1974. Estimation of comparative water transmission in two pairs of adjacent virgin and cultivated pedons in Wisconsin. Geoderma, in press.

Relating hydraulic conductivity to soil suitability for disposal of  
septic tank effluent

- Bouma, J. 1971. Evaluation of the field percolation test and an alternative procedure to test soil potential for disposal of septic tank effluent. *Soil Sci. Soc. Amer. Proc.* 35:871-875.
- Bouma, J., W. A. Ziebell, W. G. Walker, P. G. Olcott, E. McCoy, and F. D. Hole. 1972. *Soil absorption of septic tank effluent*. Information Circular No. 20, Geological and Natural History Survey, University of Wisconsin--Extension, 235 p.
- Walker, W. G., J. Bouma, D. R. Keeney, and F. R. Magdoff. 1973. Nitrogen transformations during subsurface disposal of septic tank effluent in sands: I. *Soil Transformations. J. Env. Qual.*, Vol. 2, No. 4:475-479.
- Walker, W. G., J. Bouma, D. R. Keeney, and P. G. Olcott. 1973. Nitrogen transformations during subsurface disposal of septic tank effluent in sands: II. *Ground Water Quality. J. Env. Qual.*, Vol. 2, No. 4:521-525.
- Beatty, M. T. and J. Bouma. 1973. Application of soil surveys to selection of sites for on-site disposal of liquid household wastes. *Geoderma* 10:113-122.
- Bouma, J. 1974. Use of improved field techniques for measurement of hydraulic properties of soils. *Proceedings of the Rural Environmental Engineering Conference, Warren, Vermont, in press.*
- Bouma, J. 1974. Use of soil for disposal and treatment of septic tank effluent. *Proceedings of the Rural Environmental Engineering Conference, Warren, Vermont, in press.*
- Bouma, J., J. C. Converse, W. A. Ziebell, and F. R. Magdoff. 1974. An experimental mound system for disposal of septic tank effluent in shallow soils over creviced bedrock. *Proceedings of the International Conference on Land for Waste Management, Ottawa, Canada, in press.*
- Bouma, J., J. C. Converse and F. R. Magdoff. 1974. Dosing and resting to improve soil absorption beds. *Proceedings ASAE, Vol. 17:295-298.*
- Magdoff, F. R., J. Bouma, and D. R. Keeney. 1974. Columns representing mound-type disposal systems for septic tank effluent. I. *Soil-water and gas relations. J. Env. Qual.*, Vol. 3, No. 3: 223-228.

- Magdoff, F. R., D. R. Keeney, J. Bouma and W. A. Ziebell. 1974. Columns representing mound-type disposal systems for septic tank effluent. II. Nutrient transformations and bacterial populations. *J. Env. Qual.*, Vol. 3, No. 3:228-234.
- Daniel, T. C. and J. Bouma. 1974. Column studies of soil clogging in slowly permeable soils as a function of effluent quality. *J. Env. Qual.*, in press.
- Bouma, J. 1975. New concepts in soil survey interpretations for on-site disposal of septic tank effluent. *Soil Sci. Soc. Amer. Proc.*, in press.
- Bouma, J., J. C. Converse, R. J. Otis, W. G. Walker, and W. A. Ziebell. 1975. A mound system for on-site disposal of septic tank effluent in slowly permeable soils with seasonally perched water tables. *J. Env. Qual.*, submitted.
- Otis, R. J., J. Bouma and W. G. Walker. 1974. Uniform distribution in soil absorption fields. Second National Ground Water Quality Symposium, Denver.
- Bouma, J. 1974. Innovative on-site soil disposal and treatment systems for septic tank effluent. ASAE-National Home Sewage Disposal Symposium, Chicago. (Proc. in press).
- Magdoff, F. R. and J. Bouma. 1974. The development of soil clogging in sands leached with septic tank effluent. ASAE-National Home Sewage Disposal Symposium, Chicago. (Proc. in press).
- Converse, J. C., J. Bouma, W. A. Ziebell and J. L. Anderson. 1974. Pressure distribution for improving soil absorption systems. ASAE-National Home Sewage Disposal Symposium, Chicago. (Proc. in press).
- Bouma, J. 1975. Unsaturated flow phenomena during subsurface disposal of septic tank effluent. *J. Env. Eng., Div. Amer. Soc. Civil Eng.* (submitted)

Relating hydraulic conductivity to soil mottling phenomena

- Vepraskas, M. J., F. G. Baker, and J. Bouma. 1974. Soil mottling and drainage in a mollic hapludalf as related to suitability for septic tank construction. *Soil Sci. Soc. Amer. Proc.* 38:497-501.